May 2020

Characterization of the Effect of Photobiomodulation on Peripheral Blood Mononuclear Cells and Cd4+ T Cells from Healthy Donors and Multiple Sclerosis Subjects.

Miguel Tolentino
University of Wisconsin-Milwaukee

CHARACTERIZATION OF THE EFFECT OF PHOTOBIOMODULATION ON PERIPHERAL BLOOD MONONUCLEAR CELLS AND CD4+ T CELLS FROM HEALTHY DONORS AND MULTIPLE SCLEROSIS SUBJECTS.

by

Miguel Tolentino

A Dissertation Submitted in

Partial Fulfillment of the

Requirements for the Degree of

Doctor of Philosophy

in Health Sciences

at

The University of Wisconsin-Milwaukee

May 2020

ABSTRACT

CHARACTERIZATION OF THE EFFECT OF PHOTOBIOMODULATION ON PERIPHERAL BLOOD MONONUCLEAR CELLS AND CD4+ T CELLS FROM HEALTHY DONORS AND MULTIPLE SCLEROSIS SUBJECTS

by

Miguel Tolentino

The University of Wisconsin-Milwaukee, 2020
Under the Supervision of Professor Jeri-Annette Lyons, PhD

Multiple Sclerosis (MS) is a CD4+ T cell-mediated autoimmune demyelinating disease. The pathogenesis of MS is a combination of a pro-inflammatory autoimmune response coupled with nitrosative and oxidative stress. Mitochondrial dysfunction within the central nervous system (CNS) leads to a reduction of ATP and high concentrations of nitric oxide leads to the production of reactive oxygen and nitrogen species (ROS and RNS), resulting in oxidative and nitrosative stress that damages myelin and axons, leading to axonal loss and disease progression. Nitrosative stress is present in MS even in early stages of disease even before inflammation and the myelin destruction. The currently approved therapeutics to treat MS are effective at slowing disease progression but not preventing or reversing it, presumably because these strategies target the autoimmune response but do not address the accompanying oxidative/nitrosative stress.

Photobiomodulation (PBM) is a therapeutic strategy shown to have to ameliorate chronic inflammatory and neurodegenerative conditions. During PBM, light is absorbed by cytochrome c oxidase (CCO) producing an increase in ATP production and improvement of mitochondrial function. Previously, our lab reported that 670nm light administered over the course of disease resulted in reduced IFN-ɣ, TNF-α, and

nitrosative stress, and increased IL-4, IL-10, which correlated with the reduction in disease severity in the Experimental autoimmune encephalopathy (EAE) model of MS.

Here, we evaluated the effect of PBM with different wavelengths of light administered at different doses on the immune response and nitrosative stress in MS subjects. The production of pro- and anti-inflammatory cytokines and the generation of nitrosative stress was measured in cell culture supernatants collected from peripheral blood mononuclear cells (PBMC) or isolated $CD4^+$ T cells over the course of in-vitro treatment with light. The effect of PBM was dependent on the cell population (i.e., PBMC or $CD4^+$ T cells); the wavelength of light; the dose of light administered; and severity of disease as assessed by the Patient Determined Disease Steps (PDDS) scale. The production of IFN-ɣ was higher by CD4+ T cells (735nm at $3J/cm^2$ and $10J/cm^2$) and PMBC (simultaneous 640/875/905nm, $1J/cm^2$ and $3J/cm^2$ in MS subjects with PDDS=0 compared to MS subjects with PDDS ≥1). Conversely, CD4+ T cells isolated from subjects with PDDS≥1 responded with higher levels of IL-10 compared with subjects with PDDS=0 after PBM treatment at 670nm ($3J/cm^2$).

Photobiomodulation was effective at reducing the generation of nitrite by cells isolated from subjects with MS compared to cells not receiving light treatment. The treatment of PBMC with 830nm ($10J/cm^2$) resulted in reduced ($p=0.0153$) nitrite in comparison with controls (no light treatment). In addition, the effect of PBM with 830nm light on nitrite reduction correlated with the modulation of cytokines. Treatment of PMBC with 830nm light ($10J/cm^2$) resulted in significantly reduced nitrite and increased IL-10 ($p=0.0271$). These same conditions likewise reduced IFN-ɣ produced by PBMC to a reproducible not statistically significant level ($p=0.1940$).

The results to evaluate PBM on muscle fatigue showed that all MS subjects were able to recover strength within 12% of their initial strength after a single PBM treatment with the energy dose of 120J. Extended PBM treatment showed improvement in muscle recovery in some patients, however statistical significance was not achieved. The systemic effect of regional PBM therapy was assessed by measuring serum cytokines following light treatment. Most of the IFN-ɣ, IL-6 and IL-10 values on serum samples from MS subjects were below the limit of detection, which correlates with an absence of active disease. Values of TGF-β were lower in patients with higher disability status (PDDS≥1). The extended PBM treatment with the active device increased TGF-β levels in patients with higher disability status (PDDS≥1) compared to the inactive device, however, the increase was not significant.

Collectively, the results presented show the potential of PBM to modulate immune response, reduce nitrosative stress, and improve muscle recovery. Future experiments with a more extended PBM treatment, subjects with higher disability status, and more sensitive methods to evaluate muscle recovery are needed.

TABLE OF CONTENTS

LIST OF FIGURES

LIST OF TABLES

LIST OF ABBREVIATIONS

1	APC: Antigen Presenting Cells
2	B6: C57BL/6 mice
3	BBB: Blood Brain Barrier
4	CD: Cluster of Differentiation
5	CNS: Central Nervous System
6	ConA: Concanavalin A
7	CTLA: Cytotoxic T Lymphocyte Antigen 4
8	DC: Dendritic Cells
9	DETA-NO: 2,2'-(hydroxynitrosohydrazino)bis-ethamine
10	dpi: day post immunization
11	EAE: Experimental Autoimmune Encephalomyelitis
12	ELISA: Enzyme-linked Immunosorbant Assay
13	FBS: Fetal Bovine Serum
14	FITC: Fluorescein isothiocyanate
15	HLA: Human Leukocyte Antigen
16	HSP70: Heat Shock Protein 70
17	ICAM: Intercellular Adhesion Molecule
18	IL: Interleukin
19	IFN-ɣ: Interferon gamma
20	iNOS: Inducible Nitric Oxide Synthase
21	LED: Light-emitting diode
22	LLLT: Low Level Light Therapy
23	MBP: Myelin Basic Protein
24	MHC: Major Histocompatibility Complex
25	MMP: Matrix Metalloprotein
26	MOG: Myelin Oligodendrocyte Glycoprotein
27	MOG35-55: MOG, amino acids 35-55
28	MR: Magnetic Resonance
29	MS: Multiple Sclerosis
30	NIR: Near-infrared
31	NO: Nitric Oxide
32	ONOO": Peroxynitrite
33	PBM: Photobiomodulation
34	PBS: Phosphate Buffered Saline
35	PCR: Polymerase Chain Reaction
36	PLN: Peripheral Lymph Node
37	PLP: Proteolipid Lipoprotein
38	PPMS: Primary Progressive Multiple Sclerosis
39	QPCR: Quantitative Real-time PCR
40	RANTES: Regulated upon Activation, normal T-cell Expression and Secreted
41	RNS: Reactive Nitrogen Specie

42	ROS: Reactive Oxygen Species
43	RRMS: Relapsing Remitting Multiple Sclerosis
44	SEM: Standard Error of Means
45	SC: Spinal Cord
46	SD: Standard Deviation
47	SPMS: Secondary Progressive Multiple Sclerosis
48	TGF-β: Transforming Growth factor beta
49	Th: T Helper
50	TNF-α: Tumor Necrosis Factor alpha
51	TUNEL: Terminal deoxynucleotidyl transferase dUTP nick end labeling
52	Treg: Regulatory T cells
53	VCAM: Vascular Cell Adhesion Molecule
54	WT: wild-type

CHAPTER 1. GENERAL INTRODUCTION. MULTIPLE SCLEROSIS (MS), NITRIC OXIDE (NO), AND PHOTOBIOMODULATION (PBM).

1.1 Multiple Sclerosis (MS)

Multiple Sclerosis (MS) is a CD4+ T cell-mediated autoimmune disease characterized by the development of plaques (lesions) in the central nervous system (CNS). These plaques consist of a demyelinated area with axonal damage and presence of activated macrophages with degraded myelin-derived proteins such as myelin basic protein (MBP), myelin oligodendrocyte glycoprotein (MOG), proteolipid protein (PLP) [1]. The destruction of the myelin sheath interrupts the transmission of nerve impulses from the CNS to other parts of the body causing the symptoms of MS including anxiety, depression, motor dysfunctions, tremor, pain, numbness, sexual dysfunction, weakness, and muscle fatigue (chronic fatigue) [2]. MS is not a fatal disease, but MS subjects present a reduction in life expectancy between 7 to 14 years [3].

1.2 Types of MS

Four subtypes of MS have been established based on the clinical course. Relapsing-Remitting MS (RRMS) is characterized by the sudden appearance of MS symptoms (attacks, relapses, or exacerbations) which remain for few days or months and then disappear for long periods of time (months or years), known as remission periods. Most of the MS subjects (80-85%) are initially diagnosed with RRMS [1]. RRMS subjects progress within 5-10 years of diagnosis to Secondary-Progressive MS (SPMS), which is characterized by slow but constant disease progression. In SPMS, the relapses

are not as intense as in RRMS, however, patients no longer fully recover from relapses (constant progression). The progression of the disease leads to a permanent disability due to irreversible neurological damage and axonal loss [1]. Primary-Progressive MS (PPMS) is diagnosed in approximately 10% of MS subjects who are not diagnosed with RRMS. PPMS presents a stable and continuous deterioration in neurologic disability since the onset of the disease without relapses and remission periods [2]. Progressive-Relapsing MS (PRMS) is diagnosed in approximately 5% of MS subjects who are not diagnosed with RRMS. PRMS is characterized by the continuous worsening of the symptoms since the onset of disease, relapses with and without remission can be present during all the progression of the disease [2].

1.3 MS Epidemiology

MS affects approximately 400,000 people in the US and 2.5 million worldwide [1]. MS appears between 20 and 40 years of age and affects women more frequently than men (2:1) [4]. The etiology of MS remains unclear. It has been suggested that a combination of different factors including place of birth (region), genetic susceptibility, race, environmental factors, and exposure to pathogens are involved in the acquisition and development of the disease [5-8]. For example, regions with higher incidence of MS include both Northern regions of Europe and the US with approximately 30 cases per 100,000 people. In both southern regions of Europe and the US, the incidence of MS is around 5-30 cases per 100,000 people. In central and South America, the MS incidence is approximately 10-20 cases per 100,000 people. Areas with low incidence of MS include the regions of Asia and some countries from South America with approximately

5 cases per 100,000 people [5]. Races such as African American, Native American, Mexican, Puerto Rican, Japanese, Chinese, and Filipino present less MS incidence in comparison to Caucasians [5].

1.4 Genetics and MS

Genetics play a role in the onset and development of MS. For instance, first-degree relatives of MS subjects have from 2.5 to 5% of increased risk of developing MS. Meanwhile the identical twin of someone with MS has a risk of 25% [4]. Researchers previously performed genome-wide association studies (GWAS) to identify the genetic factors involved in MS susceptibility, clinical phenotypes, and response to treatment [11]. GWAS are typically carried out in two phases: the discovery phase and the replication or confirmatory phase. GWAS generally uses microarray analysis or other large-scale gene assay to analyze thousands or millions of single-nucleotide polymorphism (SNPs) per genome in samples from several patients. These studies compare the allelic frequencies of SNPs distributed throughout the genome between samples of unrelated MS subjects and samples from control individuals [11]. The identified SNPs can be either causative SNP or tag SNP for the causative polymorphism. Causative polymorphism may affect the function, activity, timing, or location of the gene's product [11]. Current GWAS catalogs provide information of at least 100,000 SNPs and all SNP-trait associations with P values bellow $1x10^{-5}$, as well as important MS clinical associations, including IgG levels, response to drug therapy (i.e. IFN-β), disease severity, brain lesion load, age of onset, brain glutamate levels, and normalized brain volume [11, 12].

GWAS confirmed the significant association between MS and Major Histocompatibility Complex Class II (MHC-II). Some of the genes highly associated to MS include: HLA-DRB1 class II gene with a level of association of $p<4x10^{-225}$ for rs3135388) and $p<10^{-320}$ for non-attributed SNP tagging the same DRB1 gene [13, 14]. The HLA-DRB1 class II gene is located on chromosome 6 and belongs to the family of genes known as human leukocyte antigen (HLA) complex also known as major histocompatibility complex (MHC). The main function of the HLA complex is to participate with the immune system to identify the proteins that are produced by the body and foreign proteins produced by pathogens. MHC class II proteins are located on the surface of antigen presenting cells (APCs) in order to present the foreign peptides which can be recognized by the immune system and initiate an immune response [7]. The allele DRB1*1501 has been identified as the variant highly linked to MS ($p<4x10^{-225}$). Other genes include HLA-DRB1 (allele *0301), HLA-DQB1 (allele *0201), HLA-DRA (allele *0101), and HLA-DRB1 (allele *1303) [14]. Studies with transgenic mice that express the molecule alleles DRA*0101 and DRB1*1501 (humanized mouse model) have shown that after the administration of myelin basic protein (MBP) the transgenic mice developed inflammation in CNS, demyelination and clinical symptoms in a very similar way to those observed in MS [15]. GWAS studies also identified other genes related to MS for which the level of association was also highly significant ($p<5x10^{-8}$). Some of these genes include: TCF7 which is a transcription factor that participates in T cell differentiation and survival of CD4+ and CD8+ T cells; cytokines and their interleukin (IL) receptors (IL-12R, IL7R and IL2R, TNFRSF1A); costimulatory

molecules CD58 and CD86; T cell regulatory protein TAGAP, CD6 receptor (located on T cell surface [11, 16, 17].

1.5 MS Pathogenesis

The hallmark of disease pathogenesis of MS is the development of plaques or lesions in the CNS white matter, including the optic nerves, brain stem, cerebellum and spinal cord (SC). A plaque consists of a demyelinated area with relative axonal preservation, as well as the presence of macrophages containing myelin-derived proteins such as MBP, MOG, and PLP [18]. MS is a CD4+ T cell-mediated autoimmune disease. This concept is based on research using the experimental autoimmune encephalomyelitis (EAE) model. EAE is the primary animal model for MS, induced by the immunization of animals (generally mice) with a combination of myelin-derived proteins for example MBP, MOG, and PLP. EAE is characterized by inflammation in the CNS and demyelination leading to the development of relapsing-remitting or chronic progressive diseases stages similar to those in MS [19]. In addition, animal studies demonstrate that the adoptive transfer of activated myelin-specific CD4+ T cells from EAE-mice on wild type mice lead to the development of EAE [20].

1.6 T cell activation in MS.

The first step in the pathogenic mechanism of MS is the activation of naïve autoreactive T cells in the periphery and their migration into the CNS [21]. Activation of naïve T cells is carried out by a three signals mechanism. The first signal is made by the T cell receptor (TCR) by recognizing the peptides presented by the MHC on antigen

presenting cells (APCs). T cells with CD8 receptor molecules (CD8+ T cells, cytotoxic T cells) recognize MHC class I. T cells with CD4 receptor molecules (CD4+ T cells, helper T cells) recognize MHC class II [22]. MHC class I are located on the surface of nucleated cells, while MHC class II are present on professional APC (i.e. dendritic cells, B cells, macrophages) [23]. The second signal is carried out when the co-receptor molecules CD80 and CD86 on APCs (i.e. dendritic cells) bind to CD28 molecules located on T cells. The second signal produces the release of cytokines by the T cell. The binding of these cytokines to their specific receptors on T cells (signal three) will produce the final activation of T cells. For instance, IL-12 leads to Th1 differentiation and IL-4 leads to Th2 cell differentiation [22]. Once activated in the periphery, T cells are able to cross the blood brain barrier (BBB) and enter the CNS. Once in the CNS, resident APCs (microglia, B cells, astrocytes, which possess MHC class II), present myelin antigens to the autoreactive T cells, leading to reactivation and triggering the recruitment of immune cells that contribute to demyelination, loss of oligodendrocytes, and loss of axons leading to the signs and symptoms of MS [21, 24].

1.7 T cell tolerance and MS

Tolerance is the process by which autoreactive T cells that can potentially lead to autoimmune diseases are eliminated (i.e. central tolerance) or made functionally unresponsive (i.e., peripheral tolerance). When cells escape tolerance, the result is the presence of autoreactive cells in the periphery and the potential development of autoimmune disease [23, 26, 27]. **Central tolerance mechanism** is carried out in the thymus by the process of negative selection, which leads to the destruction of T cells

with high avidity interactions with self-antigens presented by the MHC complexes on APCs. The degree of avidity depends on two factors 1) the degree of affinity between the T cell receptor (TCR) and the antigen (i.e. myelin epitope) presented on the MHC complexes; and 2) the number of complexes (MHC-epitope) formed between the APC and the T cell [23, 26, 27]. Therefore, two possible mechanisms of escape from central tolerance include: 1) weak interactions between the TCRs and the antigen presented by the MHC complexes, and 2) the presence of few antigen-MHC complexes between T cells and APCs [24]. Previous studies investigated the interaction between MHC complexes and MBP peptides of different sizes. Harrington, C.J., et al., observed that the $MBP_{121-140}$ formed a complex with MHC with a half-life of 177 hours and induced tolerance. On the other hand, MBP_{AC1-11} formed a complex with MHC with a half-life of 15-30 minutes and tolerance was not produced. The results suggested that in the thymus, myelin-specific T cells can escape central tolerance mainly due to low affinity [28, 29].

Peripheral tolerance mechanisms are carried out when self-reactive T cells escape from central tolerance. These mechanisms include: destruction of auto-reactive cells (also known as deletion) and inhibitory mechanisms (i.e. anergy) [23, 26, 27]. Destruction of autoreactive cells results from the interaction between Fas (CD95 molecule) and its ligand to promote apoptosis. T cells express Fas on their surface. When T cells become activated by the antigen and IL-2 presence, the expression of Fas ligand is induced. The interaction of Fas and its ligand triggers the formation of the intracellular death-inducing signaling complex (DISC) which activates caspases to promote apoptosis [27]. T cells from MS subjects present a deregulation in the

activation of the DISC due to a reduction in the expression of Fas on the cell surface and therefore a reduction in both the Fas-ligand interaction and the activation of caspases [30, 31].

T cell activation requires the presence of the TCR signal and the costimulatory signal produced during CD28 ligation. These signals lead to the production of IL-2 which will activate the PI3KAKT-mTOR pathway to sustain cell activation. However, when the second signal is absent, a state of hyporesponsiveness known as T cell anergy results. T cell anergy is characterized by repression of TCR signaling and IL-2 expression [26]. Another inhibitory mechanism involves the CD152 molecule also known as cytotoxic-T-lymphocyte-associated protein 4 or CTLA-4, which is located on the surface of T cells and binds with higher affinity to the costimulatory receptor CD28. Binding of CTLA-4 by CD28 inhibits the activation of T cells [26]. MBP-specific T cells from MS subjects are able to become active even when CD28-mediated costimulation is blocked or absent [32-35]. This suggests that in MS subjects, T cells can escape the peripheral tolerance mechanisms because T cells are less sensitive to the lack of costimulation or these mechanisms are compromised [32-35].

The specific agents involved in the activation of T cells in the periphery by CNS antigens have not been established. One theory suggests that the presence of infectious agents could produce the activation. For example, the similarity in the structure between pathogen antigens and the structure of myelin proteins could produce the activation of T cells (molecular mimicry). Some of the pathogens implicated in activation of myelin-reactive T cells and the initiation of MS include the Epstein Barr

virus (EBV), influenza, herpes simplex virus, human papilloma virus, and human herpesvirus-6 [23].

1.8 Blood brain barrier disruption by T cells

Once activated in the periphery, activated autoreactive T cells migrate to the blood brain barrier (BBB). Autoreactive T cells adhere to the endothelium of the BBB via adhesion molecules to initiate transendothelial migration through the BBB [36]. Some endothelial molecules that participate in T cell migration include: the vascular cell adhesion molecules (VCAM), and intracellular adhesion molecule (ICAM) both expressed on endothelial cells, the α4 integrin (VLA-4, very late antigen) and the leukocyte functional antigen (LFA-1, or leukocyte function associated antigen) both expressed on T cells [21, 36].

The presence of chemokines increases both the binding affinity between T cells and the endothelium cells as well as the reversible binding between T cells and the endothelium (ICAM-1/LFA-1 and VCAM-1/VLA-4 interaction complexes). Once autoreactive T cells are firmly adhered to the endothelial surface, they start to travel on the endothelial surface looking for inter-endothelial junctions (tight junctions). T cells penetrate the endothelial basement membrane and enter the perivascular space. This migration is facilitated by matrix metalloproteinases (MMP) produced by the microglia and astrocytes which function to fracture the BBB [21, 36, 37]. Once in the CNS, autoreactive T cells are reactivated by the recognition of myelin antigens. The reactivated T cells further differentiate into CD4+ Th1 or Th17 T cells producing of pro-inflammatory cytokines (IFN-ɣ, IL-23, TNF-α, lymphotoxin) and chemokines (RANTES,

IP-10, IL-8) which further activate microglia and astrocytes, and recruit immune cells (monocytes, CD8+ T cells, B cells, mast cells) from peripheral blood into the CNS to initiate the formation of the inflammatory lesion [21, 36, 37].

1.9 Pro-inflammatory cytokines in EAE and MS

T cells are the main player in the pathogenesis of MS, thus it is necessary to understand the different T cell types, the cytokines produced by them, and their role in MS and EAE. Lymphocytes consist of the thymus-derived T cells, bone marrow-derived B cells, and natural killer (NK) cells. T cells are divided in 3 categories, CD4+ T cells (T helper), CD8+ T cells (cytotoxic), and regulatory T cells (T regs). Each category differentiates in different cell subsets depending on the presence of cytokines, chemokine receptors, transcription factors, and epigenetic modifications [23, 38]. Each cell subset produces different cytokines and performs specific functions in the immune response. Naïve CD4+ T cells in the presence of IL-12 differentiate in Th1 cells, or in the presence of IL-6, TGF-β, and IL-23 differentiate to Th17 cells. Both Th1 and Th17 cell subtypes are considered pathogenic in MS and EAE because they promote the development and progression of disease through the production of pro-inflammatory cytokines. Th1 cells produce TNF-α, IFN-γ and IL-2. Th17 cells produce IL-17, IL-6, IL-21, IL-22, and TNF-α [23, 38].

TNF-α is pro-inflammatory cytokine that participates in the development of MS and EAE. Korner et al, reported that the administration of TNF receptor (55kDa)-IgG infusion protein (TNFR-IgG, TNF-α blocker) in rats prevented the clinical signs of induced EAE without affecting the migration of CD4+ T cells to the CNS [39]. Additional

experiments showed that the timing is critical for the effectiveness of TNFR-IgG in EAE-induced rats. When TNFR-IgG infusion was administrated before the onset of disease, a reduction in the clinical signs as well as a reduction of inflammatory leukocytes in the CNS were achieved. However, if the infusion was administrated once the clinical disease was established, the disease progressed as usual. This data suggested that TNF-α plays a role in early events of disease development but not during the acute neurological deficit which is characteristic in EAE-induced rats [40]. Similarly, additional studies showed that TNF-KO C57BL/6 mice immunized with MOG_{35-55} to induce EAE presented a delay in the onset of disease as well as a reduced migration of inflammatory leukocytes into the CNS parenchyma during the onset and the peak of the disease [41]. TNF-α interacts with 2 receptors, both of which are implicated in MS and EAE. TNF-receptor-1-KO mice showed a less severe EAE characterized by a reduction in demyelination. On the other hand TNF-receptor 2 KO mice develop a more severe EAE with higher demyelination [42]. Additional studies showed that subcutaneous injections of the soluble TNF-receptor (sTNFrl) during 15 days starting the day of immunization, provided an effective inhibition of EAE induction in SJL/J mice [43]. Similarly, C57BL/6 TNF-receptor-1-KO mice immunized with MOG_{35-55} were protected against disease, characterized by a marked reduction in demyelination and lymphocyte infiltration in CNS [44].

Even though data support the role of TNF-α as pro-inflammatory cytokine that participates in the development of EAE and MS, there are studies that show that TNF-α can play a protective role, too. For instance, in one study, TNF-KO-C57BL/6 mice were immunized with MOG_{35-55} to induce EAE. TNF-KO-C57BL/6 mice with EAE developed

more severe neurological damage, higher mortality, more severe inflammation and demyelination than controls (C57BL/6 mice with EAE). Further treatment with TNF-α reduced disease severity in TNF-KO-C57BL/6 mice [45]. These data support previous findings that indicated that TNF was not necessary for induction, inflammation and demyelination but showed that TNF might play a role in limiting the degree of severity and duration of EAE and MS [45].

IFN-ɣ is another pro-inflammatory cytokine that participates in the development of EAE and MS. Studies demonstrated a positive correlation between high levels of IFN-ɣ and the clinical manifestation in EAE and MS [46-52]. In an early study, 18 RRMS subjects received recombinant IFN-ɣ at 3 different doses: low (1mcg); intermediate (30mcg); and high (1000mcg). The results showed that serum levels of IFN-ɣ were proportional to dose administrated. Seven out of 18 RRMS subjects presented exacerbation during the treatment [51]. The exacerbations occurred in all 3 dosage groups and they were not dose-related. The results suggested that the administration of IFN-ɣ activated the immune response and disease activity in the CNS, further suggesting that the attacks were immunologically mediated [51]. In a subsequent clinical trial, 45 patients with secondary progressive MS (SPMS) were divided in 3 groups of 15 patients and each group received antibodies to IFN-ɣ, TNF-α, or a placebo for 12 months. The patients taking the IFN-ɣ antibody were the only group that showed a significant improvement in disease supported MRI data in the reduction in the number of active lesions, reduction in TNF-α, and IFN-ɣ, suggesting that the use of antibodies against IFN-ɣ could be a potential treatment for SPMS subjects [52].

On the other hand, several studies demonstrated a protective role of IFN-ɣ in EAE [53-65]. For instance, Billiau et al., showed that injection of IFN-ɣ in EAE mice resulted in a reduction in disease severity, symptoms, morbidity and mortality [56]. The authors studied the effects of anti-IFN-ɣ antibody treatment in 2 different EAE models using SJL/J and C57BL/6J mice [56]. SJL/J mice show high incidence, a highly aggressive EAE and 100% mortality, under the same conditions, C57BL/6J mice are less susceptible to EAE, present lower incidence rate (20-40%), lower disease scores, and lower mortality rate. EAE was induced by injection of spinal cord homogenate, in combination with *Bordetella pertussis* and Freund's adjuvant. Anti-IFN-ɣ antibodies were injected intraperitoneally into EAE-induced C57BL/6J mice on days -6, 0, 7, and 14 relative to the time of immunization (EAE induction). These mice presented with increased incidence and mortality in comparison with controls. Histopathological examination showed that there was a positive correlation between clinical disease scores and the extent of histopathological findings. The results showed that anti-IFN-ɣ antibody treatment increases disease severity in low-EAE-susceptibility mice (C57BL6J mice) [56]. On the other hand, SJL/J mice received intraperitoneal injections of anti-IFN-ɣ antibody on days -3, 0 and 3 relatives to EAE induction. Anti-IFN-ɣ antibody did not show any effect on SJL/J mice in comparison with controls. Interestingly, when EAE induced-SJL/J mice received intraperitoneal injections of rDNA-derived IFN-ɣ on days -1, 0, 1, 3, 5, 7, and 9 relative to EAE induction, the systematic administration of IFN-ɣ produced a relative protection characterized by a reduction in the clinical scores and mortality rate [56]. These data show that it is important to differentiate between the local and systemic effects of IFN-ɣ. The local IFN-ɣ promotes inflammation whereas

systemically, it produced an anti-inflammatory effect. Based on the results obtained, the authors proposed that anti-IFN-ɣ antibodies were able to reach and neutralize the IFN-ɣ present in the circulation and peripheral body compartments but not that produced locally in the CNS, which is difficult to reach due to the presence of the blood brain barrier. Therefore, the blocking of the systemic IFN-ɣ suppresses the anti-inflammatory properties of IFN-ɣ, leading to increase of EAE severity. The endogenous IFN-ɣ formed during the induction or development of EAE can play a disease-limiting role, and thus this production should not be blocked during the inflammation of CNS. In addition, the systematic administration of IFN-ɣ may be used to reduce disease severity [56].

In additional experiments, the Billiau group investigated the role of IFN-ɣ in a chronic relapsing remitting model of EAE using SJL/J mice [61]. SJL/J mice were immunized with spinal cord homogenate in combination with Freund's incomplete adjuvant, and *Mycobacterium tuberculosis* on day 0 and 7, to induce EAE, presenting with mild EAE on day 21. The mice were divided in 3 groups and re-immunized on day 21. Group 1 received anti-IFN-ɣ antibody on days 21 and 27 (injected intraperitoneally), while Groups 2 and 3 received intraperitoneal injections of saline or rat IgG antibody (rat IgG2A). A few days after re-immunization the 3 groups presented EAE symptoms. Group 1 (anti-IFN-ɣ antibody) presented higher incidence, higher severity of attacks, and faster progression of the relapses than Group 2 and 3. The authors concluded that the induced relapses are facilitated by the administration of anti-IFN-ɣ antibody in the disease-free interval. The data showed that the enhancing effect of anti-IFN-ɣ antibody administrated before and during the primary attack did not carry over to the relapses. The data also suggested that the IFN-ɣ produced endogenously by the mice provided

some protection against disease progression [61]. Similarly, other authors also showed that the use of anti-IFN-ɣ antibody increased EAE severity [57, 58, 62]. In addition, several studies showed the protective role of IFN-ɣ in the EAE model using KO-IFN-ɣ mice. The lack of IFN-ɣ led to the development of EAE even in strains that are normally resistant to EAE [53-55, 63, 64].

Other studies reported that IFN-ɣ plays a role in the reduction in disease severity in EAE induced mice. One study reported that IFN-ɣ completely prevented the clinical disease in EAE-induced Lewis rats receiving IFN-ɣ into the ventricular system of the CNS on day 8 after EAE induction (just 2 days before the expected onset of clinical signs of EAE) [60]. Conversely, intraperitoneal injection of rats with IFN-γ on d8 resulted in a more severe disease course with high percentage of relapses [60]. These data suggest that the IFN-ɣ produced within CNS plays a disease–limiting role whereas peripheral IFNγ exacerbates disease [60].

Furlan et al., further investigated the specific and localized over expression of IFN-ɣ in the CNS of EAE-induced mice [65]. The authors used an IFN-ɣ gene-containing vector inserted in Herpes simplex virus type 1 (HSV-1) which was injected intracisternally in C57BL/6 mice (6-8 weeks of age). Mice were injected twice (days 0 and 7) and they were sacrificed at week 1 and 3. To confirm IFN-ɣ overexpression, qPCR analysis showed that mice that received the injections of vector expressing IFN-ɣ presented a significant increase of IFN-ɣ mRNA in the brain and spinal cord in comparison with controls (HSV-1 without IFN-ɣ vector). The increase in IFN-ɣ levels lasted between 3-4 weeks after vector injection. When mice received one intracisternal injection with the IFN-ɣ containing vector 1 week after EAE onset, mice partially

recovered from disease within 25 days after vector injection. On the other hand, control mice receiving the vector without the IFN-ɣ gene never recovered from EAE. When mice received intracisternal injection of the IFN-ɣ vector or control vector before the EAE onset (on the day of EAE induction and another one 7 days later), EAE-mice receiving the IFN-ɣ containing vector showed earlier disease onset, milder disease course, and increased apoptotic T cells compared to control mice. Furthermore, 83% of mice completely recovered from disease between day 22 and 28 post EAE immunization. Control mice showed later disease onset, higher EAE score, and never recovered from disease [65]. Histopathological exams performed 60 days after EAE induction on mice that received the treatment prior to disease onset showed a reduction in inflammatory infiltrates, less demyelinated areas, and reduction in axonal loss in comparison with controls. The authors conclude that their results challenged the general idea that the presence of IFN-ɣ in EAE/MS leads to the worsening of disease [65]. Altogether, the data suggest that, depending of disease stage and site of production (systemic or local), IFN-ɣ can play a dual role in MS and EAE: 1) a protective role to reduce disease severity or 2) a pathogenic role which participates in the progression and development of disease. Thus, the modulation of IFN-ɣ at any stage of MS or EAE (before, during or after relapse) could be potentially useful to reduce the clinical symptoms during the progression of the disease.

IL-6 is anti-inflammatory cytokine that participate in the development of human diseases. IL-6 secreted by immune cells such as T cells, B cells, macrophages and microglia, but also by non-immune cells such as muscle cells, adipocytes fibroblast, endothelial cells and neurons [66, 67]. IL-6 transmits its signals using a cell surface

type-I receptor complex, which include a ligand-binding glycoprotein known as IL-6 receptor (IL-6R) and a signal-transducing component gp130. There are 2 types of IL-6R the membrane bound (mIL-6R) and the soluble (sIL-6R). The sIL-6R is produced from the mIL-6R by proteolytic cleavage of metalloproteinases gene family members such as ADAM10 and ADAM17 or by splicing of IL-6R mRNA [68]. There are 2 ways IL-6 stimulates a response in a target cell. The classical signaling occurs when IL-6 binds to the membrane bound IL-6R which induces the dimerization of gp130 and then the subsequent downstream signaling. The trans-signaling occurs when sIL-6R forms a complex with IL-6 and stimulates distant cells that expresses gp130 but not the membrane bound IL-6R (i.e. neuronal cells, endothelial cells, oligondendrocytes) [69, 70]. Once the complex IL-6-IL-r-gp130 is formed, this leads to the activation on the transcription factor JAK than in turns activates different transcription factors and signal pathways such as STAT3, MAPK, and NfkB which participates in different pathological conditions such as cancer, multiple sclerosis, rheumatoid arthritis, diabetes, Alzheimer disease (AD) [67].

Studies using the EAE model have shown that IL-6 plays a role in MS and EAE development. Some studies have showed that IL-6 knockout mice were resistant to EAE [71-73]. Samoilova et al., evaluated the role of IL-6 in the development of EAE [71]. IL-6 deficient B6.129 mice ($IL\text{-}6^{-/-}$) and control mice ($IL\text{-}6^{+/+}$) were immunized with $MOG_{38\text{-}50}$ peptide. All control mice showed signs of disease 7 days after immunization. None of the IL-6 deficient mice developed EAE. Brain and spinal cord samples were collected at 10 and 28 days after immunization and used for histologic examination. The samples form the control group showed inflammatory lesion and severe demyelination.

No inflammatory lesions nor demyelination were found in samples from IL-6 deficient mice. The results suggested that in the absence of IL-6, EAE may not be induced. Next, the authors evaluated if the lack of IL-6 affect the differentiation myelin-specific cells T cells into effect T cells. Splenocytes were collected from control and IL-6 deficient mice 10 days after immunization. Cells were cultured with MOG_{38-50} peptide to evaluate cell proliferation and cytokine production. Splenocytes from control mice showed high proliferation and production of Th1 (IL2, IFN-ɣ) and Th2 (IL-4) cytokines. Splenocytes from IL-6 deficient mice showed reduced proliferation and low production of TH1 and Th2 cytokines [71]. Eugster et al., also observed that IL-6 deficient mice were resistant to MOG-induced EAE and spinal cord tissue showed no inflammatory lesion nor demyelination [73]. In addition, the authors observed that the spinal cords from MOG-induced control mice presented high expression of the adhesion molecules VCAM-1 and ICAM-1 but basal expression on IL-6 deficient mice. The entry of myelin-specific T cells into the CNS depended on the interaction of T cell VLA-4 with the adhesion molecules VCAM1 and ICAM-1 on endothelial cells. Thus, the results suggested that the low entry of myelin-specific T cells into the CNS was in part due to the low expression of VCAM1 and ICAM-1 on IL-6 deficient mice [73].

Serada et al, evaluated the role of IL-6 on Th17 cell differentiation and EAE induction [74]. The authors immunized C57BL/6J mice with MOG35-55 peptide with CFA, followed by an intraperitoneal injection of anti-IL-6R antibody or control rat IgG the same day of immunization. The mice that received the anti-IL-6R antibody presented a reduced incidence in EAE, delayed onset of disease, and reduction in the clinical score in comparison with the control group (control rat IgG). Histological examination of brain

tissue and spinal cords collected 19 days after immunization (peak of disease) showed that mice that received the anti-IL-6R antibody reduced cellular infiltration, and no demyelination in comparison with control group. These results were consistent with the reduction in the clinical score observed previously. Mononuclear cells from spinal cords were used for flow cytometry analysis. The results showed that control mice presented CD4+ T cells, CD8+ T cells, B cells, and macrophages; conversely, these cell populations were dramatically reduced in mice that received the anti-IL-6R-antibody. In addition, intracellular cytokine staining and FoxP3+ staining of spinal cord infiltrating cells, showed high infiltration of Th17, Th1 and Foxp3+ cells (Tregs) in control mice, meanwhile in anti-IL-6R antibody mice these cells were practically absent [74]. The authors collected lymph nodes from both groups 8 days after antigen stimulation (priming stage). The lymphocytes were cultured in combination with MOG_{35-55} peptide for 72h. Flow cytometry analysis showed that Th17 and Th1 cells were suppressed in anti-IL6R antibody mice compared with control mice. In addition, CFSE analysis showed that anti-IL-6R antibody reduced cell proliferation of MOG35-55 CD4+T cells in vitro. Interestingly, even though the antibody-IL-6R antibody treated group presented a reduction in cell number, these cells presented a higher population of FoxP3+ Reg T cells (Treg cells) and a lower population of Th17 cells [74]. To investigate the effects of IL-6 blockage against MOG35-55 peptide on cytokine production, lymph nodes from the anti-IL-6R antibody treated group and control group were collected at day 8, 19, and 30 (acute period or priming, peak of disease, recovery period). Cells were incubated with MOG35-55 for 72 and supernatant were used to measure cytokines. IL-17 and IFN-ɣ were suppressed in all stages in anti-IL-6R antibody treated mice. Serum samples

collected also at day 8, 19 and 30 showed also suppression of cytokines IL1β, IL-6, IL17, and TNF-α in the s stages in comparison with control group. The results suggested that the suppression of Th17 and Th1 cells by IL-6 blockage provide a protective effect against the development of EAE [74].

Elevated values of IL-6 are present in serum, plasma, cerebrospinal fluid (CSF), and brain plaques in patients with MS [75-78]. Lanzillo et al carried out a study where 45 RRMS subjects under IFN-β-1a treatment were monitored and different immunometabolic markers were measured in order to evaluate them with disease activity and progression over time. The authors found that MS subjects with higher levels of IL-6 in serum presented a higher relapse rate [77]. Maimone et al., using an immunochemistry assay, detected the presence of elevated levels of IL-6 in acute and chronic active plaques from the brain of MS subjects. IL-6 was located mainly within resident glial cells, which were located at the sites of active demyelination and immune cell damage [78]. In an EAE study Lubina-Dabrowska et al., investigated the effect of IFN-β-1a and IFN-β-1b on cytokines and myelin proteins levels in EAE-induced Lewis rats. EAE-rats received IFN-β1a or IFN-β-1b treatment 3 times per week starting 8 days prior EAE induction and continued until 14 days after EAE induction. EAE- rats were euthanized on day 14, and brain tissue was collected for quantitative RT-PCR analysis. The results showed significant increase of IL-1β, IL-6, TNF-α, and iNOS in brain tissue from control EAE-rats which correlated with the manifestation of disease. On the other hand, EAE rats receiving either IFN-β-1a or IFN-β-1b showed a reduction in IL-1β, IL-6, TNF-α, and IFN-ɣ, decreased the activation of astrocytes, and reduced demyelination, which correlated with the reduction in the severity of disease. In addition, IFN-β-1a

reduced iNOS expression and increased IL-10. On the other hand, IFN-β-1b reduced IL-10, and did not produce any change in iNOS [79].

1.10 Anti-inflammatory cytokines in EAE and MS

Naïve CD4+ T cells in presence of IL-4 can differentiate to Th2 or in presence of TGF-β and IL-2 can differentiate into regulatory T cells (Tregs) which are considered protective against the disease due to their production of anti-inflammatory cytokines [23, 38]. Th2 cells produce IL-4, IL-5, IL-6, and IL-10. Tregs cells produce TGF-β and IL-10. Th22 and Th9 cells are the other two subcategories that have been identified in MS, however, their role in MS is not yet established [23, 38]. Bitan et al., reported the participation of Th2 cells in the amelioration of EAE [80]. In that particular study, the authors studied the role of heparanase (a protein that promotes cell adhesion and migration) in autoimmunity using the EAE model. The authors found that the intraperitoneal injections of heparanase in EAE mice reduced the clinical signs of disease in a dose depend manner, increased anti-inflammatory cytokines IL-4, IL-6, and IL-10, and reduced Th1 cells pro-inflammatory cytokines TNF-α, lFN-ɣ, and IL-1[80]. Similarly, Zhang et al, evaluated the immunosuppressive properties of glucosamine in EAE mice. The authors found that oral, intraperitoneal, or intravenous administration of glucosamine in EAE mice reduced the signs of disease, CNS inflammation, demyelination, IFN-ɣ, IL-17, and increased Th2 cell cytokines IL-5 and IL-10 [81].

IL-4 has demonstrated protection in the EAE model. One study reported that C57BL/6 IL-4-KO mice immunized with guinea-pig myelin to induce EAE presented a more severe disease. This was correlated with higher cellular infiltration in the CNS and

increased mRNA expression of IFN-ɣ and TNF-α in spinal cord tissue in comparison with wild type (WT) controls [82]. Studies by Furlan et al., showed that the localized administration of IL-4 in the CNS provided protection against EAE. The authors injected in the cisterna magna of EAE mice a non-replicative herpes simplex virus (HSV) type-1-derived vector containing the IL-4 gene. The IL-4 delivery induced the localized production of IL-4 by the CNS, leading to a delay in the onset of disease, reduction in the clinical score (severity of disease), mortality, the duration of first attack and relapse, and reduced infiltrating mononuclear cells (i.e. macrophages), and microglial activation. These factors contributed to decreased production of pro-inflammatory cytokines and reduced demyelination and axonal loss in treated animals [83, 84].

The number of PBMC secreting IFN-ɣ and IL-4 was quantified in PBMC from MS subjects during relapse (n=13), in chronic stage (n=24), and healthy controls (n=20) by immunospot assay [85]. The results showed higher numbers of PBMC secreting IFN-ɣ in samples from MS subjects experiencing a relapse. The number of PBMC secreting IL-4 was higher and in comparable quantities in both MS subjects experiencing a relapse as well as the MS group on chronic stage in comparison with the control group. Additional in-vitro experiments using PBMC from the 3 groups plus myelin basic protein (MBP) to produce the activation of PBMC showed that PBMC from the MS subjects experiencing a relapse and the MS on chronic stage presented higher production of IFN-ɣ in comparison with controls, with the highest levels of IFN-ɣ produced by cells isolated from subjects experiencing a relapse [85].

Studies investigating the roles of **IL-10 and IL-4** on EAE mice showed the protective role of these anti-inflammatory cytokines in disease development [86, 87]. IL-

10 deficient mice, but not IL-4 deficient mice, presented with accelerated EAE onset in comparison with WT mice. This acceleration in disease onset was associated with a reduction in IL-4 and increase in IFN-ɣ after MOG immunization [86]. Interestingly, spontaneous recovery was present in WT and IL-4 deficient mice but recovery was not present in IL-10 deficient mice [86]. Additional studies showed that the activation of T cells from IL-10-KO mice with encephalitogenic peptide presented a stronger antigen-specific proliferation, produced higher levels of IFN-ɣ and TNF-α, and were able to induce severe EAE when they are transferred to WT mice [87]. Interestingly, the over-expression of IL-4 in transgenic mice led to a similar EAE disease course that WT mice, but the over expression of IL-10 in transgenic mice led to resistance to EAE development [87]. Altogether, these data indicate that IL-10 plays a role in progression and recovery of EAE.

Studies in MS subjects also showed increments in IL-10 levels during T cell activation. CD4+ and CD8+ T cells isolated from stable RRMS subjects and healthy controls were activated with CD3 monoclonal antibody (mAb) for 48h, then the supernatants were collected to measure cytokines. The results showed an increase in IFN-ɣ produced by both CD4+ and CD8+ T cells and increased production of IL-10 by CD4+ T cells [88]. Quantification of serum IFN-ɣ, TNF-α, IL-4, and IL-10 from MS subjects during relapse (n=42) showed higher levels of these cytokines in comparison with healthy controls (n=12). These data indicate the simultaneous activation of elevated levels of Th1 and Th2 cells during the acute stages of the disease [89]. In another study, the authors quantified serum and CFS levels of TNF-α, IL-10, and nitric oxide (NO) in 17 MS subjects during active relapse [90]. The results of serum and CSF

samples showed higher levels if TNF-α, IL-10, and NO in comparison with healthy subjects. Interestingly, 2 subjects showed higher levels of NO in CSF than in serum which indicates that a high and active production of NO in CNS can be present simultaneously as in serum. The results also showed that Th1 and Th2 cell activation is present simultaneously during an active relapse [90].

TGF-β is an anti-inflammatory cytokine that plays an important role in cell development, differentiation and immune regulation. There are 3 different isoforms of TGF-β: TGF-β1, TGF-β2 and TGF-β3. The presence of TGF-β1 in the immune system is abundant but the present of TGF-β2 and TGF-β3 is minimal [91]. Kehrl et al., reported one of the main roles TGF-β in the regulation of T cells is inhibition of IL-2 production and subsequently T cell proliferation [92]. The addition TGF-β to cultures of human T lymphocytes stimulated with Concanavalin A and IL-2 inhibited DNA synthesis between 60-80%. Some of the events related the mechanism of action of TGF-β included down regulation of IL-2 and transferrin receptors, and a five to six-fold increase in the number of TGF-β receptors per cell after cellular activation. The authors observed that activated T cells produced TGF-β mRNA and that TGF-β activity was present in supernatants suggesting that after activation, T cell themselves are a source of TGF-β. In additional experiments, CD4+ and CD8+ T cells were isolated and activated with phytohemagglutinin (PHA). TGF-β activity in supernatants showed to be increased 10-50-fold. The results suggested that TGF-β may be an antigen-nonspecific regulator of human T cell proliferation and it may participate in the modulation of T cell subtypes [92]. Bright et al., reported the mechanism by which TGF-β1 inhibits Th1 cell activation [93]. The authors reported that the activation of T cells with IL-12 led to tyrosine

phosphorylation and activation of the kinases Jak-2 and Tyk-2 as well the activation of transcription factors STAT3 and STAT4. The addition of TGF-β1 inhibited both Jak-2 and Tyk-2 kinases, and subsequently the phosphorylation of STAT 3 and STAT4. This inhibition produced a reduction in T cell proliferation and IFN-ɣ production and increase in apoptosis [93].

Gorelik et al., reported that TGF-β is necessary for immune regulation and its absence leads to the development of an autoimmune response [94]. In order to study the effects of TGF-β on the regulation of T lymphocytes the authors created transgenic mice expressing dominant-negative TGF-β receptor which blocked TGF-β signaling but allowed the expression of CD4+ and CD8+ T cells but not B cells [94]. The transgenic mice lived without any detectable problems during 3-4 months of age. After that time they developed signs of sickness, wasting and diarrhea. Histological examination showed cellular infiltration in several organs. In addition, circulating autoimmune antibodies were detected, and T cells were able to differentiate spontaneously in Th1 and Th2 cells subsets. The data suggested that the presence of TGF-β signaling is required for the regulation of T cells and immune response [94].

Several studies evaluated the role of TGFβ1 in the EAE model [95-98]. Kuruvilla et al, evaluated the anti-inflammatory role of TGF-β1 on EAE [95]. The authors reported that a daily intraperitoneal injection of TGF-β1 on SJL/j mice for 2 weeks starting the day of EAE induction delayed the onset of symptoms for 2-3 days in comparison with controls (EAE mice with no TGF-β treatment). TGF-β treatment after the first attack of EAE reduced the severity of the second episode. In an additional experiment, TGF-β was administrated daily starting 35 days after the beginning of their first episode and

continuing for at least 4 weeks. TGF-β treatment prevented the development of spontaneous relapses [95].

In another study, Racke et al., evaluated the immunosuppressive effect of TGF-β1 on chronic EAE [96] . In in-vitro experiments, TGF-β1 inhibited the activation and proliferation of myelin-basic protein specific lymph nodes cells. EAE induction was reduced when these cells were transferred to naive mice. In an additional experiment, EAE mice received TGF-β1 resulting in a reduction in the severity of the disease (clinical score), reduction of cellular infiltration in CNS, reduction in the expression of cell adhesion surface molecule lymphocyte function-associated Ag-1 (LFA-1), and reduction of MHC-II on antigen presenting cells in comparison with EAE mice without TGF-β1 treatment [96].

In MS and EAE, myelin specific effector Th1 cells participate in the inflammation in the CNS. Huss et al., studied the effect of TGF-β on effector Th1 cells using the EAE model. [99]. Splenocytes from myelin-specific T cell receptor transgenic (TCR-Tg) mice that recognize myelin basic protein peptide Ac1-11 (MBP Ac1-11) were differentiated with Ag alone or in combination with IL-12 and TGF-β. Cells in presence of MBP alone or in combination with IL-12 produced a robust Th1 response characterized by the proliferation of IFN-γ^+ cells and absence of IL-17 cells. The addition of TGF-β reduced the number of cell producing IFN-γ and the total amount of IFN-γ produced [99]. Next, the authors evaluated the role of TGF-β on the encephalitogenic capacity of myelin-specific T cells. TCR-Tg splenocytes were differentiated in vitro with Ag alone or in combination with IL-12 and TGF-β. After 72h of stimulation the cells were transferred to transgenic B10.PL mice and EAE development was monitored for 20 days. Mice that

received T cells stimulated with Ag alone or in combination with IL-12 developed a severe EAE. Mice that received T cells stimulated with Ag+TGF-β prevented the development of EAE, suggesting that the presence of TGF-β suppressed the encephalitogenicity capacity of the cells. The results from the in-vitro and in-vivo experiments suggested the presence of TGF-β during the primary differentiation on naïve TCR-Tg- T cells suppressed cytokine production, proliferation, and encephalitogenicity [99]. Next, the authors compared the effects of TGF-β on effector cells versus naïve cells. The authors differentiated TCR-Tg splenocytes in-vitro with MBP and IL-12 to create effector Th1 cells. These cells produced high amounts of IFN-ɣ and no IL-17. After 72h of stimulation, cells were rested alone for 72-96h and then re-stimulated with Ag alone or in combination with TGF-β or anti-TGF-β antibody. Reactivated Th1 cells in presence of TGF-β showed increased proliferation and increased IFN-ɣ production. Meanwhile the presence of anti-TGF-β antibody reduced in cell proliferation. These results indicated that TGF-β has opposite effects on the activation and proliferation of naïve CD4 T cells vs. effector Th1 T cells. The results showed that the presence of TGF-β during the secondary simulation increased proliferation and increased IFN-ɣ production, thus the authors hypothesized that the transference of these reactivated Th1 cell would produce a higher encephalitogenic effect in naïve recipient mice. To test their hypothesis the authors transferred effector Th1 cells restimulated with Ag alone or in combination with TGF-β or anti-TGF-β antibody into naïve B10.PL mice. Interestingly, effector Th1 cells restimulated with Ag + TGF-B reduced the capacity to cause CNS inflammation and demyelination. On the other hand, Th1 cells restimulated with Ag in combination with anti-TGF-β antibody

increased disease severity. In vitro experiments showed that Th1 cells reactivated with Ag + TGF-β produced IL-10 , reducing the encephalitogenic capacity of these cells [99]. The results from these studies suggested that the immunosuppressive role of TGF-β can be used in the treatment of MS.

1.11 Nitric oxide (NO)

Nitric oxide is a multifunctional gaseous molecule that participates in multiple cellular processes, including the immune response, signal transduction, and regulation of mitochondrial function. NO is produced by the oxidation of L-arginine to L-citruline by the nitric oxide synthase (NOS) family of enzymes [100]. Three NOS isoforms have been identified: neuronal (nNOS), endothelial (eNOS), and induced (iNOS). nNOS is located in central and peripheral neurons, the cerebellum, cerebral cortex, and hypothalamus. NO produced by nNOS participates in the communication between neurons. eNOS is expressed in endothelial tissue of blood vessels, where the NO produced participates in vasodilatation and muscle relaxation. nNOS and eNOS produce NO constitutively in a Ca^{2+} dependent manner; therefore, antagonists of Ca^{2+} reduce NO production [101].

iNOS is expressed in immune cells (i.e. macrophages, neutrophils), where it is central in the oxidative burst mediated by macrophages and neutrophils during the immune response against pathogens. NO production in these cells is Ca^{2+}-independent [101]. The levels of NO produced by nNOS or eNOS are between 0.2-2 nM [102]. Normal levels of NO produced by iNOS are 2-20 nM. When iNOS is stimulated (i.e. inflammation) NO levels are 20-200 nM [103]. In macrophages, gene expression of

iNOS is regulated by the CD14 receptor and toll like-receptors (i.e. TLR-4). Pathogens or lipopolysaccharides (LPS) bind to TLR-4 and CD14 receptor leading to the phosphorylation and activation of the IkB kinase (IKK) to phosphorylate the IkB-NFkB complex. The IkB complex is degraded in the cytosol and then NFkB can travel to the nucleus to induce the expression of genes, including iNOS. Similarly, interferon gamma (IFN-ɣ) binds to the IFN-ɣ receptor in the cell membrane, leading to the phosphorylation of the transcription factor STAT1, which travels to the nucleus to activate iNOS expression [104].

1.12 Role of NO on T cell differentiation and immunity.

NO produced by myeloid cells (i.e. macrophages, neutrophils, and monocytes) through the action of iNOS mediates the destruction of pathogens [105-109]. In addition, NO is an important regulator of the immune response. In particular, evidence supports that NO as a critical regulator of autoimmunity. For instance, different studies demonstrated that NO produced by iNOS participates as a negative regulator of the Th1 cell response, thus protecting against autoimmune attack [110-115]. Studies showed that iNOS deficient mice ($iNOS^{-/-}$) develop an enhanced Th1 cell response after infection and antigenic stimulation leading to an increase in the production of IFN-ɣ and a reduction in IL-4 in comparison with unaltered iNOS mice (WT mice) [113-115]. iNOS-deficient mice were susceptible to *Leishmania major* infection, developing significant, strong Th1 type immune response characterized by higher production of IFN-ɣ and reduction in IL-4 in comparison with WT mice [113]. In an animal model of bacterial septic arthritis, iNOS deficient mice infected with *Staphylococcus aureus* presented with

higher incidence of disease with faster development, higher septicemia, more severe arthritis, and higher mortality in comparison with infected WT mice [114]. iNOS-deficient mice expressed higher levels of TNF-α, IFN-ɣ, and reduction in IL-4 in comparison with infected WT mice, correlating with more robust Th1 cell responses. Altogether, the data suggested that NO plays a role in synovial defense against *Staphylococcus aureus* infection [114]. Infection of iNOS deficient mice with herpes simplex virus (HSV-1) showed a delay in the clearance of the disease, as well as increase in the frequency of virus reactivation in comparison with WT mice [115]. iNOS deficient mice showed an enhanced Th1 immune response in the spleens characterized by higher concentrations of IL-12 than WT mice [115].

Previously it was established that the immunization of animals with complete Freund's adjuvant (CFA) produced resistance to subsequent attempts to induce autoimmune diseases meanwhile animals immunized with incomplete Freund's adjuvant (IFA) remain susceptible [116-120]. Studies by Kahn et al., evaluated if the immunoprotective effect of CFA before EAE induction required functional iNOS [111]. The response of C57BL/6J mice to a single subcutaneous injection of CFA was compared to naïve mice not challenged with CFA. Lymph nodes and spleen were isolated to evaluate mRNA expression by qPCR. In CFA immunized mice, iNOS expression was elevated by 28 days after immunization and remained elevated for 14 months. Serum samples collected one week after CFA challenge demonstrated higher levels of nitrite (NO_2) levels by Griess reaction compared to [111]. Next, the authors evaluated the requirement of IFN-ɣ and TNF-α for iNOS induction by CFA. The authors immunized C57BL/6, C57BL/6IFN-ɣ$^{-/-}$, and C57BL/6TNFR1$^{-/-}$ with CFA then lymph

nodes and spleens were isolated 28 days after immunization to evaluated iNOS expression by qPCR. The results showed that C57BL/6IFN-ɣ$^{-/-}$, and C57BL/6TNFR1$^{-/-}$ presented lower levels of iNOS in comparison with naïve C57BL/6 mice [111]. To investigate whether iNOS induced by CFA induction would reduce EAE severity in mice, C57BL/6 mice received intraperitoneal injection of CFA 28 days before MOG-EAE induction. Mice without CFA injection before MOG-EAE induction were used as control group. Mice that received CFA pre-immunization presented with reduced disease severity (clinical score) in comparison with control group. Furthermore, C57BL/6NOS$^{-/-}$ mice pre-immunized with CFA showed a lower clinical score in comparison with the no pre-immunized CFA C57BL/6NOS$^{-/-}$ mice. However, the clinical score of both groups was higher than the pre immunized CFA WT C57BL/6 mice group. These results showed that the pre-immunization with CFA on iNOS$^{-/-}$ mice does not provide the same level of protection than in the C57BL/6 mice [111]. In additional experiments, the authors observed that WT C57BL/6 mice pre-immunized with CFA presented elevated levels of IgG and reduction in reduction in cell infiltration in spinal cords in comparison with the pre0mmunized CFA C57BL/6NOS$^{-/-}$ mice. All together, the results support the role of NO produced by iNOS in the modulation of immune response in CFA-preimmunized mice [111].

1.13 Regulatory mechanism of NO-iNOS in immune cells.

Th1 cells play a role in the development of inflammatory diseases, including MS and EAE. The IFN-ɣ produced by Th1 cells activates macrophages to induce the expression of iNOS, leading to production of high amounts of NO. Studies showed that

high amounts of NO produced by iNOS can inhibit the expansion of Th1 cells by negative feedback mechanism whereby activated macrophages inhibit IL-12, which is necessary for Th1 differentiation [121]. Fenyk-Melody et al. showed that iNOS-deficient mice presented with more severe disease compared to WT mice in the EAE model, suggesting that the NO produced by iNOS in the WT mice-EAE immunized prevented CD4+ T cells from differentiating into pathogenic Th1 cells [122, 123]. Therefore, the modulation of NO to control the immune response may be an approach to ameliorate inflammatory conditions such as MS and EAE.

Niedbala et al., carried out experiments using CD4+ and CD8+ T cells isolated from the spleen and lymph nodes from BALB/c mice to determine the effects of low and high concentrations of NO on Th1 differentiation [112]. Graded concentrations of the NO donor S-nitroacetyl-penicillamine (SNAP) were used on CD4+ T cells cultures with BALB/c spleen cells as antigen presenting cells (APC), ovalbumin peptide, plus IL-12 (to induce Th1 line) or IL-4 (to induce Th2 line). High concentrations (500μM) of SNAP inhibited the production of IFN-ɣ by the Th1 cell line, whereas low concentrations (10μM) increased the synthesis of IFN-ɣ by Th1 cell line. In addition, low concentrations (10μM) of SNAP synergistically increased the production of IFN-ɣ induced by IL-12. These results showed that NO play a role in the modulation of the immune response [112].

In further studies, Niedbala et al. evaluated the effect of low concentrations of NO in human CD4+ T cells purified from human cord blood. Cells were induced to a Th1 cell phenotype using phytohemagglutinin (PHA), IL-12, and anti-IL-4 antibody [124]. Th1 cell differentiation was enhanced with the presence of low concentrations (5mM) of the NO

donor, 2,2'-(hydroxynitrosohydrazino)bis-ethamine (NOC-18 known also as DETA-NO), and suppressed by higher concentrations (>40mM) of NOC-18 [124]. The data obtained from the human and mouse studies correlated. However, human CD4+ T cells were more sensitive to the graded (low) concentrations of NO than mouse T cells.

The next step was to investigate the mechanism of how different concentrations of NO induced Th1 cell differentiation [124]. CD4+ T cells purified from spleen and lymph nodes from BALB/c mice were cultured with a combination of anti-CD3 antibodies, IL-12 and anti-IL-4 antibody (to induce Th1 cell differentiation). Graded concentrations of the NO donor NOC-18 (5, 10, 20, 100μM) were included to evaluate if NO activates soluble guanylyl cyclase (sGC), leading to increase production of cyclic guanosine monophosphate (cGMP). The results showed an increase of intracellular cGMP in CD4+ T cells under the Th1 differentiation conditions at low doses of NOC-18 (5 and 10μM). The levels of cGMP were reduced at higher concentrations of NOC-18 (100μM). The levels of IFN-ɣ correlated with the low levels of NOC-18 and higher activity of cGMP [124]. Next, the authors tested the 1-H-oxodiazolo-(1,2,4)-(4,3-a) guinoxaline-1-one (ODQ), a competitive inhibitor of the activation of cGMP. CD4+ T cells and CD8+ T cells cultured with ovalbumin (OVA), plus IL-12, with anti-IL4 antibody (TH1 cell differentiation conditions), or IL-4 plus anti-IL12 and anti-IFN-ɣ antibodies (Th2 cell differentiation conditions), NOC-18, and ODQ (10-40μM). ODQ (at 20μM) suppressed Th1 cell differentiation but had no effect on Th2 cell differentiation at any dose. In additional experiments, ODQ also suppressed Th1 cell differentiation from CD4+ T cells in the absence of antigen presenting cells (APC). The results suggested

that at NO at low concentrations participates in Th1 differentiation by cGMP activation and this effect is exerted directly on Th1 cells and not via APC [124].

Next the authors evaluated the effect of low concentrations of NO on the selective cell differentiation of CD4+ T cells and CD8+ T cells [124]. CD4+ T cells and CD8+ T cells were cultured under Th1 and Th2 cell differentiation conditions, NOC-18 (10μM), and activated with anti-CD3 antibodies. Cells were harvested at 16h and mRNA was used to measure the levels of IL-12Rb2, IL-18Ra, and IL-4R by rtPCR. IL-18Ra (in Th1 cells) and IL-4r (in Th2 cells) did not show change compared to controls. On the other hand, Th1 cells showed increase levels of IL-12Rb2 suggesting that low levels of NO selectively and preferentially enhance the expression of IL-12Rb2 during Th1 cell differentiation. All the data put together indicates that at low concentrations of NO, NO activates sGC, leading to up-regulation of the cyclic guanosine monophosphate (cGMP), which induces IL-12 receptor β2 in T cells, producing IL-12 and TCR engagement finally leading to Th1 differentiation [124].

Similarly, Bingisser et al., studied the role of NO produced by macrophages in the modulation of the T cell inflammatory response [125]. Th1 cell activation involves IL-2R ɣ-chain, the Janus kinase 3(Jak3) and the signal transducer and activator of transcription 5 (STAT5). For T cell activation, STAT5 has to be activated (phosphorylated) by Jak3. Once STAT5 is activated, it travels to the cell nucleus and functions as transcription factor to induce cell activation [125]. Activated T cells are unable of proliferate in the presence of NO produced by alveolar macrophages despite the presence of IL-2R and secretion of IL-2. Supporting *in vitro* experiments showed similar results where T cell proliferation was suppressed by S-nitroso-N-

acetylpenicillamine (NO donor), whereas T cell proliferation occurred in presence of NG-methyl-L-arginine (NO synthase inhibitor). Immunoprecipitation assays with T cell lysates showed a significant reduction of tyrosine phosphorylation of Jak3 and STAT5 in the presence of NO. This NO-mediated T cell suppression was reversible by guanylate cyclase inhibitors methylene blue and LY-83583. Additional *in vitro* experiments showed that NO-mediated T cell suppression was reproduced using a cell membrane analogue to cyclic GMO, suggesting that guanylcyclase activation is a critical step in the inhibition of T cell activation by NO [125]. Similarly, independent studies by Mazzoni and Sato groups found that NO produced by myeloid suppressor cells (MSC) participated in the inhibition of T cells [126, 127]. The NO produced by MSC suppressed the activity (phosphorylation) of Jak1, Jak3, STAT5, extracellular signal–regulated kinase (Erk) and Akt [126, 127].

1.14 Axonal degeneration in MS

The formation of lesions or plaques in the CNS is the pathologic hallmark of MS. The development of these plaques involves the breakdown of the BBB, multifocal inflammation, demyelination, loss of oligondendrocytes, reactive gliosis and axonal degeneration. Even though all these events are involved in the development of MS, the progressive axonal loss is the main cause of neurological disability in MS [1]. Some of the changes present in MS lesions which indicate acute damage in axons include: increased distribution of Na^+ channels along the axons, axonal transport alterations i.e., accumulation of amyloid precursor protein (APP), axonal transections, axonal loss and axonal degeneration [1, 128-131].

1.15 Increased distribution of Na^+ channels along the axons

The destruction of myelin is a pathological hallmark present in the progression of MS. Under normal or healthy conditions, neurons contain axons which are covered (insulated) by myelin sheaths. The myelin sheaths are a lipid-rich extension of plasma membrane produced by Schwann cells in the peripheral nervous system (PNS), and by oligodendrocytes in the CNS. The myelin sheath along the length of the axon is interrupted by regions known as nodes of Ranvier which serve to facilitate the rapid conduction of nerve impulses or action potential (messages) along the axon from one neuron to another [132]. The saltatory conduction of action potentials (jumps) from one node of Ranvier to another is carried out due to the proper insulation or covering provided by the myelin sheaths as well as the high concentration of voltage-gated Na^+ channels at the nodes of Ranvier [133]. In normal conditions, the Na^+/K^+ ATPase is in charge of pumping out the excess of Na^+. However, when demyelination is present, there is an increase in the expression and distribution of the Na^+ channels along the axon in order to keep the salutatory conduction of action potentials [133]. This increase in Na^+ produces an increase in the activity of the Na^+/K^+ ATPase and ATP consumption. Therefore, the cell increases the number of mitochondria, and activates glycolysis in order to compensate for the increase in energy demands. When the ATP demands exceed the production of ATP by the mitochondria, the activity of Na^+/K^+ ATPase is reduced, leading to intracellular accumulation of Na^+ and membrane depolarization [134]. A high concentration of Na^+ will lead to reverse the Na^+/Ca^{2+} charger, causing to the transport of Ca^{2+} to inside the cell. Intracellular accumulation of Ca^{2+} induces mitochondrial dysfunction and cell death [134]. The accumulation of Ca^{2+} in the

axoplasm leads to activation of Ca^{2+}-dependent enzymes (i.e. calpain, phospholipases, protein kinase C, NO-synthase) to produce axon damage [135]. The high concentration of Ca^{2+} in the axoplasm produces the influx of the Ca^{2+} into the mitochondria [136]. The increase of Ca^{2+} in the mitochondria induces the opening of the permeability transition pore (PTP) which will induce mitochondrial dysfunction by the swelling of the matrix, rupture of the outer mitochondrial membrane, releasing cytochrome C and activating the apoptotic pathway to produce cell death [136].

1.16 Axonal transport alterations

Demyelination can be present during active or inactive inflammation. Studies on active cerebral MS lesions showed a positive correlation between axonal damage and the degree of inflammation in active MS lesions, as determined by quantification of proteins that are transported in the axons. Accumulation of such proteins allows for the evaluation of disturbances of axonal transport or axonal transection. One common protein used in this analysis is the amyloid precursor protein (APP). Immunochemistry using an antibody recognizing APP showed that APP accumulated in the axons due to disruption of axonal transport and presence of axonal transections. Investigators noted increased accumulation of APP in damaged axons within acute multiple sclerosis lesions in advanced stage of disease and at the borders of less acute lesions [128, 130].

1.17 Axonal transection

Magnetic Resonance Spectrophotometry (MRS) and Magnetic Resonance Imaging (MRI) studies demonstrate that axonal degeneration is present in absence of active inflammation since early stages of MS. This early axonal loss contributes to the permanent disability produced in chronic stages of the disease [137]. In one study, Trapp, B.D., et al., evaluated changes in axon morphology at different stages of MS using brain tissue samples obtained from MS subjects. The authors collected 14 active lesions, 33 chronic active lesions, and samples from the white matter without presence of lesions. The sections were evaluated by immunochemistry and confocal microscopy to evaluate the degree of demyelination, inflammation and pathologic changes in axons [131]. All 47 lesions presented axonal transection characterized by the presence of terminal axons ovoids. The number of transected axons was positively correlated with the degree of inflammation in the lesions. The quantification of transected axons in active lesions showed the presence of 11,236 transected axons/mm^3 on average, the border of chronic lesions presented 3,138 transected axons/mm^3, the center of chronic active lesion presented 875 transected axons/mm^3, and normal white matter samples presented less than 1 transected axons/mm^3 [131]. The results indicate that axonal loss is present in active lesions since the early stages of the disease.

1.18 Axonal loss and axonal degeneration

The degeneration of axons in MS presents rapid Wallerian degeneration which is distal to the site of transfection. On the other hand, the myelin present in CNS can remain for a longer period of time after proximal fiber transfection. The remaining myelin

sheaths will be present as empty tubes or they will degenerate to ovoids [130]. Interestingly, axonal damage has been observed in MS normal appearing white matter (NAWM), even though active lesions were not present on MRI images or histological examination. For example, it was reported that NAWM samples from the lateral column cross-sectional area from MS subjects in an early stage of disease showed a reduction in total nerve fiber density from 19 to 42% [138]. In another study, axonal loss and axonal degeneration was quantified in cervical spinal cords samples obtained from SPMS subjects. Samples of plaques with presence of demyelination, NAWM, and control samples were used in the immunostaining analysis of the neurofilaments. The results showed a reduction in axonal density (number of axons/mm^2) in both demyelinated plaques (61% of reduction) and NAWM samples (57% of reduction). The results support that axon degeneration is present in apparently uninjured samples (NAWM) but its progression leads to the irreversible disability [139]. These results were corroborated in subsequent studies, were axonal loss was quantified in 10 chronic inactive samples obtained from MS subjects with chronic disease (12 to 39 years). The authors found that the samples showed an average of 68% axonal loss and a reduction of 58% in axonal density [140].

1.19 Additional mechanism involved in axonal degeneration

Interestingly, the protein, cyclophilin D (CyPD), which is a structural protein of the PTP, is an important element in the formation and regulation of the opening of PTP [142, 143]. Under normal conditions, PTP allows the transport of Ca^{2+} from the mitochondria to the cytoplasm and vice versa. Mice deficient in CyPD due to targeted

disruption of the CyPD gene (CyPD-KO mice) were still capable of the formation of the PTP pore, but the mitochondria maintain a double concentration of Ca^{2+} in the cytoplasm [142]. This indicates that more Ca^{2+} is needed to open the PTP, suggesting that CyPD participates as a regulator of the PTP-opening. Interestingly, mitochondria obtained from liver, heart, and brain of CyPD-KO mice were resistant to Ca^{2+} overload, mitochondrial swelling, permeability transition, and whole cells were resistant to cell death induced by oxidative stress [142]. In another study, EAE was induced in CyPD-KO mice (CyPD-KO-EAE mice). Mice presented with the typical clinical signs of EAE model, However, CyPD-KO-EAE mice presented a less severe disease. The spinal cords obtained from the CyPD-KO-EAE mice showed similar inflammation but a reduction of axonal loss in comparison with EAE mice [143]. In addition, induced mice were resistant to nitrosative stress produced by reactive oxygen species (ROS) and reactive nitrogen species (RNS) [143]. The results suggest that the lack of CyPD helped to maintain proper mitochondrial function fundamental to reduce axonal destruction.

Some studies have used different animal models to study axon damage. For instance, in myelin associated glycoprotein (MAG)-deficient mice, the lack of MAG produces a progressive reduction in the caliber of the axon, neurofilament spacing, phosphorylation in the neurofilaments, and Wallerian degeneration at 90 days of age [144]. Another model is the cyclic nucleotide phosphodiesterase (CNP)-null mice. In the oligodendrocytes, CNP is necessary for axonal survival but not for myelin assembly. Therefore, CNP-null mice present with axonal swelling, neurodegeneration, hydrocephaly, and premature death [145]. Another model is the proteolipid protein (PLP)-null mice model. In the PLP-null mice, the oligodendrocytes are able to produce

compacted myelin sheaths on the axons. However, the stability of the myelin sheaths is lost, the lack of stabilization leads to myelin break down, demyelination, and oligodendrocytes death. Therefore, one of the functions of PLP is to hold together the myelin sheaths on the axons to maintain its integrity independently of its roles in the production of myelin [146]. The results of the studies carried out on the MAG-, CNP-, and PLP-knock out mouse models suggest that the axon degeneration is produced not due to the lack of myelin production but by the loss of trophic support necessary for axon survival [144-147].

1.20 Compensatory mechanisms during axonal loss and axonal degeneration

Studies in the EAE model further investigated the effect of chronic demyelination, axonal damage, and axonal loss in disease progression. Wujek, J.R., et al., showed that the clinical score assigned to each mouse (i.e. disease severity) correlated with axonal loss in the inflammatory lesions present in the spinal cords (SC) of affected mice, from the beginning through the last stages of the disease [148]. For example, EAE mice in chronic stages of the disease with a clinical score of 4 (permanent limb paralysis) presented a total axonal loss of 43% and 60% in lumbar and cervical SCs respectively. On the other hand, EAE mice with a clinical score of zero (no signs present) presented an axonal loss on average of 30% in cervical SCs and 15% in lumbar SCs, indicating that even in the absence of clinical signs, pathologic consequences of the disease process were evident [148]. The results also suggested that adaptive mechanisms exist to delay the presentation of clinical signs and permanent disability, but once the

threshold is exceeded the disease will worsen and neurological disability will be present [148].

Axonal degeneration is present in MS beginning with the onset of the disease. It has been proposed mitochondrial dysfunction participates in the degeneration of axons and axonal dysfunction at the onset of MS. N-acetyl aspartate (NAA) is a metabolite produced from aspartate and acetyl CoA in the mitochondria of neurons, dendrites, and axons. MRS and MRI studies demonstrated reduced levels of NAA in brain of RRMS and SPMS subjects which correlated with the progression of disability, functional impairment, axonal damage, and axonal loss [149-152]. Therefore, NAA reduction may be a possible marker to detect mitochondrial dysfunction and axonal damage. Reversible acute inflammatory events are characteristic of RR-MS. The amelioration of the inflammatory attacks is established by the resolution of the clinical symptoms. Mechanisms involved in the resolution of the clinical symptoms include remyelination, compensatory cortical adaptation, and redistribution of the Na^+ channels along the axon [153-155]. Reddy et al., evaluated if cortical adaptive responses contributed to the maintenance of normal motor function in MS subjects [155]. The authors used MRSI and functional MRI (fMRI) on MS subjects with unpaired hand function. The results showed that simple hand movements increased until 5 fold the activity of the ipsilateral sensorimotor cortex in comparison with healthy controls. The increase correlated with a reduction in the levels of NAA in brain [155]. This study suggests that cortical adaptive responses are activated to compensate for the brain damage and clinical disability noted in MS. However, once the damage and axonal loss exceed the compensatory

mechanisms in CNS, the worsening of the clinical symptoms and irreversible disability result, leading to the progression from RRMS to SPMS [147, 155] .

1.21 Mitochondrial function

The mitochondrion is the cellular organelle responsible for the production of ATP via the process of oxidative phosphorylation. The process begins in the cytosol, where glucose is converted to pyruvate. Pyruvate is transported to the mitochondrion to be metabolized to acetyl coenzyme A (CoA), which is used in the tricarboxylic acid cycle to produce nicotine adenine dinucleotide (NADH) and flavin adenine dinucleotide ($FADH_2$). NADH and $FADH_2$ are used in the mitochondrial respiratory chain to produce ATP [156]. The respiratory chain is constituted of 5 complexes: NADH dehydrogenase (complex I), succinate dehydrogenase (complex II), cytochrome c reductase (complex III), cytochrome c oxidase (CCO, complex IV), and ATP synthase (complex V). NADH and $FADH_2$ are oxidized by complex I and II respectively. The electrons released are transported by 2 electron transporters: coenzyme Q10 transports electrons from complex I and II to complex III, and cytochrome c transports electrons from complex III to complex IV (CCO) [156]. During the transport of electrons, energy is released and is used to transport protons (H^+) from the mitochondrial matrix to the mitochondrial intermembrane space (IMS), creating a proton gradient throughout the mitochondrial inner membrane (MIM). The proton gradient force is used by complex V to produce ATP. The ATP produced is then transported by the adenine nucleotide translocator to the cytosol for use in cellular reactions [156].

Cytochrome c oxidase (CCO or complex IV) is a key regulatory component in the respiratory chain. CCO contains two oxygen binding sites: the iron heme a_3 (reduced site) and the copper (Cu_B, oxidized site). Under normoxic conditions (20-130 mM O_2), the oxygen binds to these two binding sites. CCO catalyzes the reduction of oxygen to produce water [157-159]. During this reaction, there is transfer of electrons to ATP synthase, with the subsequent production of ATP. The leakage of electrons leads to the production of different reactive oxygen species (ROS) [i.e. superoxide (O_2^-), peroxide (H_2O_2), and hydroxyl (OH^-)]. Nitric oxide (NO) also plays a role as regulator of cellular respiration. Under either hypoxic conditions or high concentration of NO, NO competes with oxygen and binds reversely to the iron heme a_3 (CCO-NO). This leads to the inhibition of CCO and the reduction of ATP production [160-162].

In addition, NO at high concentrations reacts with oxygen to produce reactive nitrogen species (RNS) such as nitrite (NO_2^-), dinitro trioxide (N_2O_3), peroxynitrite ($ONOO^-$), and S-nitrosothiols (RSH). NO also participates in the production of ROS such as superoxide (O_2^-) and peroxide (H_2O_2) [164-166]. The excess of NO and RNS inhibits the activity of complexes I, II, IV and V of the respiratory chain leading to mitochondria dysfunction and reduction in ATP production [167-169].

1.22 NO and glutamate excitotoxicity in MS

NO and glutamate are involved in MS development and progression and the common pathway that they share is the damage to mitochondria (mitochondrial dysfunction. Studies of mechanisms of neurodegeneration demonstrate the role for high levels of NO, ROS and RNS in the death of neurons. Microglia are the resident

macrophages of the CNS and a common source of ROS/RNS. Microglial activation is frequent in CNS pathologies, including MS, leading to the elevated production of NO via iNOS. *In vitro* experiments showed that the activation of microglia and the high levels of NO produced lead to the inhibition of cellular respiration (depletion of ATP) in co-cultured neurons, leading to the release of glutamate from the neurons and contributing to cell death by excitotoxicity [170-173].

Glutamate is an excitatory neurotransmitter which binds to the α-amino-3-hydroxy-5-methyl-4-isozolepropionic acid (AMPA) and N-methyl-D- aspartate (NMDA) receptors located on the post-synaptic membrane of neurons The binding of glutamate to the AMPS and NMDA produces the transmission of stimulus and also allows the opening of ion channels in order for Na^+, K^+, and Ca^{2+} to transmit the impulse [173]. Excitotoxicity results when excessive glutamate is released, reaching high synaptic concentrations. The overstimulation of NMDA and AMPA receptors leads to excessive stimulation of ion channels and cell death.

In MS, the presence of high concentrations of glutamate produced by microglia, produce a deregulation in the ion gradients. At high concentrations of glutamate, Ca^{2+} can enter to the mitochondrion, producing the opening of the permeability transition pore (PTP) and release of CCO into the cytosol producing mitochondrial dysfunction [174]. The accumulation of Ca^{2+} in the mitochondria produces an increase in the activity of the reversal ATP synthase in order to compensate the entrance of Ca^{2+} leading to a depletion in ATP. The depletion of ATP will lead to a deregulation of Ca^{2+} via inhibition of the plasma Ca^{2+}-ATPase and inhibiting the activity of the enzymes involved in the glycolysis pathway [175]. High levels of Ca^{2+} due to activation of NMDA receptors leads

to the activation of the protease calpain I, located in the cytoplasm of neurons. Calpain I activation induces the degradation of cytoskeleton, neurofilaments, and ion channels, leading to cell death. Moreover, it has been found that Calpain I induces the cleavage of the apoptosis-inducing factor (AIF) and its translocation from the mitochondria to the nucleus inducing cellular death [176]. During the translocation of AIF to the nucleus, there is also a translocation of the proapoptotic factor BH3-interacting domain death agonist (Bid) to the mitochondria. Bid is a member of the bcl-2 family, the accumulation of Bid in the mitochondria leads to loss of the integrity of the mitochondrial membrane and therefore its destruction [177].

1.23 Nitrosative stress and mitochondrial dysfunction in MS and EAE

MS studies demonstrated that mitochondrial dysfunction is produced in part by high concentrations of ROS and RNS, leading to the generation of nitrosative stress [147, 178-184]. Using immunohistochemistry assays, Lu et al. observed an increase in the oxidative damage of mitochondrial DNA (mtDNA) in cells from chronic active plaques obtained from MS subjects. The oxidative damage in mtDNA correlated with reduced activity of complex I (NADH dehydrogenase) of the respiratory chain and a possible compensatory increase in the activity of complex IV (CCO) [178]. The results suggested that the oxidative damage in mitochondria was related to the chronic inflammatory process in the CNS [178]. To support the role of mitochondrial dysfunction in axon degeneration in MS, Dutta et al. used microarray assays to compare the expression of 33,000 genes in postmortem motor cortex samples from 6 MS subjects and 6 healthy controls. The authors found that 488 transcripts were reduced and 67

were increase in MS samples in comparison to controls. From these, 26 mitochondrial genes were reduced, as well as the activities of the complexes I and III of the respiratory chain. These results indicate that mitochondrial dysfunction in demyelinated axons leads to reduced ATP production and participates in the progression to permanent disability in MS [179].

Immune cell infiltration is considered the main contributor to axonal destruction. However, studies by Qi et al. in the EAE model showed that mitochondrial dysfunction due to oxidative stress was present in the CNS of immunized mice before the infiltration of immune cells [180]. EAE was induced in DBA/1J mice by immunization with spinal cord homogenate emulsified in complete Freund's adjuvant (CFA). DBA/1J mice injected just with CFA were used as controls. Three days after sensitization, mice were euthanized and the optic nerves, retinas, brains, and spinal cords were obtained [180]. None of the mice showed clinical signs of EAE disease at this time-point. The ROS activity in tissue samples was evaluated by the presence of nitrated proteins. Nitrated proteins were detected in all of the samples obtained from the mice primed with autoantigen. On the other hand, nitrated proteins were not detected in the CFA-only immunized control mice. Interestingly, the samples from immunized mice did not contain inflammatory cells. The identity of nitrated proteins in samples from neuroantigen-primed mice was further analyzed by mass spectrophotometry analysis of isolated mitochondria. These experiments showed that the nitrated proteins corresponded to heat shock protein 70, NADH dehydrogenase (complex I), cytochrome c oxidase (CCO, complex IV), and glyceraldehyde 3-phosphate dehydrogenase (GAPDH). The authors next measured mitochondrial ATP production and found that the ATP production in the

optic nerve, retina and brain did not show significant differences in samples from SC-homogenate primed mice in comparison with control tissues. On the other hand, ATP production in samples from the spinal cords of immunized mice was reduced 79% in comparison with control tissues [180]. Spinal cord samples showed a significant reduction of mitochondrial membrane potential (MMP), to approximately 33% ($p<0.05$) in comparison with controls. The loss of MMP leads to DNA fragmentation and apoptosis. This led the authors to evaluate apoptosis in the samples from immunized mice using TUNEL staining. They found TUNEL-positive cells in optic nerve, retina, brain and SCs samples. Immunofluorescent microscopy revealed that the TUNEL-positive cells were oligodendrocytes. Furthermore, tissues isolated from mice primed for EAE, but not adjuvant-inoculated control animals, showed positive iNOS immunofluorescence and the presence of iNOS by immunoblot assay. Histological analysis of spinal cords from diseased mice showed the presence of mitochondrial vacuolization and dissolution of cristae, but this was not observed in controls. These changes in the structure of mitochondria correlate with the presence of oxidative stress and the degeneration of axons at early stage of EAE [180]. Collectively, these results demonstrate the presence of nitrosative stress, oligodendrocyte death, and axonal degeneration an early stage of EAE (3 days post sensitization) in the absence of immune cells [180]. These authors subsequently observed H_2O_2 and superoxide in the mitochondria from the optic nerve obtained from EAE mice collected 3 days after sensitization. As observed previously, ROS production was present in absence of inflammatory cell infiltration [181]. Moreover, apoptotic oligodendrocytes were observed in the retina and optic nerve of the EAE mice by immunohistochemical methods.

Interestingly the suppression of SOD2 gene in the eyes of EAE mice increased the damage in myelin fibers by 27%. On the other hand, the overexpression of SOD2 in the eyes of EAE mice reduced the damage in myelin fibers by 51%. Therefore the authors suggest that the overexpression of SOD2 can be used to reduce the optic neuritis produced due to oxidative stress in EAE mice [181].

Lewis rats immunized with myelin basic protein, complete Freund adjuvant are characterized by a monophasic disease, full recovery, do not relapse, and develop resistance to further reinduction of disease. O'Brien et al. used this model to investigate the role of NO in disease development [182]. The authors observed elevated serum NO_2^- during the active period of disease which persisted into the recovery period. The results suggested that NO plays a role in the development of disease especially during an active state [182]. In separate experiments, Jolivalt et al. investigated the effect of the nitric oxide scavenger NOX-100 on EAE induced in SJL/J mice [183]. The authors found that NOX-100 reduced disease progression, CNS inflammation, pro-inflammatory cytokines and iNOS. The results suggest that therapies to reduce oxidative stress can be a suitable approach to reduce the progression of EAE and MS [183].

Calabrese et al. evaluated different nitrosative stress markers in cerebrospinal fluid and plasma samples collected from MS subjects and matched healthy controls [184]. Western blot analysis using CSF showed that samples from MS subjects presented an increase of approximately 24% in iNOS activity in comparison with controls. The use of aminoethylisothiourea (ITU), an iNOS inhibitor, on CSF samples from MS reduced the iNOS activity to similar levels to control samples. Nitrotyrosine immunostaining of CSF proteins was elevated in MS patient but was not detectable in

controls. CSF samples were used to measured nitrite levels by Griess reaction and peroxynitrites by luminol dependent enhanced chemiluminescence. Nitrite and peroxynitrites were elevated by 81% and 61% respectively in samples form MS patient in compassion with controls. CSF samples also showed an increase of approx. 38% in S-nitrosothiol is MS samples in comparison with controls. Levels of the antioxidant glutathione were reduced in CSF and plasma in MS samples in comparison with healthy controls. All these results supported the participation of nitrosative stress in the development of MS [184].

1.24 MS therapies

Therapeutic agents currently approved for the treatment of MS affect disease by modulating or suppressing the immune system in general or the autoreactive T cells, specifically. These drugs are approved for the treatment of RRMS, characterized by the inflammatory demyelination. They act to reduce the frequency and number of relapses and the number and size of the lesions present in the CNS, reduce disability, and slow the progression of disease [185, 186]. However, they do not prevent long-term disability and are ineffective for the treatment of progressive disease because they fail to offer significant neuroprotection as well as reduction in nitrosative stress that is mainly present in chronic stages [185, 186]. Neuroprotective strategies that can be used throughout the disease process are urgently needed. The combination of neuroprotection and immune modulation are considered necessary to target the innate and adaptive responses that arise during the progression of the disease and guard

against the axonal loss contributing to disease progression. The primary therapeutic agents currently approved are summarized below and in Table 1.

Interferon beta (IFN-β). The critical step in the pathogenic mechanism of MS is the activation of naïve autoreactive T cells in the periphery which then migrate to the CNS to cause disease [21]. This naïve T cell activation is carried out by the three signals mechanism discussed above. Briefly, the first signal in T cell activation occurs when TCR on CD4+ T cells recognizes the myelin peptides or their mimics presented by the MHC-II located on APC (i.e. dendritic cells, B cells, macrophages) [22, 23]. The second signal is carried out when the co-receptor molecules CD80 and CD86 on APCs (i.e. dendritic cells) bind to CD28 molecules located on T cells. The second signal produces the release of cytokines by the T cell. The binding of these cytokines to their specific receptors on T cells (signal three) will produce the final activation of T cells, for instance, IL-12 leads to Th1 differentiation and IL-4 leads to Th2 cell differentiation. Once activated in the periphery, T cells are able to cross the blood brain barrier (BBB) and enter the CNS [22].

IFN-β is available as IFN-β-1a (Avonex®, Rebif®, and Plegridy®) and IFN-β-1b (Betaseron®). Human IFN-β is a polypeptide of 166 amino acids forming five α helices naturally produced by human fibroblasts, dendritic cells, and retinal glial cells. IFN-β-1a is produced in Chinese hamster ovary cells, and it is pharmacologically identical to the natural form (found in humans). IFN-β-1b is produced in E, coli, and it has 165 amino acids instead of 166 (Met1 is absent) and the amino acid Cysteine at position 17 is replaced by Serine [187]. Betaseron® and Rebif® are administrated subcutaneously

every other day. Avonex ® is administrated intramuscularly once a week. Plegridy® is administrated subcutaneously every 2 weeks [188].

IFN-β affects disease pathogenesis by multiple mechanisms. The drug reduces the inflammatory T cell response by inhibiting the stimulation and activation of T cells. Specifically, IFN-β reduces the expression of MHC-II as well as the co-stimulatory molecules CD80 on APCs and CD28 on T cells [186, 189-191]. Th1 and Th2 subsets play and important role in MS development: Th1 cells participate during the initial phase of inflammation, while Th2 mediated response is important during recovery. IFN-β produces changes in the Th1/Th2 cell balance, leading to a shift from Th1 cell phenotype to a Th2 cell phenotype characterized by a reduction Th1 cell pro-inflammatory cytokines (IL-2, IL-12, IFN-ɣ, TNF-α) and an increase in Th2 cell anti-inflammatory cytokines (IL-4, IL-10, TGF-β) [186, 191, 192]. IFN-β also affects cell migration into the CNS by reducing the expression of the adhesion molecule VLA-4 located on the surface of activated T cells. This prevents the adhesion of activated T cells to the surface of the BBB [189]. Finally, IFN-β reduces the expression of matrix metalloproteinases (MMP) by microglia and astrocytes, which participate in breaking down of the BBB. These actions prevent the entrance of activated T cells and immune cells into the CNS where they can cause damage [189].

A five year clinical study reported that IFN-β-1b reduced the exacerbation rate and MRI lesion burden compared to placebo [193]. Another study also reported the use of IFN-β-1b produced a reduction in the exacerbation rate in comparison with placebo group and most of the patients that received IFN-β-1b were relapse free at 2 years compared with the placebo group [194]. In another clinical trial IFN-β-1a (Avonex®) was

administrated intramuscularly once per week to RRMS subjects with Expanded disability status scale (EDSS) ≤ 3.5 or >3.5. patients with a EDSS ≤ 3.5 % presented a 31.7% reduction in relapse, RRMS patient with EDSS> 3.5 presented a reduction of 37% in relapse [195].

Glatiramer acetate (GA) (Copaxone®) is a synthetic polymer made of four amino acids (L-glutamate, L-lysine, L-alanine and L-tyrosine) that mimics the primary structure of myelin basic protein (MBP). This similarity in structure allows GA to compete with MBP to bind to MHC-II on APCs as well as displace the MBP already bound to MHC-II. In fact, GA binds to MHC-II with higher affinity and faster rate than MBP [185, 186]. The GA binding to MHC-II produces a shift in T cell responses, from Th1 to Th2 cell phenotype. This was demonstrated in the EAE model by the reduced clinical severity, proliferation of MOG-reactive T cells, Th1 cell response, and IL-2 production after GA administration [196-198]. Similarly, human studies on MS subjects showed that GA treatment led to a shift in T cell responses from Th1 to Th2, evidenced by reduced Th1 cell pro-inflammatory cytokines (IFN-ɣ) and increased Th2 cell anti-inflammatory cytokines (IL-4, IL-5, IL-10) [199-201]. In the brain, GA is able to induce the production of brain derived neurotrophic factor (BDNF) by Th2 cells that might be neuroprotective [202]. One study showed that the administration of GA to EAE mice provided neuroprotection. The administration of GA at different points of the disease provided a reduction in the neuronal and axonal damage in comparison with the control group. In addition, cell proliferation, migration and cell differentiation (neurogenesis) of oligodendroglial and neuronal progenitor cells were elevated in EAE mice with GA treatment in comparison with control group [203].

A clinical trial used 20 mg of GA or placebo administrated daily on subcutaneous injections on RRMS for 2 years showed that RRMS presented a 29% reduction in the annual relapse rate (ARR) [204]. Another study showed that RRMS subjects receiving GA presented with a reduction in the total number of gadolinium-enhancing lesions, reduction in the size of lesions, and reduction in the number of new lesions observed by MRI. These trials also demonstrated a reduction in the relapse rate in comparison with placebo group [205]. A long term (15 years) follow up study showed that patients on GA presented a reduction in relapse rates, reduction in disability progression and reduction in the transition to SPMS in comparison with placebo group [206].

Fingolimod (Gilenya®) is a synthetic sphingosine-1-phosphate (S1P) analogue. S1P is a signaling molecule that participates in the regulation of trafficking of T cells and B cells from the blood to the lymph nodes. Activation of S1P receptors expressed by T cells and B cells leads to the migration of these cells from peripheral blood and sequesters them within the secondary lymph organs, thus reducing the numbers of T cells and B cells in the blood [207, 208]. Similarly, FTY720 binds to S1P receptor preventing the exit of naïve T cells form the lymph nodes and sequesters them within the secondary lymph nodes [207-210]. This reduces the number of T cells that can cross the BBB and reach the CNS where they can potentially being activated to produce inflammation and damage [207-210].

An early study investigating the effects of FTY720 on EAE in Lewis rats demonstrated that starting FTY720 treatment the same day of EAE induction led to dramatic protection against disease. [210]. This protection was associated with the reduction in the number of T cells in the spinal cords evaluated by

immunohistochemistry. The RT-PCR analysis of spinal cords also showed a reduction in the mRNA of Th1 cell cytokines, IL-2, IL-6, and IFN-ɣ. In addition, passive transfer of T cells isolated from FTY72-treated EAE rats into naïve rats, produced EAE with low incidence and disease severity [210]. The results showed that FTY720 produced an anti-inflammatory effect due to the reduction of T cell responses, their migration to the CNS, and reduction in Th1 cell pro-inflammatory cytokines [210]. Another study demonstrated that FYT720 promoted remyelination, the extension of oligondendrocytes progenitor cells, the maturation of oligondendrocytes, and increased the number of microglia cells in organotypic mouse cerebellar slice cultures [211].

Two clinical trials have evaluated the effects of FTY720 in RRMS in comparison with placebo. In the first clinical trial, RRMS subjects received a daily dose of 0.5mg or 1.25 mg/day for a period of 12 months. Patients on FTY720 showed a reduction in the annual relapse rate in comparison with the placebo group [212]. In the FREEDOMS trial, RRMS subjects received a daily dose of FTY720 0.5mg/day or 1.5 mg/day for a period of 4 years. Patients receiving FTY720 showed a reduction in the annualized relapse rate (ARR) of approximately 50%, a reduction in the brain volume loss (BVL). In addition, more patients were free from 3-month confirmed disability progression (CDP) in comparison with the placebo group [213]. MRI showed a reduction in both new enhancing and non-enhancing lesions in patients on FTY720 in comparison with the placebo group [213].

Dimethyl fumarate (DMF) (Tecfidera ®) is a methyl ester of fumaric acid. This drug treatment focuses on the reduction of oxidative stress, dendritic cell maturation and subsequent T cell activation. DMF reduces the production of pro-inflammatory

cytokines (i.e. IFN-ɣ, TNF-ɣ, IL-6) and nitric oxide (NO), and increases the production of nicotinamide adenine dinucleotide phosphate quinone reductase 1 (NQO1), a detoxification enzyme, and glutathione, an antioxidant. Glutathione and NQO1 participate in the reduction of free radicals and RNS which potentially can cause damage in the CNS [214-218].

Peng et al. evaluated the effect of DMF on dendritic cell maturation and the subsequent T cells responses mediated by dendritic cells [218]. Bone marrow-derived dendritic cells from C57BL/6 mice were stimulated with LPS in the presence or absence of DMF. Cytokine analysis at 6 and 24h showed that DMF significantly reduced the production of the pro-inflammatory cytokines, IL-12 and IL-6, which participate in Th1 and Th17 differentiation, respectively. Flow cytometry analysis showed that LPS stimulation enhanced the expression of MHC-II^{high}, CD80, and CD86^{high}, but the presence of DMF completely inhibited the up-regulation of the surface molecules [218]. The cytokine and flow cytometry data suggested that DMF inhibits the maturation of dendritic cells by preventing the expression of surface markers required for effective presentation of antigens to T cells and the subsequent the suppression of pro-inflammatory cytokines IL-12 and IL-6 needed for Th1 and Th17 differentiation [218]. Next, the authors evaluated whether DMF affected the activation of T cells by dendritic cells. Dendritic cells were stimulated with LPS in presence (LPS/DMF-DCs) or in absence (LPS-DCs) of DMF for 24h, then, washed to remove LPS and DMF. The treated dendritic cells were then co-cultured with T cell receptor transgenic T cells specific for MOG_{35-55} in the presence of MOG_{35-55} peptide for 72h. Flow cytometry data showed that LPS/DMS-DCs generated a lower percentage of CD4+ T cells expressing

the CD44 maker in comparison with those exposed to LPS/DCs [218]. IFN-ɣ and IL-17 were reduced in supernatants from LPS/DMF-DCs + MOG_{35-55}-specific T cells. In addition, T cells co-cultured with LPS/DMF-DCs presented with reduced cell proliferation. These data suggested that DMF is able to reduce dendritic cell maturation, and subsequent T cell activation, leading to a reduction in cytokines production and cell proliferation of MOG-specific T cells [218]. To investigate the how DMF impairs the maturation of dendritic cells, the authors evaluated the NF-kB pathways which participate in the maturation of dendritic cells by Toll-like receptors. The authors found that DMF reduced the nuclear translocation and phosphorylation of p65 unit, which inhibited NFkB signal pathway. Thus, the results suggested that DMF suppresses the NFkB pathway, inhibiting dendritic cell maturation, and subsequently Th1 and Th17 differentiation [218].

Studies in the MOG35-55-induced model of EAE in mice with showed that DMF administrated twice per day starting 3 days after MOG immunization produced a reduction in the clinical score and macrophage infiltration in the spinal cords, and increased plasma IL-10 [219]. In a human study, the authors evaluated the effect of DMF on the production of cytokines and development of Th subsets. The authors collected peripheral blood mononuclear cells and CD4+ T cells from healthy donors, and cells were activated with CD2/CD8 monoclonal antibody in presence and absence of DMF. The presence of DMF increased IL-4 and IL-5 without affecting the levels of -2 and IFN-ɣ. Next, the authors activated PBMC with mycobacterium tuberculosis, which induces a Th1 cell response characterized by high production of IFN-ɣ. Similar to results

with $CD4^+$ T cells, cultures with DMF exhibited increased IL-4 and IL-5 and no changes in IFN-ɣ, suggesting a shift from Th1 to Th2 cell response [220].

In a clinical trial evaluating the effect of DMF on RRMS, subjects were divided into 4 groups, each receiving a different dose of drug: 1) 120mg, once a day, 2) 120mg 2 times per day, 3) 240mg 3 times a day, 4) placebo. The results showed that groups receiving 240mg 3 times per day presented with a 69% reduction in the mean number of enhancing lesions on MRI as well as a reduction of 32% in the annual relapse rate [221]. Two additional clinical trials evaluated the effect of DMF on RRMS using doses of 240 mg two times per day, 3 times per day and placebo. The results showed a reduction of the annual relapse day of 44% (2 times/day dose) and 51% (3 times/day dose), reduction in disability progression in 21% (2 times/day dose) and 24% (3 times/day dose), and both groups also showed a reduction in the number of new or enlarging lesions by MRI [222-225].

Teriflunomide (Aubagio®) inhibits the proliferation of T and B cells by interfering with the cell cycle. When lymphocytes are activated, they undergo cell division. The synthesis phase (S phase) is the portion of the cell cycle when DNA is copied. The S phase requires pyrimidine and purine bases for DNA synthesis. Terifluonomide blocks the synthesis of pyrimidine by inhibiting the mitochondrial enzyme, dihydroorotate dehydrogenase (DHODH). This enzyme is necessary for the de novo synthesis of pyrimidine ribonucleotides and is highly expressed in proliferating lymphocytes [226-228]. Resting or naïve lymphocytes use nucleotides from degrading DNA and RNA (nucleotide salvage pathway) and do not need DHODH, therefore the immune responses are preserved and the viability of immune cells is not affected [226].Thus, the

suppression of DHODH by stopping mitosis reduces the proliferation of activated T cells and B cells in the periphery, reducing the number of cells that can reach and cross the BBB. All these events protect the CNS from autoimmune damage [229].

In-vitro studies using cultured rat microglia demonstrated that Teriflunomide was not cytotoxic to microglia but reduced the co-stimulatory molecule CD86, and increased IL-10 production after lipopolysaccharide activation [230]. The drug also decreased microglial proliferation in a dose dependent manner. Teriflunomide at low concentrations (0.25-1μM) did not have an effect on activation or proliferation of microglia, while Teriflunomide at 5μM produced a reduction in proliferation of approximately 30%. All together the results suggested that Teriflunomide can reduce microglial proliferation (activation) and produce anti-inflammatory effect due to the production of IL-10 [230].

Animal studies showed that Teriflunomide reduced damage to axons within the spinal cords in the EAE induced in dark Agouti rats [231, 232]. Rats treated with oral Teriflunomide everyday starting either on the day of immunization or the day of disease onset presented with a reduction on EAE clinical score, improvement of neurophysiological status of descending motor tracts, and reduction in axonal damage compared to placebo treated rats. The results suggested that the reduction in axonal loss and improvement in motor functions may be due to a reduction in both inflammation and demyelination in the CNS [231, 232].

Human studies showed that MS subjects on Teriflunomide experienced a reduced annual relapse rate, a longer time to first relapse, and reduction in disability progression and lesions detected by MRI in comparison with the placebo group. [233,

234]. In one study, 1088 RRMS patients between 18-55 years of age with a score of 0 to 5.5 in the expanded disability status scale and 1-2 relapses in the previous 2 years were recruited to evaluate the effects of Teriflunomide in a period of 108 weeks [233]. Patients were divided into 3 groups: group 1 received a dose of 7mg/day; group 2 received 14 mg/day; and group 3 received a placebo. The results showed that subjects receiving Teriflunomide experienced reduction in the annualized relapse rate with relative risk reductions of 31.2% (group 1) and 31.5% (group 2) compared to subjects receiving placebo. Similarly the proportion of subjects with confirmed progression of disability was 21.7 (group 1 7, mg/day, 20.2% (group 2 14mg/day) and 27.3% (group 3, placebo) [233]. In a second study, the effects of Teriflunomide administered at 7 and 14mg/day on RRMS for a period of 48 weeks was evaluated. The authors also found that 7 and 14 mg/day doses produce a reduction in the annual relapse rate in comparison with placebo. The 14mg/day also reduced disability progression in comparison with the placebo. The 7mg/day dose did not reduce disability progression in comparison with the placebo group [234].

Ocrelizumab (Ocrevus®, Genentech, Inc., San Francisco, CA, USA). B cells also play an important role in the development of MS. In MS, B cells express higher surface levels of MHC-II and co-stimulatory molecules which participate in the activation of T cells. In addition, B cells also produce antibodies that participate in the pro-inflammatory and demyelination processes in the CNS. Thus, ocrelizumab has been used to reduce the number of B cells in MS [186, 235]. Ocrelizumab is a humanized monoclonal antibody that targets the surface molecule CD20 on B cells causing their elimination. Ocrelizumab does not eliminate plasma cells and hematopoietic stem cells

because they do not express CD20 molecule [235]. One clinical trial compared the effect of Ocrelizumab and IFN-β1a on RRMS subjects [236]. Patients were divided in 2 groups: group 1, received an intravenous dose of 600 mg of Ocrelizumab every 24 weeks for 96 weeks; Group 2 received a subcutaneous dose of 44μg of IFN-β-1a 3 times per week. Both groups received treatment and were monitored for 96 weeks. The results showed that the group on Ocrelizumab in comparison with the IFN-β-1a group presented a 46% lower rate in the annual relapse rate, a lower disability progression at 12 weeks (9.1% vs 13.6%) and 24 weeks (6.9 vs 10.4) of treatment, a reduction in the number of lesions detected by MRI, as well as improvement in walking speed, upper-limb movements and cognition tasks [236]. In a second clinical trial, RRMS subjects were divided in 2 groups: group 1 received Ocrelizumab at 600 mg; group 2 received a placebo. Both groups received treatment every 24 weeks for at least 120 weeks [237]. The results showed that after 12 weeks of treatment, the percentage of patients with confirmed disability progression on ocrelizumab was 32.9% in comparison 39.3% with the placebo group. At week 24, the percentage of patients with confirmed disability was 29.6% in comparison to 35.7% with placebo. At 120 weeks, patients on ocrelizumab in comparison with the placebo group, presented an improvement in the 25-foot walk, a reduction in the rain lesions and brain loss detected by MRI [237].

Table 1. Mechanism of Action for MS	
Drug	**Mechanism of action**
IFN-β®	Inhibits stimulation and activation of Th1 cells [186, 189-191]. Shift T cell responses from Th1 to Th2 [186, 191, 192]. Prevent the expression of cell adhesion molecule VLA-4 and reduces the expression of metaloproteinases [189].
Glatiramer acetate (Copaxone®)	Inhibits of T cell activation. Shift T cell responses from Th1 to Th2 [196-198]. Reduces Th1 cell pro-inflammatory cytokines (IFN-ɣ) and an increase in Th2 cell anti-inflammatory cytokines (IL-4, IL-5, IL-10) [199-201].
Fingolimod (Gilenya®)	Prevent the exit of CD4+ and CD8+ t cells and B cells from secondary lymph tissues which reduces the number of cells thatn can cross the reach and cross the BBB to produce damage in the CNS [207-210].
Dimethyl fumarate (Tecfidera®)	Inhibits MHC-II expression which prevents T cell activation. Reduces the production of pro-inflammatory cytokines (i.e. IFN-ɣ, TNF-ɣ, IL-6) and nitric oxide (NO), and increases the production of nicotinamide adenine dinucleotide phosphate quinone reductase 1 (NQO1) [214-217]. Reduces the production of the pro-inflammatory cytokines IL-12 and IL-6 which participate in Th1 and Th17 differentiation [218]. Inhibits MHC-II expression on antige presenting cells preventing the activation of T cells [218]. Inhibits NFkB signal pathway which inhibits dendritic cell maturation, and subsequently Th1 and Th17 differentiation. [218]
Teriflunomide (Aubagio®)	Inhibits T cells and B cells proliferation by blocking the synthesis the mitochondrial enzyme dihydroorotate dehydrogenase (DHODH). This reduces the number of cells that can reach the CNS. [226-228].
Ocrelizumab (Ocrevus®)	Monoclonal antibody that targets the surface molecule CD20 on B cells causing their elimination. The reduction of B cells prevents the activation of T cells and production of antibodies against myelin-like proteins [235].

1.25 Photobiomodulation (PBM)

Photobiomodulation (PBM) is a therapeutic approach shown to have beneficial effects in the treatment of different pathologies, including wound healing, chronic inflammatory conditions, and neurological disorders [238]. PBM has been used in the biomedical field since the invention of the ruby laser and the helium-neon laser in the early 1960's. The light applied by PBM devices is absorbed by the tissue, leading to a biological effect. The wavelengths used in PBM fall into the visible red (VIS) and near

infrared (NIR) wavelengths, 600-1100 nm, which is known as the “optical window” [238]. The mechanisms of action of PBM are still under investigation.

It is proposed that the biological effects of PBM are elicited through improvement of mitochondrial function. Previous studies demonstrated that VIS/NIR light is absorbed by cytochrome c oxidase (CCO, complex IV) located in the inner membrane of the mitochondrion [239-242]. Absorption of light by CCO initiates as cascade of events culminating in increased transcription and translation of mitochondrial proteins, and increased ATP production [239-242]. Initial experiments to investigate the mechanism of PBM Greco et al., evaluated the effect of light treatment on the synthesis of RNA and proteins by the mitochondria. Isolated mitochondria obtained from rat liver received light treatment He-Ne laser lamp at 632.8 nm, 4mW/cm2, 5J/cm2. After light treatment, the mitochondria showed increase in synthesis of both RNA and protein (transcription and translation of proteins) [240]. In an additional study, He-Ne laser (632nm, 10mW, 200s, 2J/cm^2) administered to mitochondrial extract from rat liver led to an increase in electron transfer (proton pumping activity), CCO activity, and ATP production [242]. Pastore et al studied the effect of light treatment on cytochrome C oxidase (CCO). Purified CCO solution received light treatment at 632.9nm using 10mW/cm2. Subsequent experiments showed that light-treated CCO was able to oxidize cytochrome C faster compared with control (no light treated CCO) [239].

Wong-Riley et al., carried out in-vitro studies to evaluate the effect of PBM at 670, 728, 770, 830, and 880nm (power intensity of 50mW/cm^2, energy density of 4J/cm^2) on CCO activity and ATP production in primary neuronal cultures from rat visual cortex [243]. Primary neuronal cultures were incubated with tetrodotoxin (TTX)

(concentration of 0.4 μM), a sodium channel blocker which reduces neuronal impulse activity, CCO activity, and ATP consumption. PBM treatment at 670nm and 830nm was the most effective in recovering CCO activity and ATP production to similar levels to those observed in controls (cultures incubated with TTX without PBM treatment). Conversely, PBM treatment at 728nm failed to show a significant effect. The action spectra of CCO activity and ATP content in neuronal culture subjected to the five PBM treatments were plotted in order to determine the relationship with the action spectra of the CCO. The plot showed that there is positive correlation between the action spectra of CCO activity and the ATP content (at 670nm and 830nm) with the absorption spectrum of CCO, while there was a smaller correlation at 728 nm [243].

Hu et al., investigated the potential effect of PBM on cell proliferation and the possible mechanism involved [245]. After treating the melanoma cell line A2058 with He-Ne laser (632.8nm, 10mW/cm^2, 0, 5, 1, 2J/cm^2), the authors observed increased cell proliferation, CCO activity, mitochondrial membrane potential (MMP), ATP, cAMP, and activation of the Jun N-terminal kinase (JNK) and the transcription factor, AP-1 [245]. The experiments showed that the increased cAMP was due to increased ATP production induced by PBM. Moreover, the cAMP induced the increased activation of JNK/AP-1 after light treatment. AP-1 is a transcription factor that induces the expression of genes related with cell proliferation, survival and angiogenesis. Therefore, increased activation of A-A1 by PBM is responsible for many of the noted effects of attributed to PBMT [245]. Karu et al., also investigated the role of the mitochondrion in the mechanism of action of PBM using HeLa cells. Immediately after treating HeLa cells with He-Ne laser (632.8nm, 100J/m^2, 10s) the authors measured ATP production using

a luciferin-luciferase bioluminescent assay. The log phase reached the maximum peak 20min after PBM treatment. The increase of ATP production correlated with the increase in cell proliferation reaching the highest peak at 170.8% in comparison with controls (no PBM treatment). ATP production returned to base levels 60min after the light treatment [246].

1.26 PBM parameters

In order for PBM to produce a therapeutic effect, it is necessary to apply the correct light dose. Energy [Joules (J)] is used to define the light dose administered during light treatments, where Energy (J) = Power (Watts) x Time (s). The amount of power and the time used are fundamental to define the amount of energy that is administrated and the biological effects obtained. If two treatments provide the same amount of energy (J) but in one treatment the amount of power is twice folded and the time is reduced to half then a different or non-effect will be produced [244]. The dose parameters involved in PBM are presented in Table 2.

Table 2. Light dose parameters [247].

Parameter	Units	Description
Irradiance, intensity or power density	Watts/cm^2	Power (in watts) of light treatment divided by the area (cm^2)
Energy	Joules (J)	Power (watts) of light treatment applied multiplied by time of treatment. Energy (J) = Power (Watts) x Time (s).
Energy density or fluence	Joules/cm^2	Used to describe the dose applied during light treatment
Irradiation time	Seconds (s)	Time used during the application of light treatment

1.27 Biphasic dose response in Photobiomodulation (PBM)

Photobiomodulation (PBM) exhibits a biphasic or inverted U-shape dose response curve. A biphasic curve indicates that at low energy doses, there is not

enough energy to produce an effect (below threshold). When the energy dose is increased, the energy threshold is achieved and a biologic effect is observed. If more energy is administered, the threshold is crossed, and the biologic effect is inhibited (Figure 1). Several lines of research have studied the effects of biphasic dose responses in different systems [244, 248-252].

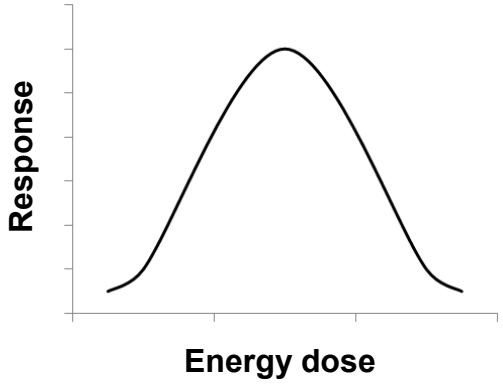

Figure 1. Biphasic dose response curve observed in PBM [244].

Sharma et al, studied the effects of 810nm laser on primary cortical neurons [248]. Pregnant female C57BL/6 mice were sacrificed at 16 weeks post-conception. Primary cortical neurons were isolated from the brains from embryonic mice. Brain tissue was triturated, washed, and cells obtained were platted and maintained for 8 days before the PBM treatment. Light treatment was applied using diode laser at 810nm in a continuous wave mode with a power density of 25 mW/cm^2 and different energy densities (0.03, 0.3, 3, 10 and 30 J/cm^2) [248]. Intracellular levels of reactive oxygen species (ROS), nitric oxide, and calcium, ATP production, and mitochondrial membrane potential were measured 5 min after PBM treatment. The results showed that PBM at lower fluences (0.03, 0.3 and 3 J/cm^2) produced an increase in ATP and mitochondrial membrane potential in comparison with base line being the 3 J/cm^2 the best dose.

However, PBM effect on ATP and mitochondrial membrane potential was reduced or returned to basal levels at higher energy densities (10, 30 J/cm^2) [248]. PBM led to increased ROS at all doses, reaching a double peak at 3 and 30 J/cm2. Nitric oxide production showed a similar double peak as ROS but the increase was less significant. High levels of ROS production, mitochondrial membrane potential and ATP coincided at 3J/cm^2. The results suggested that low levels of energy delivered by PBM treatment can be enough to induce the activation of cell signals which participate in the modulatory effects of PBM. The results also showed that there is a threshold where PBM can produce an effect of cells. Once the threshold is passed, the activity or induction of cellular mediators will be reduced and possibly detrimental mediators such as ROS and nitric oxide can be elevated or induced [248].

Chen et al., evaluated the effect of PBM at 810nm on the transcription factor NFkB [249]. Mouse embryonic fibroblasts (MEFs) from pregnant female HLL mice (NFkB luciferase reporter mice, C57B6/DBA background) were used in the study. PBM treatment was applied using 810nm (1 to 30 mW/cm^2) using energy densities of 0.003, 0.03, 0.3, 3 and 30 J/cm^2. After PBM treatment cells lysates were collected and used to measure luciferase activity [249]. The results showed a biphasic dose curve. Low energy doses produced increased NF-kβ activation, reaching the maximum at 0.3 J/cm^2, then going down at 3 and 30 J/cm^2. The increase in the activation of NFκβ reached its highest expression at 10 hours after PBM treatment and returned to basal levels at 24h (Figure 2). The addition of antioxidants blocked the activation of NFκβ, indicating that the activation of NFκβ was mediated via mitochondrial ROS. ROS production in response to PBM also demonstrated a biphasic dose response. ROS

production was measured 30 min after PBM, 0.3, 3 and 30J/cm^2 produced a significant increase in comparison with no PBMT treatment, being 3J/cm2 the energy density with the highest ROS generation (Figure 2). PBM also resulted in increased ATP production. The maximum production of ATP was reached 5 min after PBM treatment and it returned to its basal levels in 4 hours [249]. The results suggested that PBM at low doses of energy improve mitochondrial function and induced the production of small amount of ROS that might participate as signal molecules. For example, it was already established that ROS activate NFkβ pathway [254]. Some of the cellular targets of the NFκβ include chemokines, immune receptors, adhesion molecules, stress response genes, apoptosis regulators, transcription factors, growth factors, enzymes cell cycle regulators [255]. Thus, it could be possible that small amount of ROS is needed to activate the NFkβ pathway, but high amount of energy leads to the production of high amount of ROS that can produce damage in the cell [253].

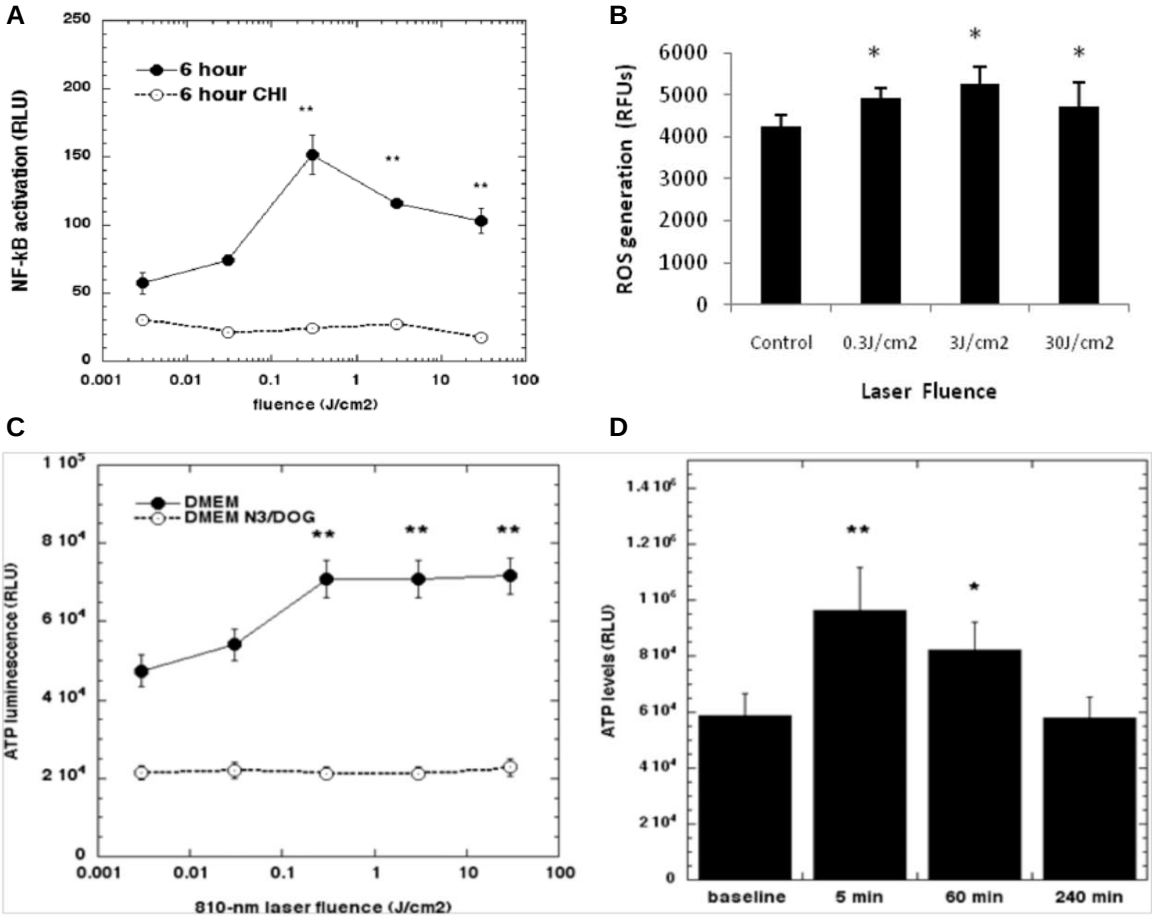

Figure 2. Biphasic dose curve for NfkB activation, ROS generation and ATP production. Light treatment (810 nm laser irradiation) on mouse embryonic fibroblast using different energy doses (0.3, 3, 30J/cm^2) A) Changes in NFkB activation, (B) Changes in ROS levels, C) ATP production at different energy doses, D) ATP production overtime using 3Jcm^2. (CHI= cycloheximide, NFκβ inhibitor) [249].

1.28 Effects of PBM on Nitric oxide (NO).

Data supports the notion that NO is a key mediator of the beneficial effects produced by PBM. Several studies demonstrate increased NO production immediately after PBM treatment, suggesting the release of NO from an intracellular source rather than de novo synthesis resulting from increased expression of NOS enzymes. For instance, Ball et al., carried out *in vitro* studies to characterize the effects of PBM on the

CCO-H_2O and CCO-NO reactions previously discussed (mitochondrial function section) [256]. Under hypoxic conditions, NO production by mouse brain mitochondria increased in presence of succinate (nitrite donor) and L-NAME (iNOS inhibitor) which was dependent on a source of NO_2^-. The results suggested that these mitochondria produced NO independently from iNOS in this experimental system. The authors also observed increased NO synthesis when a CCO donor (detergent solubilized mitochondria, TMPD, and cytochrome c) was added to the system. These results indicated the presence of CCO/NO activity due to CCO in mouse brain mitochondria. In further experiments, the authors evaluated the effect of PBM on the activity of CCO-NO of mouse brain mitochondria. They found that He-Ne light at 590nm ($40W/m^2$) increased CCO-NO activity, increasing NO production. However, the PBM did not have any effect on CCO-H_2O reaction (consumption of oxygen). Because the CCO/H_2O reaction was not affected during PBM, this indicates that there is not an increase in the rate of electron transference chain. Therefore, the rate of transference of electrons in CCO/NO is not affected either. These results suggest that CCO-NO reaction does not participate in the generation of NO. These observations therefore suggest that the increase of NO is due to the dissociation of NO from the complex CCO-NO [256]. This wavelength (i.e., 590nm) correlates with the stimulatory range of absorption of heme-proteins, (509-691nm) [257]. Additionally, the results showed that under hypoxic conditions, the production of NO after light treatment is dependent of both CCO and NO_2^-. Due to the observations, it has been proposed that the PBM induces the dissociation of NO from CCO producing its release to participate in different functions including signal molecule, vasodilator, messenger, and anti-cell adhesive.

Zhang et al., investigated the effect of PBM treatment on hypoxic and reoxygenation-induced injury in vitro using Sprague-Dawley rat cardiomyocytes [258]. The results showed that PBM treatment (670nm, 5, 25, 50mW/cm^2) applied 5 min after hypoxic and re-oxygenated injured cardiomyocytes reduced cell membrane injury, apoptosis, increased survival rate, NO production, and ATP production in comparison with control (no PBM treatment) [258]. The authors found that PBM treatment led to the release of NO bound to CCO. In addition, measuring NO following light treatment in the presence of different combinations of NO scavengers and NOS inhibitors demonstrated a reduction in NO and in the beneficial effects of PBM, suggesting that NO is produced by NOS and other NO stores and supporting the role of NO in the therapeutic mechanism of PBMT [258].

1.29 Photobiomodulation (PBM) on neurodegeneration.

Photobiomodulation (PBM) therapy is proving effective at ameliorating pathology and clinical severity for various neurodegenerative conditions, including traumatic brain injury (TBI), acute ischemic stroke (AIS), familial amyotrophic lateral sclerosis (FALS), spinal cord injury (SCI), Alzheimer disease (AD) and Parkinson disease (PD), [250, 259-268]. Yu, Z., et al studied the neuroprotection mechanisms involved during PBM on neurodegenerative conditions [259]. The authors evaluated if PBM at 810nm was able to reduce the mitochondrial dysfunction in neurons subjected to hypoxia/ischemia damage. The authors used an *in vitro* model to mimic conditions presented in neurodegenerative conditions such as stroke, brain trauma and neurodegeneration. Primary cortical mouse neurons were deprived of oxygen and glucose for 4h and then

reoxygenated for 2h, followed by PBM applied in a single treatment for 2min (810nm, 25mW/cm^2). Neurons that received PBM treatment presented with increased mitochondrial viability and a reduction in neuronal death. Furthermore, PBM led to an increase in mitochondrial membrane potential (MMP) ATP production compared to neurons without PBM treatment (control). The results suggest that one possible mechanisms of neuroprotection of PBM is by ameliorating mitochondrial dysfunction and restoring the depletion of energy as a consequence of oxygen and glucose depravation [259].

Xuan, et al. evaluated the effect of PBM on **traumatic brain injury (TBI)** using a BALB/c mice model. Mice were subjected to TBI induced by controlled cortical impact and subsequently divided into 4 experimental groups: 1) no PBM treatment, 2) a single PBMT treatment 4h post TBI, 3) 3 PBM treatments per day, 4) 14 PBM treatments per day. PBM was applied transcranially using 810nm laser (25.8mW/cm^2, 38s, 18J/cm^2) starting 4 h post TBI. Mice were sacrificed at 0, 4, 7, 14 and 28 days post-TBI for histology, histomorphometry. In addition, mice were injected with bromodeoxyuridine (at day 21-27) to allow the identification of proliferating cells [250]. Mice that received a single and 3 daily PBM treatments presented improved pathology as evidenced by reduced neurological severity score (NSS) and wire-grip and motion test (WGMT) scores. Mice that received 14 daily PBM treatments did not present significant change in comparison with control group [269]. Mice that received a single and 3 daily PBM treatments presented reduced lesion size and fewer degenerating neurons at 28 days after TBI induction in comparison with 14 daily PBM treatment and control group. In addition, histological assay showed that mice receiving single and 3 daily PBM

treatments presented BrdU-positive cells in the site of lesion in comparison with the 14 daily PBM treatments, and control group, suggesting that PBM treatment increased neurogenesis. The authors suggest that PBM may be effective for the treatment of TBI as long as the appropriate PBM treatment protocol (dose and time period) is used [250].

Familial amyotrophic lateral sclerosis (FALS) is characterized by the presence of oxidative stress, mitochondrial dysfunction, loss of motor neurons, and neuronal death. Moges et al. used the transgenic G93A SOD1 mouse model to study the therapeutic potential of PMBT for the treatment of FALS. This model presents with similar signs and symptoms to those patients with FALS, including hind limb weakness, walking problems, paralysis, neurogenic atrophy, and the inability to drink and eat, leading to severe weakness. PBM with 810nm light (140mW/cm^2, 2min, 12J/cm^2) for 3 consecutive days per week for a total of 7 weeks resulted in improved motor function early in disease in comparison with mice without PBM treatment (Sham controls) [261].

Alzheimer disease (AD) is characterized by the formation of plaques composed of amyloid-β (Aβ) peptide in the brain made of patients. The analysis of brain tissue samples from AD patients showed that Aβ protein plaques contain high numbers of activated of microglia and astrocytes that produce NO via iNOS-NFkβ activation [270-272]. Microglia activation produces tumor necrosis factor-alpha (TNF-α), which also increases NO production [273]. In addition, the neurofibrillary tangles (NFTs) found in the hippocampus of AD patients showed high expression of iNOS [274, 275]. Activated microglia participate in the activation of inflammatory mediators such as NADPH oxidase (PHOX), which activates NFκβ-iNOS increasing NO production [276]. High levels of NO produce nitrosylation and nitrotyrosination of proteins contributing to AD

pathology. RNS mediate glutamate excitotoxicity, inhibition of the complexes I and IV (CCO) of the respiratory chain, and organelle fragmentation (mitochondria and Golgi apparatus) [277]. PBM studies on AD demonstrate beneficial effect. One study using the APP/PS1 mice and NIR light at 670 nm (90 s, 4 J/cm^2, 5 days/week) for 4 weeks found that PBM reduced the clinical pathology. The size and number of Aβ plaques in neocortex and hippocampus of APP/PS1 mice were reduced following PBMT [266]. Another study, using transcranial laser therapy at 808 nm (1.2 J/cm^2, 3 times/week/6 months) on the Aβ protein precursor (AβPP) transgenic mouse model, showed a reduction in Aβ plaques and plasma and cerebrospinal fluid (CSF) Aβ levels and improved mitochondrial function, ATP production, and neurological functions [278]. A third study showed that PBM at 1072 nm (1.8 J/cm^2, 5 mW/cm^2, 6min, two consecutive days, 5 months) on TASTPM mice increased heat shock proteins (HSP), and reduced tau-phosphorylation, Aβ proteins in plasma and CSF, and Aβ plaques in the cerebral cortex. These results suggest that the increase in HSP prevents the misfolding of proteins avoiding their precipitation, aggregation, and formation of plaques [267].

Parkinson's disease (PD) is characterized by oxidative stress and mitochondrial dysfunction leading to a reduction in axonal transport and loss of dopaminergic neurons within the substantia nigra [268]. Several lines of investigation using different models of PD suggest that PBMT is affective against disease progression [268, 279-286]. For instance, Trimmer et al., used neuronal cell cultures obtained from PD patients and healthy donors to evaluate the effect of PBM treatment on mitochondrial velocity (mitochondrial movement). PBM at 810nm (50 mW/cm^2, 40s) was applied to neuronal cultures and cells were stained with MTRed. Mitochondrial movement was recorded for

2h with a microscope equipped with epifluorescence. The velocity of mitochondria was reduced in neurons from PD patients in comparison with neurons obtained from healthy donors. However, after the light treatment the velocity of mitochondria from PD-patients was significantly increased and comparable to the velocity of mitochondria from healthy controls. The results indicate that PBM improves mitochondrial function which might increase axonal transport [268].

A second study suggested that PBM treatment could reduce dopaminergic cell loss in the substantia nigra pars compacta (SNc). Local inflammation and microglial activation was induced in male Sprague-Dawley rats following intracranial injection of after lipopolysaccharide (LPS) [284]. Rats were divided in 3 groups: group 1) vehicle only injection no PBM treatment; group 2) LPS injection no PBM treatment; group 3) LPS injection with PBM treatment. Intracranial injection was applied using 10 or 20μg of LPS. PBM treatment (670nm, 50mW/cm^2, 88s) was applied 1cm above the head, 2 times/day (9 am and 6pm) for a total of 7 days starting the day of injection. Rats were sacrificed 7 days after administering LPS, and brain tissue was extracted and stained with tyrosine hydroxylase. The results showed that PBM treatment prevented dopaminergic cell loss in rats receiving 10μg of LPS, but not in rats receiving 20μg. In addition, rats that received 10μg of LPS and PBM treatment presented with improved motor function in comparison with those with 20μg of LPS with or without PBMT treatment. The results suggested that PBMT provided protection against cellular death, however there is a threshold of nigral inflammation and cellular death at which PBM stop its therapeutic effect to prevent cell death [284].

One study evaluated the effect of PBM on a PD animal model using the neurotoxin, 1-methyl-4-phenyl-1,2,3,6-tetrahydropyridine (MPTP) [285]. MTPT produces damage in the nigrostriatal dopaminergic pathway as well in the vasculature of the brain. C57BL/6 mice were injected with MPTP or isotonic saline (controls) and perfused with fluorescein isothiocyanate FITC-labeled albumin at different time points during the course of the experiment. The PBM treatment group received daily transcranial PBM treatment (670nm, 50mW/cm^2, 3min/day) starting 24h after MPTP injection. Seven days after MPTP injection, mice presented leakage of FITC labeled albumin in the substantia nigra and caudate putamen complex (located in the center of the brain). Mice receiving PBM treatment presented with reduced leakage of FOTC-labelled albumin in the substantia nigra and caudate putamen complex. The results suggested that PBM has the potential to reduce neuronal and vascular damage in the brain [285]. A small pilot study evaluated the effect of PBM on eight late stage PD patients, each patient during 2 weeks received daily PBM treatment on the brain stem and lobes including bilateral occipital, parietal, temporal and frontal lobes. The results showed that all patients compared to baseline presented an improvement in gait, cognitive function, and speech [286].

1.30 PBM on Experimental Autoimmune Encephalomyelitis (EAE)

Previously, our laboratory studied the effects of PBM in the EAE model of MS [287, 288]. C57BL/6 wild-type (WT) mice were immunized with MOG peptide 35-55 to induce EAE. Peripheral lymph nodes (PLN) were isolated 10 days after the immunization, and the lymphocytes obtained were cultured with MOG_{35-55},

Concanavalin A (ConA, a mitogen), or no stimulation. Beginning on the first day of culture and continuing daily for 96 hours, the cells received light treatment at 670 nm (LED array 75cm^2, fluence of 5J/cm^2). Cell cultures without light treatment were used as controls. Supernatants were collected every 24h and cytokines production was analyzed by ELISA. The results showed an antigen-specific effect of light on the cytokine production in cells cultured with MOG_{35-55}. Light treatment produced a significant reduction of IFN-ɣ ($P<0.0001$, pro-inflammatory cytokine) and a significant increase in IL-10 ($P<0.0001$, anti-inflammatory cytokine) expression in comparison with untreated light cells (Figure 3). However, PBM of lymphocytes incubated with ConA did not result in significant changes in IL-10 expression in comparison with similar cultures without light treatment. On the other hand, there was a significant increase in IFN-ɣ in cell cultures incubated with Con A and light treated just at 96h in comparison with similar groups without light treatment. The results suggest that the PBM effect on cytokine production was antigen-specific [287].

The *in vitro* experiments demonstrated that PBM at 670 nm modulates the immune response in a manner predicted to ameliorate clinical disease. Therefore, these experiments were extrapolated to in vivo experiments, where MOG_{35-55} immunized mice received PBM treatment at 670 nm (5 J/cm^2, LED lamp, applied on the dorsal surface of mice) starting the day after immunization for a total of 10 days (**suppression protocol**). Mice without light treatment were used as controls. The results showed that mice on PBM treatment presented a reduction in the clinical severity of the disease in the acute phase of disease in comparison with mice without PBM treatment. The clinical score of mice receiving light treatment was reduced (score range 2 to 3.5) in comparison with

mice without light treatment (score range 3 to 4) (P<0.01). However, by the end of the experiment, the clinical score of mice on PBMT treatment went back up to similar levels to controls (Figure 3). In additional experiments, a new PBM treatment protocol was developed. MOG_{35-55} immunized mice received PBM at 670 nm for 7 days starting on the day of disease onset (**onset protocol**). The results showed reduction in the clinical severity of the disease similar to the suppression light treatment protocol (data not shown) [287].

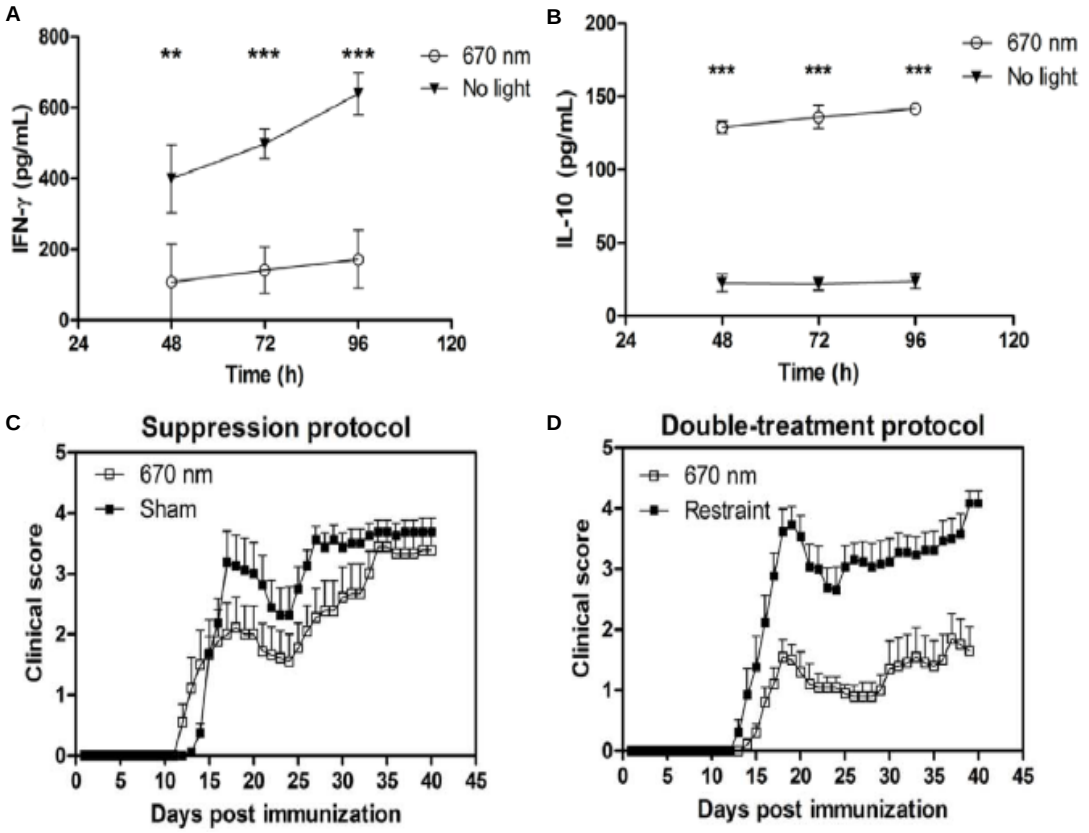

Figure 3. Modulation of cytokine production and clinical severity by PBM at 670 nm. Lymphocytes from PLN from EAE mice were incubated with MOG_{35-55} and light treated at 670 nm every 24 h for a total of 96. PBM at 670 nm produced a significant reduction on IFN-γ (A) and IL-10 (B). MOG_{35-55} immunized mice received PBM at 670 nm (5 J/cm^2 starting the day after immunization for a total of 10 days (suppression protocol) (C) or for 7 days starting the day the initiation of the clinical symptoms followed by 7 days without light treatment and then 7 more days of light treatment (double-treatment protocol) (D). The double treatment protocol showed to produce a more significant reduction in the clinical score of disease in comparison with the suppression protocol [287].

The results obtained led to the development of a new treatment protocol with the goal of having a longer lasting effect on the disease. The double treatment protocol consisted of the application of light for 7 days starting with the day of onset of clinical signs, followed by a period of 7 days without light treatment, with light treatment resuming on days 8 through 14 [287]. The results showed that mice that received the double-treatment protocol presented a more significant reduction in the clinical severity of the disease (score range 1 to 2) in comparison with light untreated mice (score range 3 to 4) ($P<0.01$), and the effect was sustained (Figure 3). Moreover, the reduction in clinical severity was more significant in comparison with mice that received the suppression protocol.

PLNs and SCs were obtained from EAE-affected mice over the course of light treatment experiments. Gene expression was quantified by qPCR. In both PLNs and SCs, the suppression protocol produced a significant down regulation of IFN-ɣ and TNF-α (pro-inflammatory cytokines), and a significant up-regulation of IL-4 and IL-10 (anti-inflammatory cytokines) (Figure 4) [287].

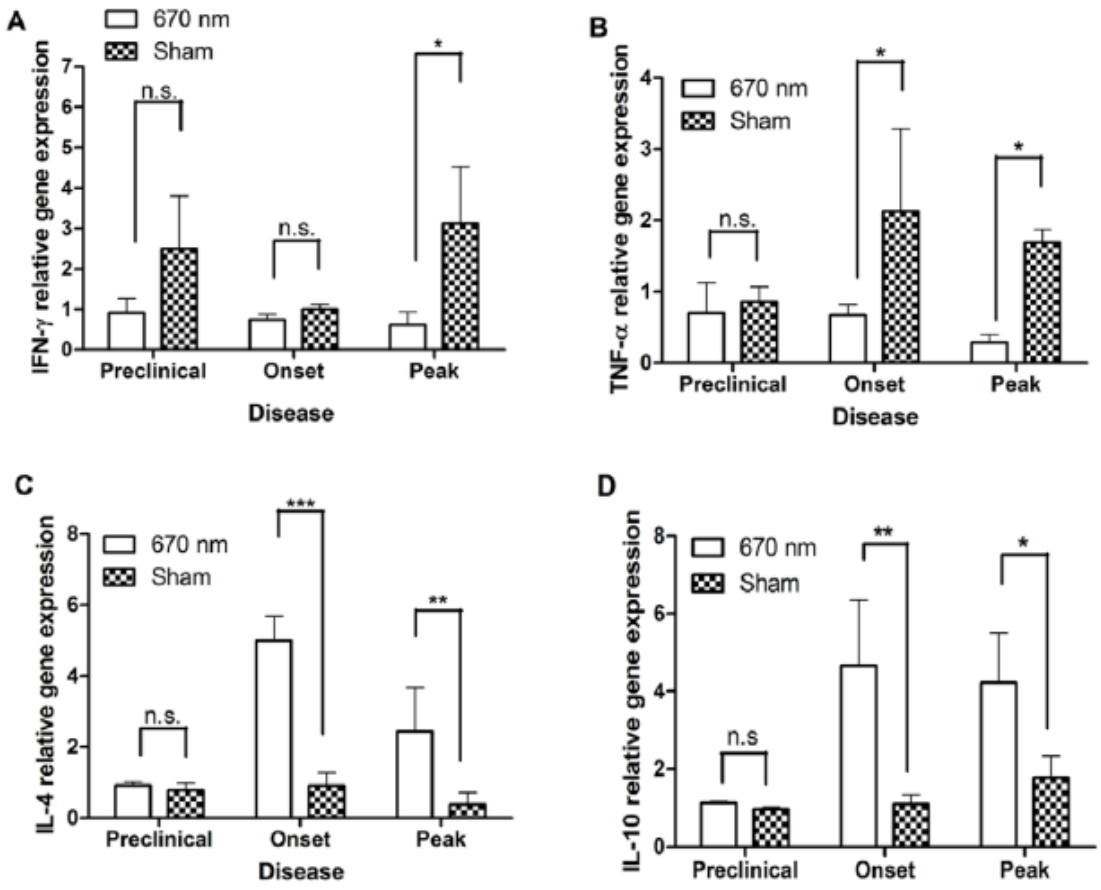

Figure 4. Modulation of immune response in EAE mice on PBM at 670 nm with suppression protocol. Suppression protocol on EAE-induced mice produced a significant reduction during chronic stage of disease on IFN-γ **(A)** and significant reduction in both acute and chronic stages of disease on TNF-α **(B)**, IL-4 **(C)** and IL-10 **(D)** [287].

On the other hand, the double-treatment protocol did not produce significant changes in IFN-ɣ and TNF-α at any point of the disease (Figure 5), but it did produce a significant up-regulation of IL-4 (during the acute stage) and IL-10 (during the chronic stage) (Figure 5) [287]. Even though the double treatment protocol did not produce significant changes in the levels of pro-inflammatory cytokines, it is important to point out that the up regulation of IL-4 and IL-10 was approximately 100 times increased. This huge increase in the expression of anti-inflammatory cytokines correlates the reduction of clinical severity showed in EAE mice that received the double treatment protocol (Figure 5) [287].

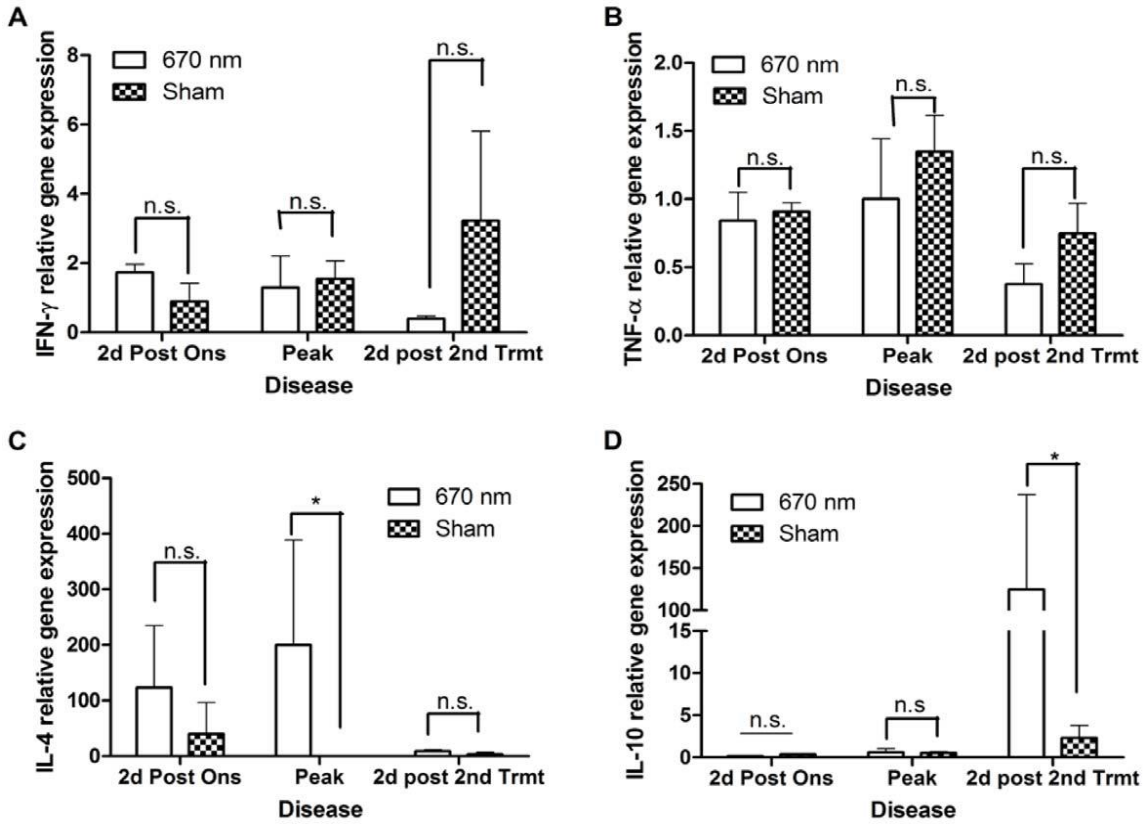

Figure 5. Modulation of immune response in EAE mice on PBM at 670 nm with double treatment protocol. Double treatment protocol did not produce significant changes on IFN-γ (A) and TNF-α (B) at any at either acute or chronic stage of disease. Double treatment protocol produced a significant increase of IL-4 (C) and IL-10 (D) during the acute and chronic stages respectively [287].

Nitrosative stress and mitochondrial dysfunction are linked to the pathogenic progression of EAE and MS. The observed effect of PBM on the clinical course of EAE demonstrated a significant beneficial effect on the progression of disease. Thus, the effect of the double treatment protocol with 670 nm light on the modulation of nitrosative stress using the EAE model was evaluated. C57BL/6 mice were immunized with MOG_{35-55} and the PLN were removed at 10 days post immunization. The isolated lymphocytes were cultured with MOG_{35-55} or ConA and were light treated at 670 nm beginning 2 hours after plating cells and continuing every 24h, for a total of 96h. Extra sets of lymphocytes cultures with MOG_{35-55} or ConA without light treatment were used

as controls. The supernatants were collected every 24h and nitrite (NO_2^-) levels were measured using a colorimetric assay based on the Griess reaction. Cell cultures incubated with MOG_{35-55} receiving PBM treatment showed a significant reduction in NO_2^- over the course of the whole experiment in comparison to cells without PBM treatment ($P<0.0001$) (Figure 6). Interestingly, the lymphocytes incubated with ConA receiving PBM treatment showed a reduction in the levels of NO_2^- at 72h ($p<0.0001$). These results support previous findings suggesting that the effect of PBM was antigen specific [288].

The effect of PBM on iNOS gene expression over the course of EAE in light treated mice was also evaluated. Spinal cords were obtained from mice receiving the double treatment protocol over the course of the disease, and iNOS gene expression was analyzed by qPCR. The results showed no significant changes on iNOS expression during the acute phase of the disease, however there was a significant down-regulation in the chronic phase of the disease ($p<0.05$) (Figure 6) [288]. In order to further investigate the role of iNOS in the EAE model, iNOS knockout ($iNOS^{-/-}$) mice and WT C57BL/6 mice were immunized with MOG_{35-55} and were subjected to the double light treatment protocol. The double light treatment protocol produced amelioration in the clinical severity of the disease in WT mice but did not produce amelioration in $iNOS^{-/-}$ mice. These results suggest that the presence of NO produced by iNOS (NO-iNOS) is necessary in the beneficial effects of PBM in our model (Figure 6). To further investigate, LN-lymphocytes were obtained from MOG_{35-55} immunized $iNOS^{-/-}$ mice. The lymphocytes were incubated with MOG_{35-55} antigen or Con A and treated daily with light at 670 nm for a total of 96 h. The results showed no significant increase in nitrite

production at any time point in any of the cell cultures (data not included). Together, results obtained in vivo and *in vitro* suggest that the NO produced by iNOS is necessary for the amelioration of EAE by PBM [288].

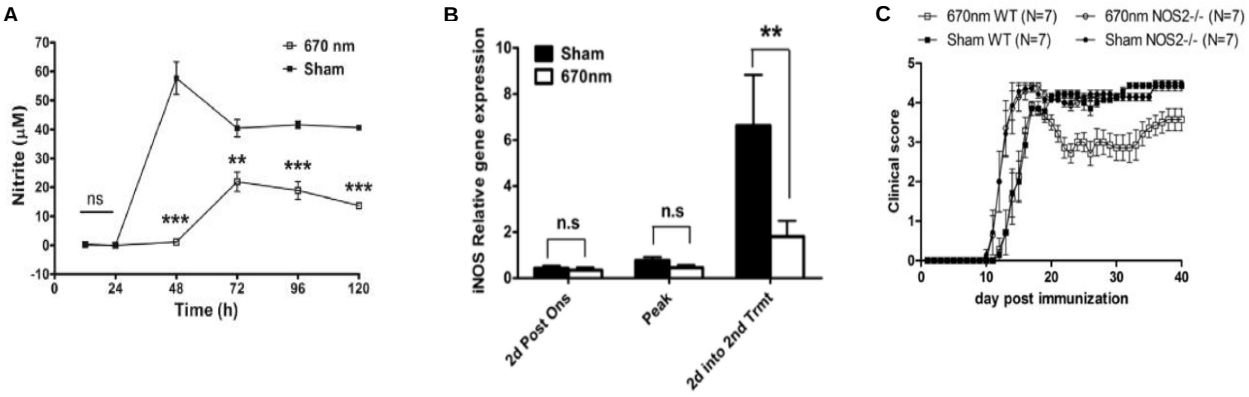

Figure 6. PBM at 670 nm reduces nitrosative stress. A). PBM at 670 significantly reduced NO_2^- in PLN-lymphocytes obtained from EAE-mice. B) Double treatment protocol on EAE mice produced a significant reduction in the gene expression of iNOS. C) Double treatment protocol did not reduce the clinical score on $iNOS^{-/-}$-EAE mice [288].

1.31 Photobiomodulation on chronic fatigue and muscle performance

Approximately 80% of MS subjects present with muscle weakness and fatigue due to a combination of events, including alterations in both the central motor drive and intramuscular function [223, 289-294]. Fatigue is additionally related to alterations in skeletal muscle, such as reduction in the size of muscle fibers and the levels of mitochondrial enzymes involved in energy production, including succinic dehydrogenase (SDH) and glyceraldehyde 3-phosphate dehydrogenase (GAPDH) [294]. Studies show that PBM reduces skeletal muscle fatigue, exercise-induced oxidative stress, improves strength, increases exercise performance, and enhances muscle rehabilitation [295-303].

PBM treatment of skeletal muscle improves muscle performance, delays and reduces skeletal muscle fatigue, and reduces the accumulation of biochemical markers related to muscle damage (i.e. creatine kinase activity, C-reactive protein, lactate dehydrogenase) [295-298]. The effect of PBM on muscle fatigue and performance was investigated in professional volleyball players. During the first session, all players performed as many voluntary biceps contractions as possible with a load of 75% of the maximal voluntary contraction force (MVC). One week later, players (N=12) were split into 2 groups, with one group received PBM (655nm, 20J, 6.7min) and the other receiving placebo before the exercise. The group that received active PBM showed a significant increase in the number of repetitions compared to session 1 compared the placebo group [295]. In further experiments, the authors tested PBM (810nm, 60J, 2.5min) on volleyball players in a crossover study to evaluate muscle performance and biochemical markers for muscle recovery [297]. PBM treatment produced an increase in exercise performance (number of repetitions), reduced muscle fatigue, and reduction in serum levels of creatine kinase activity and C-reactive protein [297] compared to placebo. Baroni et al., evaluated the effects of PBM on LDH and CK serum levels, both of which are direct markers of muscle damage [298]. PBMT (810nm, 180J, 6min, n=18) and placebo treatment (device turned off, n=18) were applied to the knee of healthy men before knee extensor eccentric exercise. PBM produced an increase in the maximal voluntary contraction (MVC) and significant reduction on the levels of LDH and CK at 24 and 48h in comparison with the placebo group [298]. Similarly, Toma et al., studied the effect of PBM treatment on skeletal muscle fatigue in elderly women (60-70 yoa) [299]. PBMT (808nm, 56J, 10min, n=12) and placebo treatment (device turned off,

n=12) were applied to the rectus femoris muscle of the dominant leg immediately before the fatigue protocol which consisted in voluntary isotonic contractions of knee flexion-extension performed with a load corresponding to 75% of one maximal repetition during 60s. Patients that received PBM treatment showed an increase in the number of repetitions in comparison with placebo [299]. All together these results showed the potential use of PBMT to improvement in muscle performance and faster recovery.

In a crossover study designed to evaluate the effect of PBMT on exercise performance and oxidative stress, 22 male untrained volunteers received PBM treatment (810nm, 30J, 2.5min) or placebo treatment 5min before a standardized progressive running protocol. PBM treatment compared to placebo improved exercise performance, reduced the super dismutase enzyme, lactate dehydrogenase (LDH), further supporting the ability of PBMT to improve in muscle performance and decrease exercise-induced oxidative stress [300].

In conclusion, PBM is a new alternative therapeutic approach with tremendous potential for the biomedical field, including the resolution of chronic inflammation and treatment of neurodegenerative diseases. Previous data from our lab showed that the application of 670 nm light modulated the mechanisms involved in EAE pathogenesis leading to amelioration of clinical signs. The next step in our line of research was to extrapolate these experiments to in vitro and in vivo assays using samples as well the participation from MS subjects. The goal of this project was to characterize the potential effect of PBM treatment on MS subjects. We hypothesized that PBM treatment would reduce pro-inflammatory cytokines, nitrosative stress, muscle fatigue, and increase anti-inflammatory cytokines in MS subjects.

CHAPTER 2. CHARACTERIZATION OF THE EFFECTS OF PHOTOBIOMDULATON ON IMMUNE CELLS OBTAINED FROM HEALTHY DONORS AND MULTIPLE SCLEROSIS SUBJECTS.

2.1 Abstract

Multiple Sclerosis (MS) is a CD4+ T cell-mediated demyelinating autoimmune disease characterized by the development of plaques in the central nervous system (CNS). Currently, there is no cure for MS. Available drug treatments focus on the modulation of the immune response during initial stages of disease in order to slow down its progression but they are not effective in chronic stages. Therefore, the development of alternative approaches to effectively treat acute or chronic stages of disease is needed. Photobiomodulation (PBM) is a therapeutic approach proving effective at ameliorating various neurodegenerative conditions. It is proposed that the therapeutic effects of PBM are produced by the improvement of mitochondrial function, mediated by the absorption of VIS/NIR light by cytochrome c oxidase (CCO, complex IV). Previously our lab showed that PBM at 670nm on the Experimental Autoimmune Encephalopathy (EAE) model of MS, reduced IFN-ɣ and TNF-α and increased IL-4 and IL-10 which correlated with a reduction in the severity of disease.

Here we studied the effects of PBM on immune cells from MS subjects. Peripheral blood mononuclear cells (PBMC) and CD4+ T cells from MS subjects were activated with phytohemagglutinin (PHA) or CD3/CD28 activator, respectively, and received different PBM treatments. MS subjects were divided in 2 groups based on the Patient Determined Disease Steps (PDDS) scale: PPDS=0 and PDDS≥1. The results

revealed that the severity of disease affected the response to PBM. MS subjects with higher severity in disease (PDDS≥1) presented an anti-inflammatory effect after PBM treatment, while those with normal functions (PDDS=0) presented with a pro-inflammatory response. For instance, PBM treatment with 735nm light (3J/cm^2 or 10J/cm^2) and type 2b device (640/87/905nm, 1J/cm^2 or 3J/cm^2) increased the production of IFN-ɣ by CD4+ T cells and PBMC from MS subjects with PDDS=0, but not PDDS≥1. PBM with 670nm light (3J/cm^2) produced no change in IFN-ɣ production by PBMC and CD4+ T cells but increased in IL-10 by CD4+ T cells in MS subjects with PDDS≥1 but not PDDS=0. The results suggest that PBM has the potential to participate in the modulation of the immune response in MS subjects. The clinical stage of disease for each patient has to be considered before the administration of PBM treatment.

2.2 Introduction

Multiple Sclerosis (MS) is a CD4+ T cell-mediated autoimmune disease characterized by the development of plaques (lesions) in the central nervous system (CNS) [1]. The destruction of the myelin sheath interrupts the transmission of nerve impulses from the CNS to other parts of the body causing the symptoms of MS [2]. CD4+T cells are the main player in the pathogenesis of MS and its animal model, Experimental Autoimmune Encephalomyelitis (EAE). Naïve CD4+ T cells activated in the presence of myelin protein and IL-12 differentiate in Th1 cells, or in the presence of IL-6, TGF-β, and IL-23 differentiate to Th17 cells. Both Th1 and Th17 cell subtypes are considered pathogenic in MS and EAE because they promote the development and progression of disease through the production of pro-inflammatory cytokines. Th1 cells

produce TNF-α, IFN-γ and IL-2. Th17 cells produce IL-17, IL-6, IL-21, IL-22, and TNF-α [23, 38]. Studies demonstrated a positive correlation between high levels of IFN-ɣ and the clinical manifestation in EAE and MS [46-52]. Conversely, studies demonstrated the role of IL-10 in the amelioration of EAE and MS and EAE [86, 87].

Currently, there is no cure for MS. Current treatments focus on early stages of disease to suppress the immune system, but they are not effective in stopping the progression of disease nor are they effective against chronic disease. It is necessary to develop treatments to reduce progression and symptoms at any stage. Photobiomodulation (PBM) is a new therapeutic approach proven to be effective in the treatment of different pathologies, including wound healing, chronic inflammatory conditions, and neurological disorders [238]. In particular, PBM therapy is proving effective at ameliorating pathology and clinical severity for various neurodegenerative conditions, including traumatic brain injury (TBI), acute ischemic stroke (AIS), familial amyotrophic lateral sclerosis (FALS), spinal cord injury (SCI), Alzheimer disease (AD) and Parkinson disease (PD) [250, 259-268]. It is proposed that during PBM, VIS/NIR light is absorbed by cytochrome c oxidase (CCO, complex IV) leading to improvement of mitochondrial function and increased ATP production [239-242]. Our lab previously reported that PBM treatment with 670nm light of MOG-induced EAE in C57BL/6 mice reduced pro-inflammatory cytokines (IFN-ɣ, TNF-α) and nitrosative stress and increased anti-inflammatory cytokines (IL-4, IL-10), which correlated with a reduction in the severity of disease [287, 288]. Here, we report the first studies investigating the effect of PBM on cytokine production by peripheral blood mononuclear cells (PBMC) and $CD4^+$ T cells isolated from MS subjects and healthy donors. Based on data from our animal

studies, we hypothesized that PBM would reduce IFN-ɣ and increase IL-10 in PBMC and CD4+ T cells from MS subjects. We found that 735nm light (3J/cm^2 or 10J/cm^2) and type 2b device (640/87/905nm, 1J/cm^2 or 3J/cm^2) increased IFN-ɣ by CD4+ T cells and PBMC from MS subjects with PDDS=0. Meanwhile, 670nm light (3J/cm^2) increased IL-10 production by CD4+ T cells and produced no change in IFN-ɣ production by PBMC and CD4+ T cells in MS subjects with PDDS≥1.

2.3 Materials and Methods

Subject population. Recruitment of subjects was carried out following the guidelines of the Institutional Review Board of the University of Wisconsin Milwaukee (IRB# 18.020) and Marquette University (IRB# HR-1710020115). All patients were informed about the project and consent forms were signed by the patient and the lab personnel providing the information. Inclusion criteria (RRMS, n=23): Relapsing-remitting MS (RRMS) male and female subjects between 18-80 years of age with no history of relapse or immunosuppressive therapy in the previous 6 months. Any current disease-modifying treatment was recorded. Exclusion criteria: RRMS subjects with any current infection, any additional neurodegenerative, autoimmune, or mitochondrial disease. Healthy donors (control group, n=17) between 18-80 years of age with no history of neurodegenerative disease, autoimmune disease, or current infection were included (Table 3). Selection of RRMS and healthy donors was carried out using a questionnaire in order to evaluate optimal state of health. Measurement of hematocrit was performed before the collection of blood in order to document that anemia was not present. Hematocrit was obtained by finger stick. Briefly, the fingertip of the index finger was

wiped with an alcohol pad and pricked with a sterile lancet. The first 2-3 drops of blood were discarded and the hematocrit tube was filled until the two-thirds of capacity. Two hematocrit tubes were filled to validate results. One side of the tubes was sealed and spun down in a microhematocrit centrifuge for 5 min at high speed. Hematocrit values were measured using a ruled hematocrit reader. The normal ranges considered were: male 42-54%, female 38-46%.

Table 3. MS and Healthy subjects recruited.	
# Healthy men above 50yo=	1
# Healthy women above 50yo=	7
Total	8
# Healthy men below 50yo=	6
# Healthy women below 50yo=	3
Total	9
# MS men above 50yo=	2
# MS women above 50yo=	12
Total	14
# MS men below 50yo=	2
#MS women below 50yo=	7
Total	9
# Healthy subjects in total	17
# MS subjects in total	23
Total	40

MS subject classification. MS subjects were classified based on the Patient Determined disease steps (PDDS) scale. PDDS scale is a subject reported outcome of disability of multiple sclerosis. PDDS scale is based on motor and ambulatory dysfunction present in MS subjects. PDDS scale has 7 levels ranging from 0= normal to 6= Confined to wheelchair. A summary of PDDS scale is presented in Table 4, a complete PDDS scale form can be found in the indicated references [304, 305].

Table 4. Patient Determined disease steps (PDDS) scale [304, 305].		
Score	**Disability status**	**Characteristics**
0	**Normal**	Normal motor functions. Minor abnormalities on examination. The course is relapsing-remitting with a return to baseline with or without treatment.
1	**Mild disability**	Mild symptoms or dysfunctions present. No visible problems of gait. Some findings include: sensory abnormalities, minor incoordination, weakness, and fatigue. The pattern of disease is relapsing-remitting, but patients may not have a full return to baseline following attacks.
2	**Moderate disability**	Visible problems of gait present. Patients do not require ambulation aids. The pattern of disease is relapsing-remitting or progressive.
3	**Early cane**	Intermittent use of cane or other unilateral support. Patient use unilateral support for longer distances, but they are able to walk at least 25 feet without it. The pattern of disease is relapsing-remitting or progressive.
4	**Late cane**	Constant use of cane or unilateral support. Patients cannot walk 25 feet without support. Use of a scooter for greater distances The pattern of disease is relapsing remitting or progressive.
5	**Bilateral support**	Patients require bilateral support to walk 25 feet (eg, two canes or two crutches or a walker). They may use a scooter for greater distances. The pattern of disease is relapsing-remitting or progressive.
6	**Confined to wheelchair**	Constant use of a wheelchair or scooter. Patients may walk a few steps but are unable to walk 25 feet, even with bilateral support.
U	**Unclassifiable**	Patients who cannot be classified in any of the previous scores. Patients present significant cognitive or visual impairment, fatigue, bowel or bladder impairment, etc.

Cell isolation and cell culture conditions. Blood (50ml) from RRMS or healthy donors was drawn into vacutainer tubes containing EDTA (BD Vacutainer, Franklin lakes, NJ US). Peripheral blood mononuclear cells (PBMC) were isolated by ficoll-paque (MP-Biomedicals, Solon, OH) gradient centrifugation (400g, 30min) and washed with PBS. CD4+ T cells were isolated from PBMC using EasySep Human CD4+ T cell isolation kit (Stemcell Technologies, VA, CA) following manufacturer instructions. PBMC and CD4+ T cells were cultured (300,000 cells/ml) and activated with phytohemagglutinin (PHA 10µg/mL, MP-Biomedicals, Solon, OH) or CD3/CD28 complex (50µg/mL, Stemcell Technologies, Cambridge, MA), respectively in RPMI medium [supplemented with 10% FCS, penicillin (100U/ml)/streptomycin (100Mg/mL), L-glutamate (2mM), sodium pyruvate (0.1mM), 2-mecarptoethanol (50mM)] with 1% AB human serum and incubated at 37C, 10% CO_2. Cells received PBM treatment every 24h for a total of

120h. Cells and supernatants were collected at 48, 72 and 120h. Supernatants were stored at -80°C until analysis.

Photobiomodulation. Two types of light devices were used (Table 5). Type 1 devices emitted a continuous wave of light at 670, 735, or 830nm (VIS, light emitting diode [LED]) (Quantum Devices, Barneveld, WI). Type 2 devices emitted a pulsed wave of light (Multiradiance Medical, Solon OH). Type 2 devices were divided in two groups depending on the wavelengths delivered. Type 2A delivers a single pulsed wavelength at 640nm (VIS, light emitting diode [LED]). Type 2B delivered 3 pulsed wavelengths simultaneously: 640nm (VIS, light emitting diode [LED]), 875nm (NIR; LED) and 905nm light (NIR; super-pulsed Galium Arsenic laser). Dosing parameters applied for each device are summarized in Table 5. All PBM treatments were applied every 24h for a total of 120h starting 2h after initial plating. Light devices were placed on the top of the covered cell culture plate during treatment.

Table 5. Photobiomodulation parameters

Wavelength	Device	Power Density (W/cm^2)	Time (sec)	Energy Density (J/cm^2)
670 nm	LED (QBMI Spectralife, $75cm^2$)	0.010 W/cm^2	300 sec	3 J/cm^2
		0.028 W/cm^2	360 sec	10 J/cm^2
830 nm	LED (QBMI Spectralife, $75cm^2$)	0.010 W/cm^2	300 sec	3 J/cm^2
		0.0333 W/cm^2	300 sec	10 J/cm^2
735 nm	LED (QBMI Spectralife, $75cm^2$)	0.010 W/cm^2	300 sec	3 J/cm^2
		0.0333 W/cm^2	300 sec	10 J/cm^2
Type 2A 640 nm	Pulsed LED (MRM)	0.0025 W/cm^2	400 sec	1 J/cm^2
			1200 sec	3 J/cm^2
Type 2B 640 nm 875 nm 905 nm	LED LED Superpulsed laser (MRM)	0.033 W/cm^2	10 sec	0.3 J/cm^2
			31 sec	1 J/cm^2
			91 sec	3 J/cm^2
			304 sec	10 J/cm^2

Carboxyfluorescein diacetate succinimidyl ester (CFSE) staining. Cell proliferation resulting from the activation of PBMC with PHA (MP-Biomedicals, Solon, OH) and CD4+ T cells with CD3/CD28 activator (Stemcell Technologies, Cambridge, MA) was monitored every 24h by flow cytometry using CFSE staining. CFSE dye penetrates the cell membrane and binds to long-lived intracellular molecules to produce fluorescence. The fluorescence intensity is reduced by half in new clones during each cell division. The decreasing fluorescence intensity, indicative of cell division, is monitored by flow cytometry until 8 cell divisions, at which point the fluorescence is reduced to background of unstained cells [306]. CFSE staining was carried out following an standardized protocol [306]. Briefly, CFSE (LifeTechnologies, Eugene, OR) was diluted in DMSO to get a stock concentration of 5 mM. The PBMC or CD4 + T cells were suspended in PBS at $50x10^6$ cells/ml, and CFSE was added to obtain a concentration of 1µM. The cells with the CFSE were incubated for 5min at RT, washed 3 times with 10 volumes of PBS containing 5% (v/v) heat inactivated fetal calf serum (HI-FCS), and centrifuged at 500g for 10min at RT. The CFSE labeled cells (PBMC or CD4+ T cells) were cultured with PHA or CD3/CD28 activator accordingly, at 300,000 cells/well in 48wells/plate. PBM treatment was applied every 24h. The cells were harvested every 24h and cell proliferation analyzed by flow cytometry on a FACSCalibur (BD Biosciences, San Diego, CA). The decrease in the fluorescence intensity of CFSE was analyzed by FlowJo (FlowJo software LLC, Ashland, OR).

Flow cytometry. After CD4+ T isolation, flow cytometry staining was carried out in order to determine the purity of isolated cells. Cell purity was typically 90-95%. Surface markers used to identify cell populations included anti-human CD3 (T cells), anti-human CD4 ($CD4^+$ T cells), and anti-human CD19 (B cells) antibodies (BioLegend, San Diego, CA). Cell staining was performed using standardized protocols in our lab. Briefly, after CD4+ T isolation, 100,000 isolated CD4+ T cells were washed with FACS buffer (phosphate buffer saline, 0.1% sodium azide, 1% fetal bovine serum, 3000g, 5min), suspended in 100µL FACS buffer and split in 2 tubes (negative and positive staining). Next, 200µL of human Fc receptor binding inhibitor were added to each tube and incubated in ice for 20min. Cells were centrifuged and washed once with FACS buffer (3000g, 5min, 4°C). Cells were resuspended in 50µl FACS buffer, then the antibodies anti-human CD3, anti-human CD4, and anti-human CD19 antibodies were added (Positive Sample). Fluorochrome-matched mouse IgG isotype control antibodies (K, heavy, and light chain) were used as negative control. Cells were incubated on ice for 30min, and washed twice with FACS buffer. Cells were resuspended in 500µL FACS buffer and analyzed using a FACS Calibur flow cytometer. Data analysis was done based on 10,000 cells collected using BD Cell Quest Pro 5.1.1 software.

Cytokine quantification by ELISA. Collected supernatants were used for quantification of IL-10 (<31.3pg/mL detection limit) and IFN-ɣ (<15.6 pg/mL detection limit) by ELISA (Duoset Elisa, R&D systems, MN) following manufacturer instructions. Absorbance was measured using a plate reader (Bio-Tek, model KC4, Winooski, VT) at 450nm, levels of cytokines were calculated according to a standard curve.

Data analysis. Data were analyzed with GraphPad Prism 7 (La Jolla CA, USA). Statistical analysis was performed with SAS 9.4 (Cary, NC). Fisher exact test was performed as appropriate. $P<0.05$ was considered significant. Statistical analysis was carried out by Chi Cho, MS, in the college of Health Sciences, University of Wisconsin Milwaukee.

2.4 Results

Photobiomodulation treatment modulates cytokine production in PBMC and CD4+ T cells in MS subjects and healthy subjects.

Blood samples from healthy subjects were collected and PBMC and CD4+ T cells were isolated, activated, and received PBM treatment as indicated in materials and methods. We first investigated whether the effect of PBM on the modulation of cytokines differed between MS subjects and healthy subjects. In order to determine the effect of PBM treatment on cytokine production, the production of cytokines (IFN-ɣ or IL-10) after PBM treatment was obtained by subtracting the production of cytokines under no PBM treatment (no light treatment or control). Due to significant variation in the absolute values of IFN-ɣ and IL-10 detected, data was analyzed based on a ±20% change in cytokine production over the baseline (no light treatment). Significant results are summarized in Table 6. All other conditions tested failed to result in a significant difference in cytokine production between MS subjects and healthy donors.

Table 6. Photobiomodulation effect on cytokine production by PBMC and CD4+ cells from MS subjects and healthy donors.					
Cells cytokine	**Device**	**Energy Density (J/cm^2)**	**Time point**	**P value (Fisher exact test)**	**Outcome**
CD4-IFNɣ	670nm	10 J/cm^2	48h	0.042229	Significant
	Type 2B device (640/875/905nm)	3 J/cm^2	48h	0.031929	Significant
	Type 2B device (640/875/905nm)	10 J/cm^2	120h	0.012516	Significant
PBMC-IFNɣ	Single pulsed 640nm	3 J/cm^2	48h	0.021625	Significant
	Type 2B device (640/875/905nm)	0.3 J/cm^2	120h	0.040956	Significant
CD4-IL10	670nm	10 J/cm^2	72h	0.044509	Significant

Patient distributions for PBM treatments that showed significant results are presented in Tables 7 to 12. For instance, 670nm (10J/cm^2, 48h, Table 7) and Type 2b device 3J/cm^2, 48h, Table 8) increased IFN-ɣ by CD4 T cells in 41.67% and 54.55% of MS subjects respectively. The response from healthy donors was mixed, with cells from the majority of subjects increasing IFN-ɣ in response to this dose of 670nm light.

Table 7. Effect of 670nm (10J/cm^2, 48h) on IFN-ɣ production by CD4+ T cells from MS subjects and healthy donors - Patient distribution. P=0.042229 (Fisher exact test).				
Patient	**Increase 20%**	**NO CHANGE (-20% TO 20%)**	**Reduction 20%**	**Total**
Healthy	7 46.67%	3 20.00%	5 33.33%	15
MS	5 41.67%	7 58.33%	0 0.00%	12
Total	12	10	5	27

Table 8. Effect of Type 2B device (640/875/905nm, 3J/cm^2, 48h) on IFN-ɣ production by CD4+ T cells from MS subjects and healthy donors - Patient distribution. P= 0.031929 (Fisher exact test).				
Patient	**Increase 20%**	**NO CHANGE (-20% TO 20%)**	**Reduction 20%**	**Total**
Healthy	5 35.71%	8 57.14%	1 7.14%	14
MS	6 54.55%	1 9.09%	4 36.36%	11
Total	11	9	5	25

Table 9. Effect of Type 2B device (640/875/905nm, 10J/cm^2, 120h) on IFN-ɣ production by CD4 +T cells from MS subjects and healthy donors - Patient Distribution. P= 0.012516 (Fisher exact test).				
Patient	**Increase 20%**	**NO CHANGE (-20% TO 20%)**	**Reduction 20%**	**Total**
Healthy	2 18.18%	6 54.55%	3 27.27%	11
MS	6 75.00%	0 0.00%	2 25.00%	8
Total	8	6	5	19

Table 10. Effect of single pulsed 640nm (3J/cm^2, 48h) on IFN-ɣ production by PBMC from MS subjects and healthy donors – Patient distribution. P= 0.021625 (Fisher exact test).				
Patient	**Increase 20%**	**NO CHANGE (-20% TO 20%)**	**Reduction 20%**	**Total**
Healthy	3 20.00%	4 26.67%	8 53.33%	15
MS	5 33.33%	9 60.00%	1 6.67%	15
Total	8	13	9	30

Table 11. Effect of Type 2B device (640/875/905nm, 0.3 J/cm^2, 120h) on IFN-ɣ production by PBMC from MS subjects and healthy donors – Patient distribution. P= 0.040956 (Fisher exact test).				
Patients	**Increase 20%**	**NO CHANGE (-20% TO 20%)**	**Reduction 20%**	**Total**
Healthy	8 66.67%	4 33.33%	0 0.00%	12
MS	2 18.18%	7 63.64%	2 18.18%	11
Total	10	11	2	23

Table 12. Effect of 670nm (10 J/cm^2, 72h) on IL-10 production by CD4+ T cells from MS subjects and healthy donors – Patient distribution. P= 0.044509 (Fisher exact test).				
Patients	**Increase 20%**	**NO CHANGE (-20% TO 20%)**	**Reduction 20%**	**Total**
Healthy	0 0.00%	14 82.35%	3 17.65%	17
MS	6 28.57%	13 61.90%	2 9.52%	21
Total	6	27	5	38

Disease severity affects the response of MS subjects to Photobiomodulation treatment of PBMC and $CD4^+$ T cells.

Data in other systems suggests that the degree of pathology or severity of disease may affect the response to PBM treatment. To determine if this held true in MS, the response of MS subjects to PBM treatment was assessed to determine if it differed in subjects with no physical deficit (PDDS=0) compared to those with some level of disability (PDDS ≥1). Due to the variation in the absolute values of cytokine production, data was analyzed based on a ±20% change in cytokine production over the baseline (no light treatment). Significant results are summarized in Table 13.

Table 13. Photobiomodulation effect on cytokine production using ±20% cut-off point

Device	Energy Density (J/cm^2)	Treatment Time-point	Cells, cytokines	P value (Fisher exact test)	Outcome
830nm	10 J/cm^2	48 h	PBMC-IFNɣ	0.00979	SIGNIFICANT
Type 2B (640/875/905nm)	1 J/cm^2	48 h	CD4-IFNɣ	0.00476	SIGNIFICANT
735nm	10 J/cm^2	72 h	CD4-IFNɣ	0.04928	SIGNIFICANT

Patient distributions for PBM treatments that showed significant results are presented in Tables 14-16. In most cases, cells isolated from subjects with PDDS=0, did not respond to PBM therapy. On the contrary, although the response was variable, the cells isolated from majority of subjects with PDDS ≥1 responded to PBM treatment with changes in cytokine secretion. For instance, PBM with type 2B device (640/875/905nm, 1J/cm^2, 48h) 100% of MS subjects with PDDS≥1 showed increase in IFN-ɣ by CD4+ T cells, whereas 75% of subjects with PDDS=0 did not respond to this device with changes in IFN-ɣ secretion (Table 15). An exception was noted with treatment with the 735nm (10J/cm^2, 72h) device: 67% of subjects with PDDS=0 increased IFN-ɣ secretion

in response to this device, while 62.5% of MS subjects with PDDS≥1 showed reduction in IFN-ɣ by CD4+ T cells (Table 16).

Table 14. Effect of 830nm (10J/cm^2, 48h) on IFN-ɣ production by PBMC from MS subjects with PDDS=0 vs PDDS≥1. Patient distribution. P=0.00979 (Fisher exact test).				
PDDS	**Increase 20%**	**NO CHANGE (-20% TO 20%)**	**Reduction 20%**	**Total**
0	0 0.00%	4 100.00%	0 0.00%	4
1	4 44.44%	1 11.11%	4 44.44%	9
Total	4	5	4	13

Table 15. Effect of Type 2B device (640/875/905nm, 1J/cm^2, 48h) on IFN-ɣ production by CD4+ T cells from MS subjects with PDDS=0 vs PDDS≥1. Patient distribution. P= 0.00476 (Fisher exact test).				
PDDS	**Increase 20%**	**NO CHANGE (-20% TO 20%)**	**Reduction 20%**	**Total**
0	0 0.00%	3 75.00%	1 25.00%	4
1	6 100.00%	0 0.00%	0 0.00%	6
Total	6	3	1	10

Table 16. Effect of 735nm, 10J/cm^2, 72h) on IFN-ɣ production by CD4+ T cells from MS subjects with PDDS=0 vs PDDS≥1. Patient distribution. P=0.04928 (Fisher exact test).				
PDDS	**Increase 20%**	**NO CHANGE (-20% TO 20%)**	**Reduction 20%**	**Total**
0	4 66.67%	2 33.33%	0 0.00%	6
1	2 25.00%	1 12.50%	5 62.50%	8
Total	6	3	5	14

To further investigate the effect of disease severity on cytokine production after PBM treatment in our MS population, we evaluated the magnitude of cytokine production for each MS subject based on disease severity (PPDS score=0 vs, PDDS

≥1). Unlike the previous section, the ±20% cut-off point was not considered. Significant differences are summarized in Table 17.

Table 17. Photobiomodulation effect on cytokine production by PBMC and CD4+ T cells from MS subjects depending on disease severity PDDS=0 vs PDDS≥1.

Cells cytokines	Device	Energy Density (J/cm^2)	Time point	P value (Fisher exact test)	Outcome
CD4+ T IFNɣ	670nm	3 J/cm^2	48h	0.018163	significant
	Type 2B device (640/875/905nm)	1 J/cm^2	48h	0.014214	significant
	735nm	10 J/cm^2	72h	0.016925	significant
	735nm	3 J/cm^2	120h	0.008010	significant
PBMC IFN-ɣ	735nm	3 J/cm^2	48h	0.037243	significant
	Type 2B device (640/875/905nm)	1 J/cm^2	120h	0.002856	significant
	Type 2B device (640/875/905nm)	3 J/cm^2	120h	0.014668	significant
CD4+ T IL-10	670nm	3 J/cm^2	72h	0.039170	significant

Analysis revealed that the nature and magnitude of the response of cells to particular devices and to particular doses of light differed in subjects with PDDS=0 vs. PDDS≥ (Figures 7-10). CD4+ T cells isolated from subjects with PDDS≥1 produced significantly greater IFN-ɣ in response to the 670nm device (3J/cm^2, at 48h, p=0.018163) and type 2b device (640/875/905nm, 1J/cm^2, at 48h, p=0.014214) than did cells from MS subjects with PDDS=0. Similarly, PBM with the 735nm device (3J/cm^2, at 48h, p=0.037243), increased IFN-ɣ production by PBMC in MS subjects with PDDS≥1 in comparison with cells from MS subjects with PDDS=0 (Figure 7). Conversely, cells from subjects with PDDS=0 produced a greater response to 735nm light at a higher dose (10J/cm^2, 72h, p=0.016925) and 3J/cm^2 (at 120h, p=0.008010) than did cells from subjects with PDDS≥1 (Figure 8).

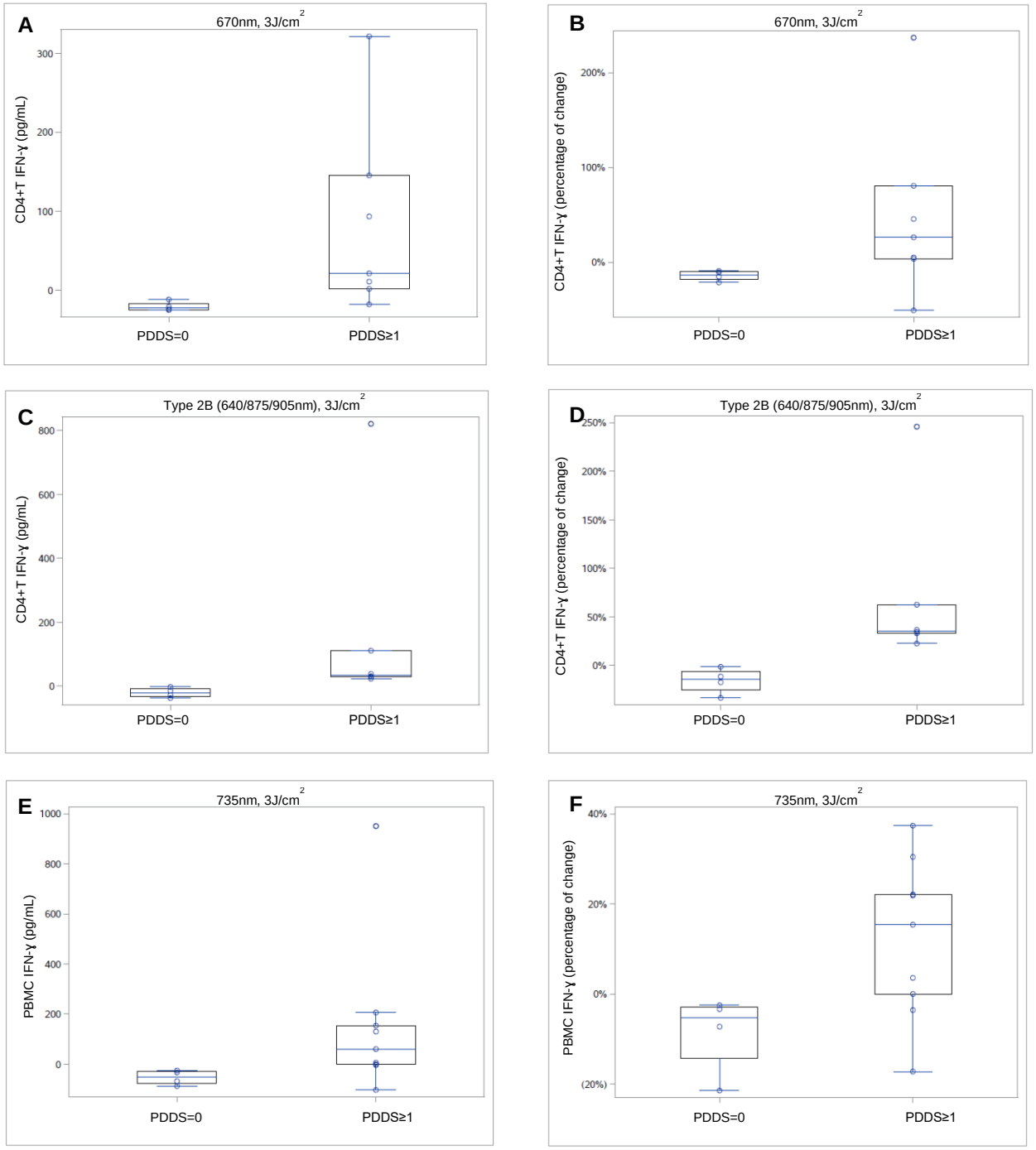

Figure 7. Comparison of PBM treatment effect on IFN-ɣ production by CD4+ T cells and PBMC cells at 48h from MS subjects with PPDS=0 and PDDS≥1. 670nm, (3J/cm^2, CD4 T cells, p=0.018163), A) change in pg/mL, B) percentage of change over baseline (no light treatment). Type 2b device (640/875/905nm, 1J/cm^2, CD4+ T cells, p=0.014214), C) change in pg/mL, D) percentage of change over baseline (no light treatment). 735nm (3J/cm^2, PBMC, p=0.037243), E) change in pg/mL, F) percentage of change over baseline (no light treatment). Box represents interquartile range (75%-25%). The bar within the box is the median. The whiskers are 1.5x the interquartile range. Anything outside these bars is an outlier.

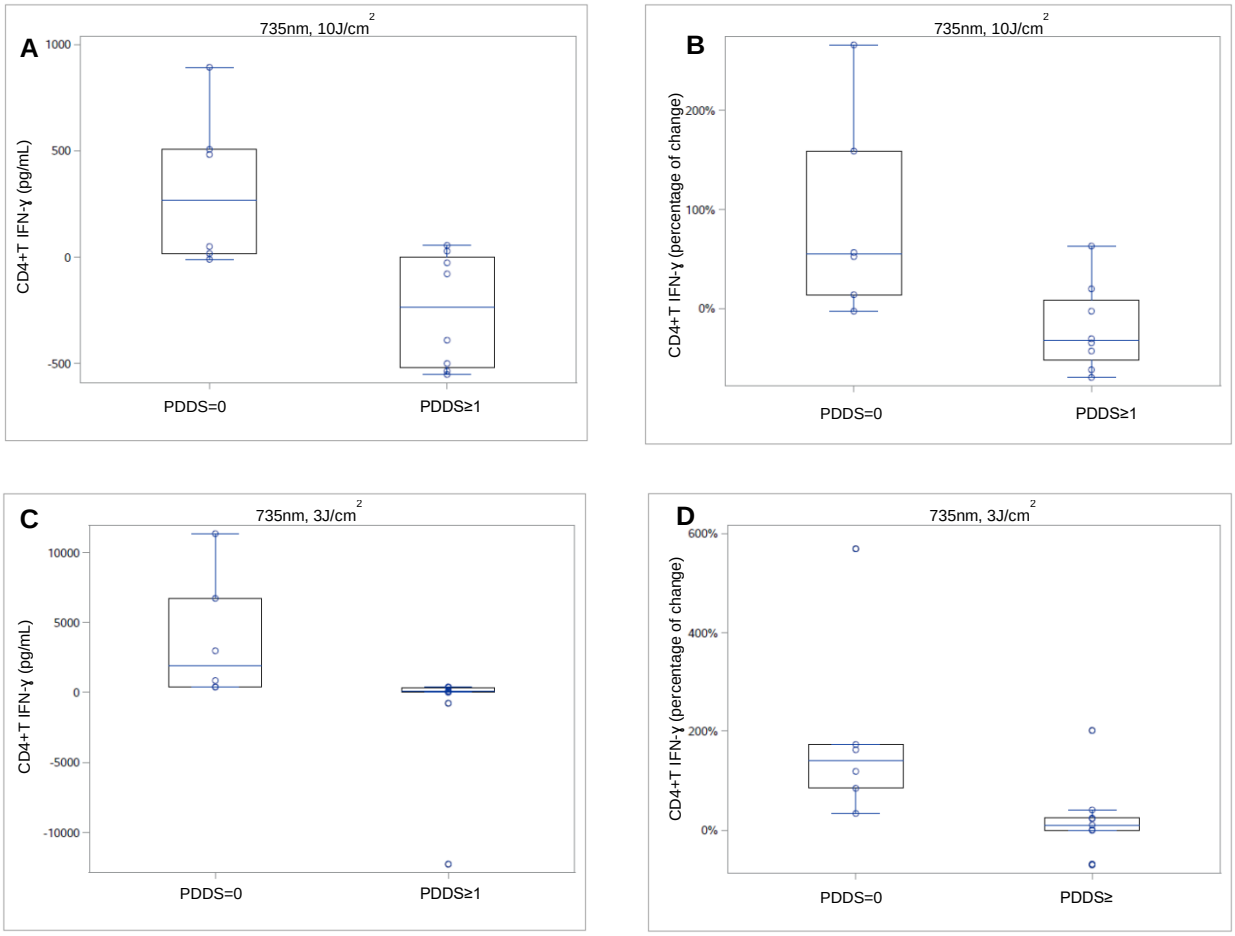

Figure 8. PBM treatment with 735nm on IFN-ɣ production by CD4 T cells. Energy density of 10J/cm^2 at 72h, A) change in pg/mL, B) percentage of change over baseline (no light treatment). Energy density of 3J/cm^2 at 120h, C) change in pg/mL, D) percentage of change over baseline (no light treatment). Box represents interquartile range (75%-25%). The bar within the box is the median. The whiskers are 1.5x the interquartile range. Anything outside these bars is an outlier.

A similar difference in the nature of the response was noted by PBMC from subjects with PDDS=0 vs. PDDS≥1 (Figure 9). Contrary to the response of $CD4^+$ T cells noted above, increased IFN-ɣ by PBMC from MS subjects with PDDS=0 was noted with the Type 2B device (640/875/905nm) at 1J/cm^2 (72h, p=0.002856) and 3J/cm^2 (120h, p=0.014668) but not MS subjects with PDDS≥1.

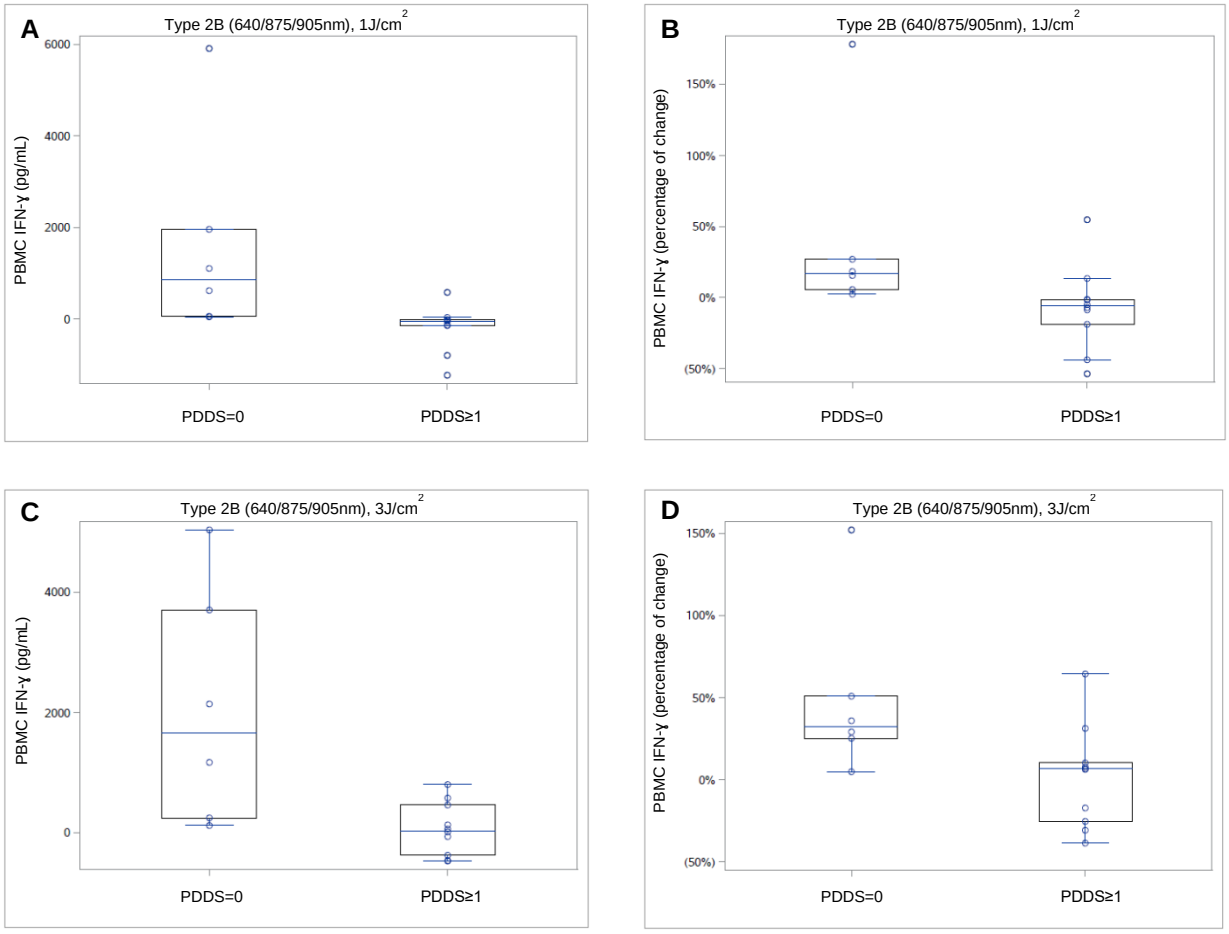

Figure 9. PBM treatment with active device on the production of IFN-ɣ by PBMC. Energy density of 1J/cm^2 at 120h, A) change in pg/mL, B) percentage of change over baseline (no light treatment). Energy density of 3J/cm^2 at 120h, C) change in pg/mL, D) percentage of change over baseline (no light treatment). Box represents interquartile range (75%-25%). The bar within the box is the median. The whiskers are 1.5x the interquartile range. Anything outside these bars is an outlier.

Of note, only PBM treatment with 670nm light at 3 J/cm^2 (72h, p= 0.039170) increase the production of anti-inflammatory IL-10 by CD4+ T cells from MS subjects with PDDS≥1. Furthermore, MS subjects with PDDS=0 responded with minimal change, or a decrease in IL-10 to this wavelength at this dose (Figure 10).

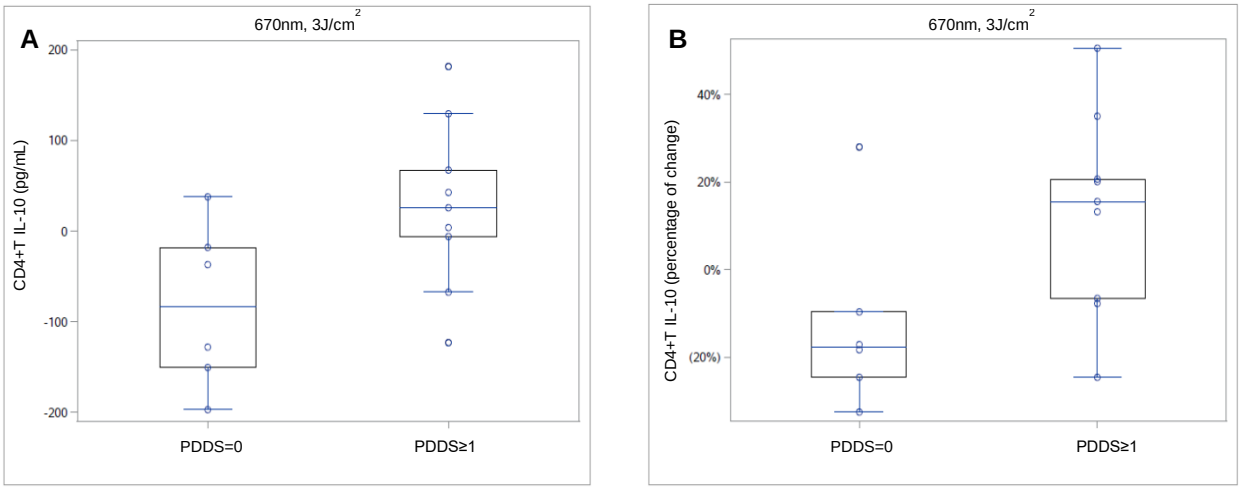

Figure 10. PBM treatment with 670nm increased IL-10 production by CD4 T cells from MS subjects with PDDS≥1. Energy density of 3J/cm^2 at 120h, A) change in pg/mL, B) percentage of change over baseline (no light treatment). Box represents interquartile range (75%-25%). The bar within the box is the median. The whiskers are 1.5x the interquartile range. Anything outside these bars is an outlier.

Discussion

Multiple Sclerosis (MS) is a CD4+ T autoimmune disease characterized by the development of plaques in the central nervous system (CNS) [1]. Photobiomodulation (PBM) is proven to be effective at ameliorating different neurodegenerative conditions [250, 259-268]. Previously, our lab reported that PBM at 670nm was effective in ameliorating the clinical severity in mice with EAE [287]. MOG_{35-55} immunized C57BL/6 mice receiving PBM treatment at 670nm (5J/cm^2) for a total of 10 days starting the day after immunization (suppression protocol) presented with a significant reduction in the clinical severity of the disease in comparison with controls [287]. In addition, MOG_{35-55} immunized C57BL/6 mice that received a PBM treatment for 7 days starting with the day of onset of clinical signs, followed by a period of 7 days without light treatment, with

light treatment resuming on days 8 through 14 (double treatment protocol) presented significant reduction in the severity of disease in comparison with controls. RT-PCR analysis of spinal cords and lymph nodes collected during the course of experiments showed that suppression protocol down-regulated IFN-ɣ and TNF-α, and up-regulated IL-4 and IL-10 during the onset and peak of disease [287]. Interestingly, the double-treatment protocol resulted in non-statistically significant but reproducible decreases in IFN-ɣ and TNF-α but significantly up-regulated IL-4 (during the acute stage) and IL-10 (during the chronic stage) [287].

The results presented here demonstrate that PBM is able to modulate cytokine production by PBMC and CD4+ cells from MS subjects. Contrary to our hypothesis, PBM also modulated cytokine production by cells isolated from healthy donors. These results support previous observations by others authors that indicated that PBM is able to produce an effect in both healthy and compromised systems [248, 249, 307-309]. First, we decided to evaluate if the modulation of cytokines was significantly different from the baseline (cells without PBM treatment). The absolute expression of cytokines (IFN-ɣ, IL-10) among subjects were quite different, thus data was analyzed based on a ±20% change in cytokine production over the baseline (no light treatment) to consider a significant change. The threshold for significance was set at ±20% based on changes expected in MS subjects over the course of disease and compared to healthy donors. Studies have indicated that MS subjects present higher levels of pro- and anti-inflammatory cytokines compared to matched healthy subjects. The increase in both pro and anti-inflammatory cytokines among MS subjects is quite variable depending of disease progression and remission periods [314-317]. CD4+ T cell isolated from healthy

donors and MS subjects showed increased IFN-ɣ in response to treatment with 670nm (10J/cm^2, 48h) and the type 2b device (640/875/905nm, 3J/cm^2, 48h). In addition, MS subjects samples also increased IFN-ɣ production by CD4+ T cells in response to the Type 2B device (640/875/905nm, 10J/cm^2, 120h) and increased IFN-ɣ production by PBMC in response to single pulsed 640nm (3J/cm^2, 48h), respectively. Healthy subjects showed increased IFN-ɣ by PBMC with Type 2B device (640/875/905nm, with 0.3 J/cm2 at 120h). Interestingly, 670nm (10J/cm^2, 72h) produced increased IL-10 produced by CD4+T cells in MS samples, but there was no significant change in samples from healthy subjects.

Analysis of data showed that the effect of PBM was different between healthy and MS subjects. Therefore, we evaluated if the modulation of cytokines significantly differed from the baseline (cells without PBM treatment) in MS subjects in relation to disease severity. Data was again analyzed based on a ±20% change in cytokine production over the baseline to be considered significant. MS subjects were divided in 2 groups—those with PPDS score=0 and those with a PDDS ≥1. The results showed that the disease severity (PDDS score) affects the response to PBM. 735nm (10J/cm^2, 72h) produced the reduction of IFN-ɣ by CD4+ T cells from MS subjects with PDDS≥1 but not subjects with PDDS=0. On the other hand, type 2B device (640/875/905nm, 1J/cm^2, 48h) and 735nm (10J/cm^2, 72h) increased IFN-ɣ production by CD4 T cells collected from MS subjects with PDDS≥1 and PDDS=0, respectively. These results suggest that PBM with 735nm (10J/cm^2) might be beneficial on patients with PDDS≥1 because it reduced the production of IFN-ɣ. Conversely, PBM with type 2B device (640/875/905nm, 1J/cm^2) and 735nm (10J/cm^2) would produce a negative effect on MS

due that they increase the production of IFN-ɣ by CD4 T cells in MS subjects with PDDS≥1 and PDDS=0, respectively.

The previous results showed that disease severity played a role in the modulatory effect of PBM on cytokines. Next, we evaluated if the cytokine production magnitude and regulation after PBM treatment in each MS subject were affected by disease severity. MS subjects were again divided in 2 groups: MS subjects with PPDS=0 and MS subjects with PDDS≥1. No cut-off point was considered. The results showed that disease severity plays a role in the levels of cytokine being produced and in the modulatory effect of PBM on cytokines. PBM treatment with 735nm (3 J/cm^2 at 120h, and 10J/cm^2 at 72h) and Type 2B device (640/875/905nm (1 and 3J/cm^2 at 120h) induced higher production of IFN-ɣ in CD4+ T cells and PBMC, respectively, in MS subjects with PDDS=0 in comparison with MS subjects with PDDS≥1. Interestingly, PBM with 670nm (3J/cm^2 at 72h) induced a higher production of IL-10 by CD4+ T cells from MS subjects with PDDS≥1, but not from subjects PDDS=0. These results indicate that the use of PBM with 670nm (3J/cm^2) on MS subjects with PDDS≥1 might be beneficial because it induces the production of the anti-inflammatory cytokine IL-10 and there is no significant increase in the pro-inflammatory cytokine IFN-ɣ. The fact that PBM treatment with 735nm and type 2b device (640/87/905nm) increased the production of IFN-ɣ by CD4+ T cells and PBMC in MS subjects with PDDS=0 will require further investigation in its potential effect on MS subjects. For some time, IFN-ɣ has been considered detrimental in MS due to its participation in the development and progression of MS and EAE MS [46-52]. However, several studies indicate that IFN-ɣ

can play a beneficial role in MS and EAE [53-65]. Thus, the increase of IFN-ɣ due to PBM treatment in MS subjects with PDDS=0 might be beneficial to ameliorate disease.

Our results agree with previous observations from other authors who indicated that the effect of PBM on a system depends on its redox status [248, 249, 307-309]. For instance, Karu group evaluated the changes in the absorption spectra of HeLa cells before and after PBM. PBM treatment (632.8nm, 103J/m^2) on HeLa cells with oxidized cytochrome c oxidase resulted in an initial reduction of cytochrome C oxidase, followed by oxidation (a bell shaped curve). Then, PBM treatment on HeLa cells with reduced cytochrome c oxidase resulted in an initial oxidation of the cytochrome c oxidase, followed by its reduction (inverted bell shaped curve). This suggested that the effect of PBM will depend of the redox status of a system [307]. Similarly, Huang group evaluated the effects of PBM under oxidative stress conditions. Primary cultured murine cortical neurons where incubated alone or with one of three oxidative stressors including hydrogen peroxide, cobalt chloride, and rotenone with or without PBM at 810nm, 3J/cm^2 [308]. The oxidative stressors increased ROS and reduced mitochondrial membrane potential and ATP production. PBM on cells alone (with no oxidative stressors) increased mitochondrial membrane potential and ATP production above baseline and a modest increase in ROS levels. Conversely, in conditions of cells with oxidative stress, PBM treatment increased mitochondrial membrane potential back to basal levels, increased ATP production, reduced high ROS levels, and reduced cell death. The results showed that PBM can reduce oxidative stress in compromised systems (oxidative stress conditions) but in healthy cells can increase ROS levels [308].

The fact that PBM induced the production of IFN-ɣ by CD4+ T cells in persons with MS with PDDS=0 and PDDS≥1 will require further investigation in the possible effect of IFN-ɣ on MS subjects. Due to its pro-inflammatory characteristics, IFN-ɣ is considered as one of the main players in the development and progression of MS and EAE. Studies demonstrated the positive correlation between the high levels of IFN-ɣ and the clinical manifestations, relapses, and disease stages in MS and EAE [46-52]. For instance, in a clinical trial, 18 RRMS subjects received recombinant IFN-ɣ at 3 different doses: low (1mcg); intermediate (30mcg); and high (1000mcg). The results showed that serum levels of IFN-ɣ were proportional to dose administrated. In addition, 7 out of 18 RRMS subjects presented exacerbation during the treatment [51].

On the contrary, several studies showed that IFN-ɣ can play a disease limiting role in MS and EAE [53-65]. For instance, several studies showed that IFN-ɣ can play a protective role in the EAE model using IFN-ɣ-KO mice. The lack of IFN-ɣ led to the development of EAE even in strains that are normally resistant to EAE [53-55, 63, 64]. In one study, the Billiau group evaluated the effect of anti-IFN-ɣ antibodies on EAE in mice [56]. Anti-IFN-ɣ antibodies were injected intraperitoneally into C57BL/6J mice on days -6, 0, 7, and 14 relative to the time of EAE induction. The mice treated with antibody mice developed EAE with higher, incidence and mortality in comparison with controls. Histological damage correlated with the clinical severity of the disease. These results suggested that anti-IFN-ɣ antibodies increased the severity of disease and therefore IFN-ɣ plays a protective role. Next the authors administrated intraperitoneally IFN-ɣ (rDNS-IFN-ɣ) to SJL/L mice on days -1, 0, 1, 3, 5, 7, and 9 relative to EAE induction. These mice presented with EAE with a reduced clinical score and mortality

rate in comparison with controls [56]. The authors suggested that IFN-ɣ can produce different effects based on local or systemic expression. The local IFN-ɣ promotes inflammation whereas the systemic IFN-ɣ produces an anti-inflammatory effect. The authors suggested that the anti-IFN-ɣ antibodies neutralized the systemic IFN-ɣ present in the circulatory and peripheral compartments but they were not able to reach the IFN-ɣ found in the CNS due to the blocking by the blood brain barrier. The neutralization of the systemic IFN-ɣ suppressed the protective role (anti-inflammatory) of IFN-ɣ leading a more severe EAE. Thus, the systemic IFN-ɣ present during EAE induction or development of EAE can play a disease-limiting role. This also explains how the administration of IFN-ɣ before the induction of EAE was useful to reduce the severity of disease [56]. Additional studies by Billiau group investigated the role of IFN-ɣ in a chronic relapsing remitting model of EAE using SJL/J mice [61]. Intraperitoneal injections of anti-IFN-ɣ antibody were administrated on days 21 and 27 (disease free interval) in EAE-induced SJL/J mice. These mice developed higher disease severity and faster progression of disease than the control group. The results suggested that the severity of disease was increased due to the administration of anti-IFN-ɣ antibody during the disease free period. This suggested that the IFN-ɣ produced during the disease free period participates in the protection against EAE [61]. Therefore, the use of PBM treatment during disease free periods in order to increase IFN-ɣ in MS subjects and its protective role in disease should be explored with extreme caution.

Our results showed that 670nmm ($3J/cm^2$, 120h, $p=0.039170$) increased IL-10 produced by CD4+T cells in MS subjects with PDDS≥1 in comparison with MS subjects with PDDS=0. This is important given the anti-inflammatory role of IL-10 in MS and

EAE. Studies demonstrate that IL-10 is an anti-inflammatory cytokine that produces a protective role in MS and EAE [86-88, 90]. For instance, Samilova et al. showed that IL-10 deficient mice, but not IL-4 deficient mice, developed accelerated EAE onset in comparison with WT mice [86]. Spontaneous recovery was present in WT and IL-4 deficient mice but recovery was not present in IL-10 deficient mice, suggesting that IL-10 is fundamental in the amelioration or recovery process [86]. In one study by Rodriguez et al., the authors quantified the levels of TNF-α, lL-10, and nitric oxide in serum and cerebrospinal fluid (CSF) from MS subjects before and during an active relapse. Their results showed that during the active relapse, MS subjects presented higher levels of TNF-α, lL-10, and nitric oxide in comparison to levels before the relapse and also in comparison with healthy subjects. The results suggested that Th1 and Th2 cell activations (pro- and anti-inflammatory responses) are present simultaneously during an active relapse [90].

In conclusion, the results presented here show the potential of PBM in the modulation of cytokines in MS subjects. The results suggest that PBM treatment on MS subjects must be applied with extreme caution. Due to the small size of our sample population and the variety in PDDS scores among MS subjects it was not possible to establish a definite wavelength or energy dose to modulate cytokine expression. Therefore, the specific wavelengths, the energy density, the clinical stage (disease severity) in combination with PPDS scores for each patient are some of the factors that need to be considered before the application and optimization of PBM treatment. In addition, the fact that PBM induces the modulation of cytokines (IFN-ɣ, IL-10) is remarkable. This suggests that in the same way that cytokines and PDDS scores are

used to monitor MS progression, and drug treatment efficacy, they could be used to monitor the effect of PBM treatment in MS subjects.

CHAPTER 3. CHARACTERIZATION OF THE EFFECTS OF PHOTOBIOMODULATION (PBM) ON NITROSATIVE STRESS IN MULTIPLE SCLEROSIS SUBJECTS.

3.1 Abstract

Multiple Sclerosis (MS) is a CD4+ T cell-mediated demyelinating autoimmune neurodegenerative disease that affects the central nervous system (CNS). Nitrosative stress and mitochondrial dysfunction are events present even in early stages of disease even before the myelin destruction. There is no a cure for MS. Current drug treatments focus on the modulation of the immune response during initial stages of disease in order to slow down progression but they are not effective in chronic stages where nitrosative stress takes control of disease progression. Therefore, alternative approaches to modulate immune response and nitrosative stress in early or chronic stages of disease are needed. Photobiomodulation (PBM) with light in the visible and near infrared regions of the spectrum is showing promise as a therapeutic strategy to treat chronic inflammation and neurological disorders. Previously our lab studied the effect of PBM with light at 670nm on the Experimental autoimmune encephalopathy (EAE) model of MS. 670nm light reduced nitrosative in in-vitro and in-vivo experiments using mice with EAE. The reduction in nitrosative stress correlated with the reduction in clinical severity of EAE. Here we evaluated the ability of PBM to reduce nitrosative stress in immune

cells from MS subjects. Peripheral blood mononuclear cells (PBMC) from MS subjects were activated with Phytohemagglutinin (PHA), and received PBM treatment. Supernatants were collected and used to measure nitrite (NO_2^-) levels. 830nm ($10J/cm^2$, 72h, p=0.0153) reduced the levels of nitrate compared to controls (no light treatment). The reduction in nitrate correlated with the increase in IL-10 by PBMC (p=0.0271) and reduction in IFN-ɣ by PBMC (not significant p=0.1940). PBM at 830nm has the potential to participate as a therapeutic tool in the reduction of nitrosative stress and modulation of immune response in MS.

3.2 Introduction

Multiple Sclerosis (MS) is a CD4+ T cell-mediated demyelinating autoimmune disease that affects the central nervous system (CNS) [1]. The destruction of the myelin sheath interrupts the transmission of nerve impulses from the CNS to other parts of the body causing the symptoms of MS [2]. Previous studies showed that nitrosative stress is present in early stages even before the myelin destruction [147, 178-184]. Under high concentration of Nitric oxide (NO), NO competes with oxygen for binding to Cytochrome c oxidase (CCO or complex IV), the enzyme that catalyzes the transfer of electrons from cytochrome c to molecular oxygen in mitochondrial electron transport, causing mitochondrial dysfunction and depletion of ATP [160-162].

There is not a cure for MS. Current drug treatments focus on the modulation of the immune response during initial stages of disease in order to slow down progression but they are not effective in chronic stages where nitrosative stress takes control of disease progression. Therefore, alternative approaches to modulate immune response

and nitrosative stress at any stage of disease are needed. Photobiomodulation (PBM) is a therapeutic approach proving effective in the amelioration of neurological disorders including traumatic brain injury (TBI), Alzheimer disease (AD) and Parkinson disease (PD) [238, 250, 259-268]. It is proposed that during PBM treatment, VIS/NIR light is absorbed by cytochrome c oxidase (CCO) improving mitochondrial function and increasing ATP production [239-242].

Our lab previously reported that PBM treatment with light at 670nm ameliorated clinical severity and reduced nitrosative stress in the Experimental Autoimmune Encephalomyelitis (EAE) model of MS [288]. Here, we extend these studies to the clinical disease, MS. We investigated the effect of PBM treatment on nitrite production by peripheral blood mononuclear cells (PBMC) from MS subjects as a marker of nitrosative stress. We hypothesized that PBM would reduce nitrite, indicative of decreased nitrosative stress. We observed that *in vitro* PBM therapy of PBMC treated with 830nm light at 10J/cm^2) reduced nitrite production in comparison with cells not receiving light treatment. This reduction correlated with increased in IL-10 and reduced IFN-ɣ secretion by PBMC.

3.3 Materials and Methods

Subject population. Recruitment of subjects was carried out following the guidelines of the Institutional Review Board of the University of Wisconsin Milwaukee (IRB# 18.020) and Marquette University (IRB# HR-1710020115). All subjects were informed about the project and consent forms were signed by the patient and the lab personal providing the information. Inclusion criteria: RRMS subjects (n=23; male=4, female=19) between 18-

80 years of age with no history of relapse or immunosuppressive therapy in the previous 6 months. Any current disease modifying therapy was recorded. Exclusion criteria: RRMS subjects with any current infection, any additional neurodegenerative, autoimmune, or mitochondrial disease. Selection of RRMS was carried out using a questionnaire in order to evaluate optimal state of health. Measurement of hematocrit was performed before the collection of blood in order to rule out the presence of anemia. Hematocrit was obtained by finger stick. Briefly, the fingertip of the index finger was wiped with an alcohol pad and pricked with a sterile lancet. The first 2-3 drops of blood were discarded and the hematocrit tube was filled until the two-thirds of capacity. Two hematocrit tubes were filled to validate results. One side of the tubes was sealed and spun down in a microhematocrit centrifuge for 5 min at high speed. Hematocrit values were measured in a hematocrit reader (ruled apparatus). Normal ranges considered: male 42-54%, female 38-46%.

MS patient classification. MS subjects were classified based on the Patient Determined disease steps (PDDS) scale. PDDS scale is a patient reported outcome of disability of multiple sclerosis. PDDS scale is based on motor and ambulatory dysfunction present in MS subjects. PDDS scale has 7 levels ranging from 0= normal to 6= Confined to wheelchair (Table 4) [304, 305].

Cell isolation and cell culture conditions. Blood (50ml) from RRMS were drawn in EDTA tubes (BD Vacutainer, NJ US). Peripheral blood mononuclear cells (PBMC) were isolated by ficoll-paque (MP-Biomedicals, Solon, OH) gradient centrifugation (400g, 30min) and washed with PBS. PBMC were cultured (300,000 cells/ml) and activated

with phytohemagglutinin (PHA, 10µg/mL, MP-Biomedicals, Solon, OH) in RPMI medium [supplemented with 10% FCS, penicillin (100U/ml)/streptomycin (100Mg/mL), L-glutamate (2mM), sodium pyruvate (0.1mM), 2-mecarptoethanol (50mM)] with 1% AB human serum and incubated at 37C, 10% CO_2. Cells received PBM treatment every 24h for a total of 120h. Supernatants were collected at 48, 72 and 120h and stored at -80°C until analysis.

Photobiomodulation. Two types of light devices were used (Table 5). Type 1 devices. Continuous wave devices at: 670, 735, and 830nm (VIS, light emitting diode [LED]) (Quantum Devices, Barneveld, WI). Doses of energy applied: 3 and 10J/cm^2, 300s. Type 2 devices. Pulsed wave devices (Multiradiance Medical, Solon OH). Type 2 devices were divided in two groups depending on the wavelengths delivered. Type 2A delivers a single pulsed wavelength at 640nm (VIS, light emitting diode [LED]). Doses of energy applied: 3 and 10J/cm^2. Type 2B delivers 3 pulsed wavelengths at the same time, these include: 640nm (VIS, light emitting diode [LED]), 875nm (NIR; LED) and 905nm light (NIR; super-pulsed Galium Arsenic laser). Doses of energy applied: 0.3, 1, 3 and 10 J/cm^2. All PBM treatments were applied every 24h for a total of 120h starting 2h after initial platting.

Nitrite quantification. Nitric oxide has a short half-life making almost impossible to quantify directly. The measurement of its final oxidized products nitrite (NO_2^-) and nitrate (NO_3^-), the final oxidized products of NO, provide an indirect method to measure nitric oxide. Supernatants were used to measure nitrite (NO_2^-) using the fluorometric

assay OxiSelect In Vitro Nitric Oxide (Nitrite / Nitrate) Assay Kit (Cell Biolabs, San Diego CA). The levels of nitrite were calculated according to a standard curve (<0.547 μM detection limit). Briefly, the nitrate (NO_3^-) in the sample is converted to nitrite (NO_2^-) by the nitrate reductase enzyme, and the amount of nitrite produced is detected with the fluorescent probe, DAN (2,3-diaminonapthalene). The fluorescence was measured using a plate reader equipped for excitation in the 360-365nm range and for emission in the 430-450nm range.

Data analysis. Data were analyzed with GraphPad Prism 7 (La Jolla CA, USA). Statistical analysis was performed with SAS 9.4 (Cary, NC). Multiple comparisons performed by Wilcoxon signed rank test, Chi-Square Test for Equal Proportions, and Fisher exact test were performed as appropriate. $P<0.05$ was considered significant. Statistical analysis was carried out by Chi Cho, MS, in the college of Health Sciences, University of Wisconsin Milwaukee.

3.4 Results

Photobiomodulation by 830nm and 640nm reduces nitrite production in vitro by PBMC from MS subjects.

To investigate the effect of PBM on nitrosative stress in MS, we determined if light treatment could reduce nitrite production by PMBC isolated from MS subjects. PBMC from MS subjects were cultured with phytohemagglutinin (PHA) and received different PBM treatments every 24h for a total of 120h (Table 5). Nitrite production was measured in cell culture supernatants using a fluorometric assay. Data showed that at

72h PBMC that received PBM treatment at 830nm (10J/cm^2, p=0.0153, Wilcoxon signed rank test) reduced the levels of nitrite in comparison with no light controls (Figure 11). No other PBM light treatments tested significantly reduced nitrite production in the cultures.

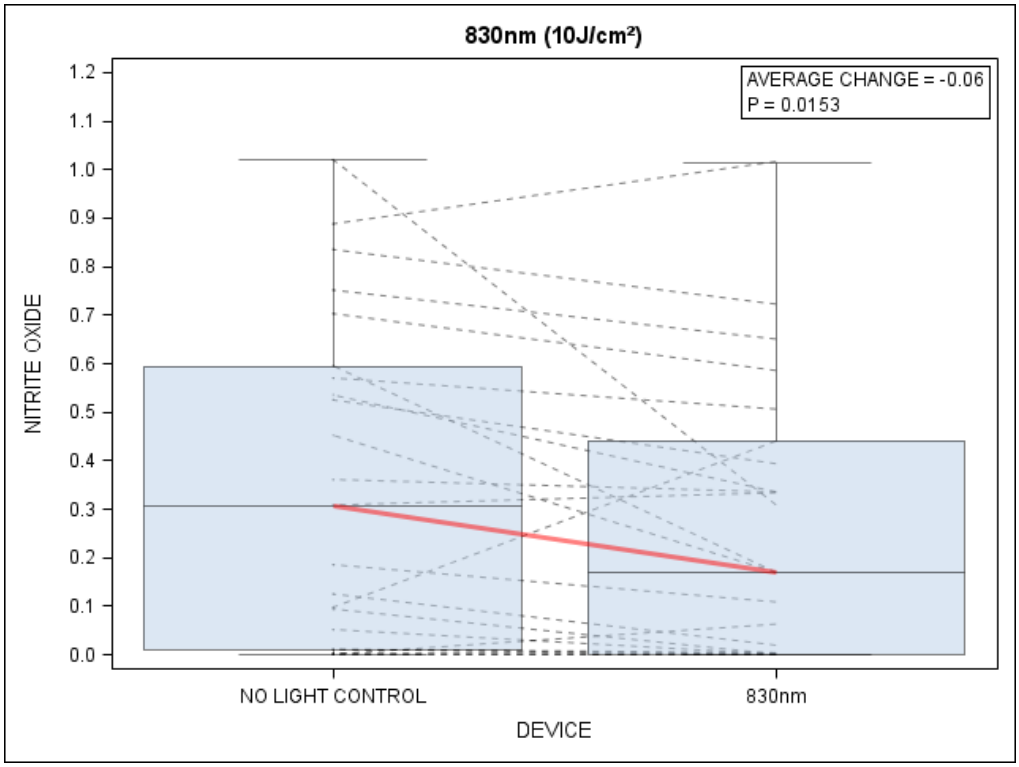

Figure 11. Photobiomodulation reduces nitrite production by PBMC from MS subjects. PBMC from MS subjects were cultured with phytohemagglutinin (PHA 10µg/mL). Cells received PBM treatment as indicated in materials and methods. At 72h continuous wavelength at 830nm (10J/cm^2, p=0.0153) reduced nitrite in comparison with controls (no light treatment). Each box represents interquartile range (75%-25%). The bar within the box is the median. The whiskers are 1.5x the interquartile range. Each line represent a MS subject and shows how they changed after PBM treatment. The red line shows the change in the average of nitrite with no light treatment (control) and after PBM treatment.

PBM induced reduction on nitrite production by PBMC correlates with the PBM-modulation of pro- and anti- inflammatory cytokines in MS subjects

Results in Chapter 2 showed that PBM treatment resulted in the modulation of pro-(IFN-ɣ) and anti-(IL-10) inflammatory cytokines produced by PBMC. In order to further evaluate the effect of PBM treatments on cytokine modulation and nitrite production, we investigated possible relationships between them. We analyzed nitrite production versus IL-10 and IFN-ɣ produced by PBMC. Photobiomodulation treatment with 830nm (10J/cm^2, at 72h) produced both a reduction in nitrite and an increase in IL-10 produced by PBMC ($p=0.0271$, Chi-Square Test for Equal Proportions) Figure 12, Table 18. In addition, 830nm (10J/cm^2, at 72h) produced a reduction in both nitrite levels and IFN-ɣ produced by PBMC, however this reduction was not significant ($p=0.1940$) Figure 13, Table 19.

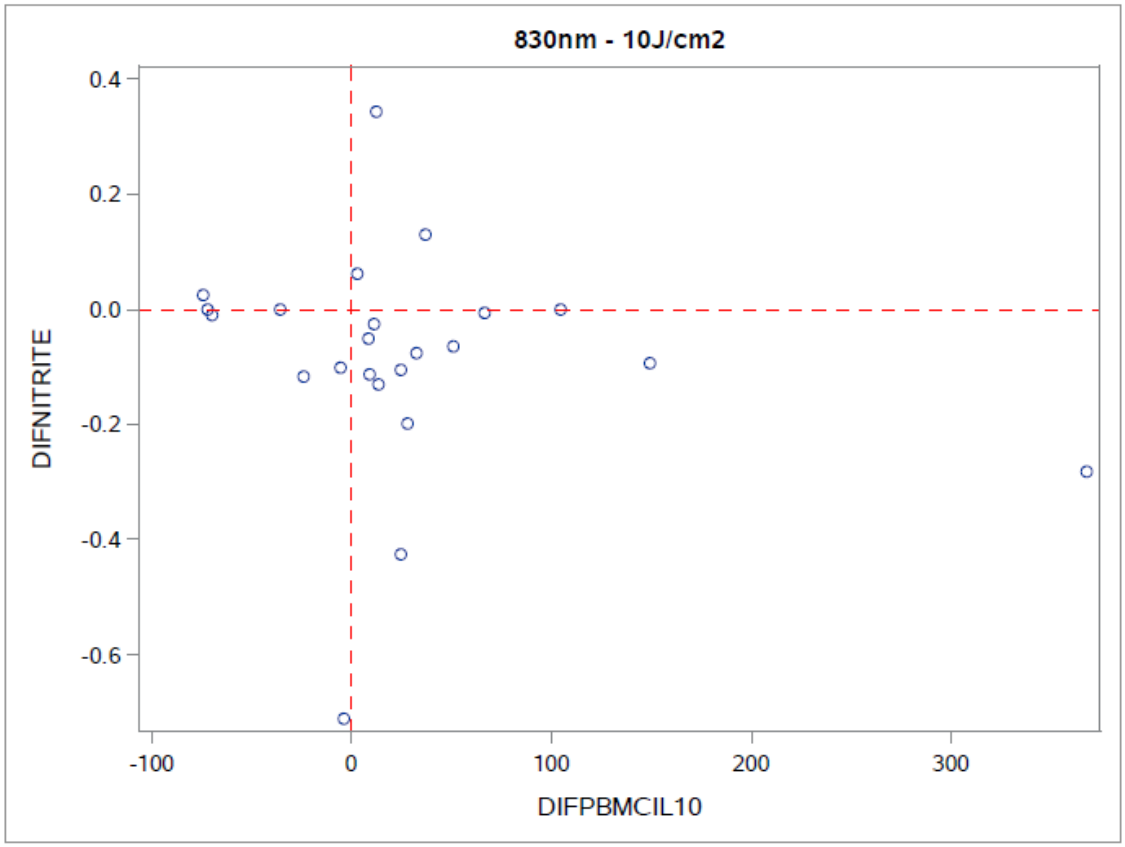

Figure 12. 830 nm (10J/cm^2, 72h) reduces nitrite and IL-10 production by PBMC from MS subjects. Analysis of data showed that there is a correlation between the reduction of nitrite and reduction of IL-10 by PBMC (p=0.0.0271). DIFNITRITE= difference in nitrite between 830nm and no-light treatment (control). DIFPBMCIL10= difference in PBMC-IL10 between 830nm and no-light treatment (control). The red lines are set at 0 for both axes, if the value is positive it means that the production is higher after 830nm than with no light treatment (control). If the number is negative then the production if lower after 830nm thank with no light treatment (control).

Table 18. Relationship between Nitrite production and IL-10 production by PBMC, 830nm 10/cm^2, 72h, n=23, p=0.0271 (Chi-Square Test for Equal Proportions)		
	Frequency	**Percent**
Increase Nitrite / Increase PBMC-IL10	4	17.39
Decrease Nitrite / Increase PBMC-IL10	12	52.17
Decrease Nitrite / Decrease PBMC-IL10	4	17.39
Increase Nitrite / Decrease PBMC-IL10	3	13.04

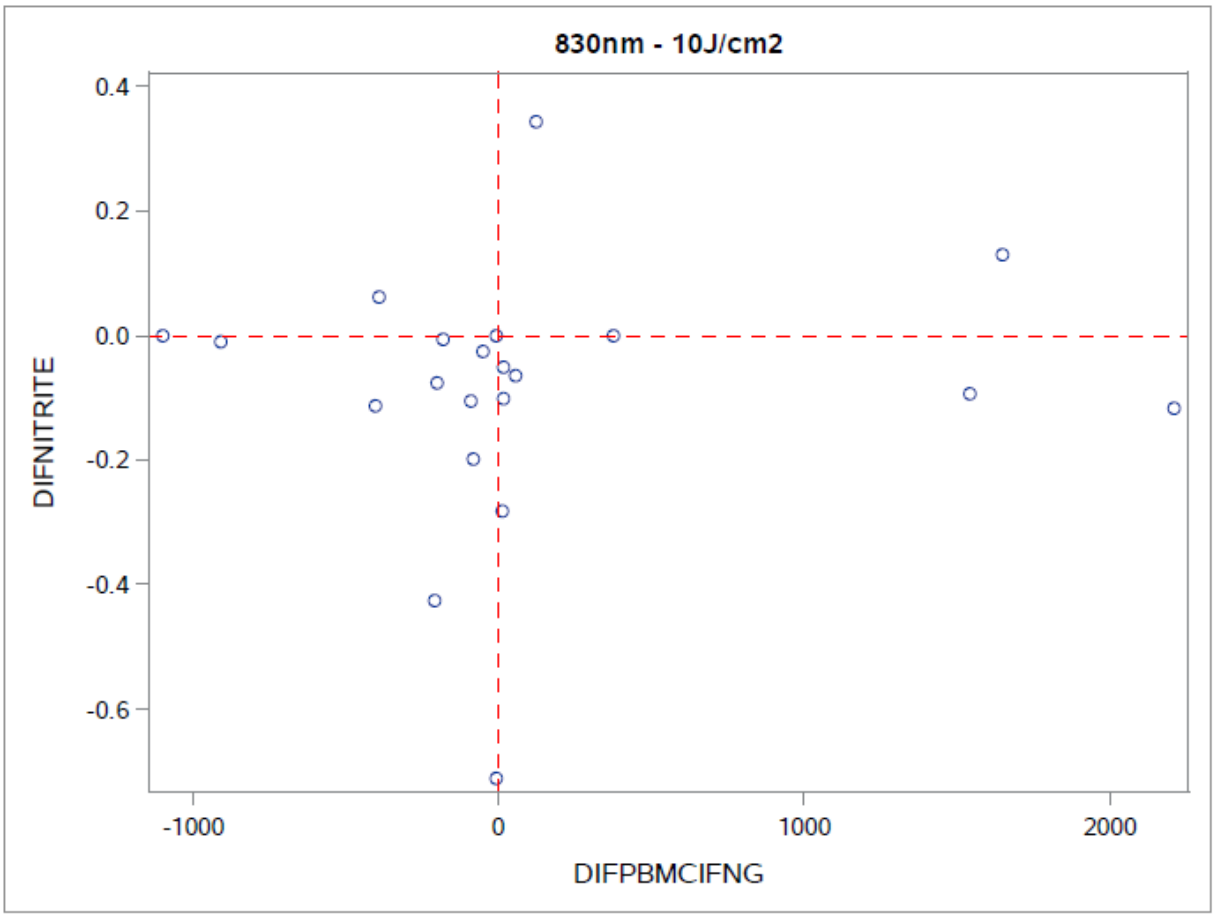

Figure 13. 830 nm (10J/cm^2, 72h) reduces nitrite and IFN-ɣ production by PBMC from MS subjects. Analysis of data showed that there is a correlation between the reduction of nitrite and reduction of IFN-ɣ by PBMC (p=0.1940). DIFNITRITE= difference in nitrite between 830nm and no-light treatment (control). DIFPBMCIFNG= difference in PBMC-IFNɣ between 830nm and no-light treatment (control). The red lines are set at 0 for both axes, if the value is positive it means that the production is higher after 830nm than with no light treatment (control). If the number is negative then the production if lower after 830nm thank with no light treatment (control).

Table 19. Relationship between Nitrite production and IFN-ɣ production by PBMC, 830nm 10/cm^2, 72h, n=23, p=0.1940 (Chi-Square Test for Equal Proportions).		
	Frequency	**Percent**
Increase Nitrite / Increase PBMC-IFN-ɣ	3	14.29
Decrease Nitrite / Increase PBMC- IFN-ɣ	6	28.57
Decrease Nitrite / Decrease PBMC- IFN-ɣ	9	42.86
Increase Nitrite / Decrease PBMC- IFN-ɣ	3	14.29

We carried out analysis of data to determine if the severity of disease (PDDS score) affected the modulation of nitrite and IL-10 and IFN-ɣ. MS subjects were divided in 2 groups depending of PDDS score, MS subjects with PDDS=0 and MS subjects with PDDS≥1. Severity of disease showed not significant effect in the modulation of nitrite, IL-10 and IFN-ɣ by PBMC receiving 830nm (10J/cm^2) (Tables 20, 21).

Table 20. Production of Nitrite and IL10 in PBMC grouped by PDDS

PDDS	INCREASE NO / INCREASE PBMC-IL10	DECREASE NO / INCREASE PBMC-IL10	DECREASE NO / DECREASE PBMC-IL10	INCREASE NO / DECREASE PBMC-IL10	Total
0	0 0.00%	5 71.43%	1 14.29%	1 14.29%	7
1	2 18.18%	5 45.45%	2 18.18%	2 18.18%	11
Total	2	10	3	3	18
Fisher's Exact Test Probability (P) 0.0713 Pr ≤ P 0.8812					

Table 21. Production of Nitrite and IFN-ɣ in PBMC grouped by PDDS

PDDS	INCREASE NO / INCREASE PBMC-IFNG	DECREASE NO / INCREASE PBMC-IFNG	DECREASE NO / DECREASE PBMC-IFNG	INCREASE NO / DECREASE PBMC-IFNG	Total
0	0 0.00%	2 33.33%	4 66.67%	0 0.00%	6
1	2 20.00%	4 40.00%	2 20.00%	2 20.00%	10
Total	2	6	6	2	16
Fisher's Exact Test Probability (P) 0.0281 Pr ≤ P 0.4181					

3.5 Discussion

Multiple Sclerosis (MS) is a CD4+ T autoimmune demyelinating disease characterized by the development of plaques in the central nervous system (CNS) [1]. MS studies demonstrated that nitrosative stress is present during acute and chronic stages of MS and EAE [147, 178-184]. Current MS treatments focus in the modulation of immune response during the initial stages of disease but they are not effective during chronic stages of disease where nitrosative stress takes control of disease over the immune response. Photobiomodulation (PBM) is proven to be effective at ameliorating different neurodegenerative conditions [250, 259-268].

Our group previously reported the effect of PBM at 670nm light to reduce clinical severity of disease and reduce nitrosative stress in the EAE model [288]. In-vitro studies using isolated lymphocytes from mice with EAE cultured with MOG_{35-55} receiving PBM with 670nm light (0.028 W/cm^2, 90s, 2.5J/cm^2) demonstrated reduction in the nitrite (NO_2^-) production in cell culture supernatants [288]. In in-vivo experiments, PBM treatment 670nm light decreased iNOS expression in spinal cord tissue isolated during the chronic stage of disease from mice with EAE [288]. In support of a role for NO in the amelioration of EAE by PBM, PBM therapy did not affect the severity of EAE induced in iNOS knockout ($iNOS^{-/-}$) mice. These results suggested that the presence of NO produced by iNOS (NO-iNOS) was necessary in the beneficial effects of PBM [288].

In order to extrapolate our previous findings of the effect of PBM at 670nm on the reduction of nitrosative stress in the EAE model, we evaluated additional wavelengths (Table 5). 670nm and 830nm wavelengths have been reported by others as useful wavelengths on different systems during PBM treatment, in addition 670 and 830nm

correlate with the absorption spectra of CCO [243]. We also evaluated devices able to deliver pulsed wavelengths. One device delivered a single pulsed 640nm wavelength and other device delivers 3 wavelengths simultaneously including 640, 875, and 905nm. We hypothesized that for the 3-wavelentgh device it could be possible to need a lower energy density in order to observe an effect. For this device a wider range of energy densities were tested including 0.3, 1, 3, and 10J/cm^2 in order to anticipate a possible biphasic dose effect.

A biphasic dose response effect is commonly observed in PBM treatments. At low energy doses, there is not enough energy to produce an effect (below threshold). When the energy dose is increased a biologic effect is observed and a threshold is achieved. If more energy continues to be administered, a threshold is crossed and the biologic effect is inhibited [244]. The effect of a biphasic dose response curve due to different wavelengths and doses of energy during PBM treatments have been studied in different systems [244, 248-252]. Based on previous data from our lab on PBM optimization, we tested 3 and 10J/cm^2 on cell cultures in order to anticipate the effect of a biphasic dose curve. The results presented here support previous findings reported by our lab where PBM at 670nm on mice with EAE reduced pro-inflammatory cytokines (IFN-ɣ, TNF-α), increased anti-inflammatory cytokines (IL-4, IL-10) and reduced nitrosative stress [287, 288]. The results showed that PBM at 830nm (10J/cm^2, 72h) on PBMC reduced the production of nitrite as marker of oxidative stress. Nitrite reduction correlated with the increase IL-10 ($p=0.0271$) and the reduction of IFN-ɣ ($p=0.1940$), however this last one was not statistically significant likely due to our small size sample. The fact that 3J/cm^2 did not produce an effect on PBMC on nitrite, IL-10, and IFN-ɣ

regulation as 10J/cm^2 did, suggest that a low dose of energy was not enough to produce a therapeutic effect. These results correlate with the biphasic dose response curve principle. Our lab previously showed that 670nm participate in the regulation of nitrite and cytokines using C57BL/6 mouse cells with EAE, here we showed that 830nm produced a regulation using human cells from MS subjects. This would suggest that 670nm is more effective in mice and 830nm in humans, however, the literature shows that both wavelengths can produce an effect in mice or humans. Therefore, wavelengths and doses of energy have to be studied together when they are applied to a particular system.

Data presented in chapter 2 showed that severity of disease (PDDS score) plays a role in the regulatory effect of PBM on cytokines. Interestingly, the analysis of data of nitrite regulation by PBM based on severity of disease (PDDS score) showed that the severity of disease does not play a role in the modulatory effect of PBM at 830nm (10J/cm^2) on nitrate and IL-10 production by PBMC. Therefore, this suggests that PBM at 830nm (10J/cm^2) can be used to reduce nitrite levels (nitrosative stress) and increase IL-10 at any point of disease. This is particularly important because as it has been mentioned, MS studies demonstrated that nitrosative stress is present during acute and chronic stages of MS and EAE [147, 178-184]. Future studies with bigger sample size and MS subjects on different stages of disease are needed to verify these results.

The fact that PBM at 830nm reduced nitrite levels is in agreement with other studies that indicate that PBM can modulate nitrosative stress on different systems [308, 310-313]. For instance, Huang group investigated the effects of PBM treatment (810nm, 20mW/cm^2, 3J/cm^2) on cultured murine cortical neurons cultured with oxidative

stressors including H_2O_2, cobalt chloride and rotenone [308]. PBM reduced ROS generation, increased mitochondrial membrane potential, and reduced cell death. These results suggested that PBM can produce a positive effect when oxidative stress is elevated [308]. Zhang group investigated the effects of 630nm to reduce brain H_2O_2 levels (reactive oxygen specie) in the senescence-accelerated prone 8 mouse (SAMP8) model of age-related dementia [311]. Age-associated H_2O_2 inhibits the formaldehyde dehydrogenase enzyme producing the accumulation of formaldehyde which inhibits choline acetyltransferase causing acetylcholine deficiency. The application of 630nm produced the activation of catalase and formaldehyde dehydrogenase in the brain and cell cultures producing a reduction in H_2O_2, reduction in formaldehyde, and restoring the levels of acetylcholine. These results correlated with the improvement in memory presented in SAMP8 mice [311].

PBM at 830nm (10J/cm^2, 72h) on PBMC reduced the production of nitrite which correlated with the increase in IL-10 ($p=0.0271$) and the reduction of IFN-ɣ ($p=0.1940$, no significant). The increase in IL-10 can be explained by the participation of both drug treatment and PBM treatment in the regulation of immune response. Most of the MS subjects were under MS drug treatment. MS drugs as well as PBM treatment shift the immune response from Th1 to Th2 responses increasing the production of anti-inflammatory cytokines. The reduction of both nitrite and IFN-ɣ by PBMC can be explained by recognized overlapping regulatory pathways for NO and IFN-ɣ [104]. In immune cells, the regulation of NO produced by iNOS is regulated TLR-4 and as well as IFN-ɣ-receptor. The binding of pathogens or lipopolysaccharides TLR-4 leads to the activation of the NfkB pathway, leading to the activation of iNOS and subsequently the

generation of NO [104]. Similarly, the binding of IFN-ɣ to IFNɣ-receptor on immune cells leads to the activation of STAT1 which activates the gene expression of iNOS [104]. Th1 cells play a fundamental role in the development and pathogenesis of inflammatory diseases, including MS and EAE. The IFN-ɣ produced by Th1 cells activates macrophages to induce the expression of iNOS, leading to production of high amounts of NO. Studies showed that high amounts of NO produced by iNOS can inhibit the expansion of Th1 cells by negative feedback mechanism whereby activated macrophages inhibit IL-12 which is necessary for Th1 differentiation and subsequent production of IFN-ɣ [112, 121]. The Chen group reported the anti-inflammatory effect of PBM with 810nm on murine bone marrow derived dendritic cells [309]. Dendritic cells were activated with lipopolysaccharide (TLR4 agonist) or CpG oligodeoxynucleotide (TLR9 agonist), then PBM treatment at 810nm at 0.3, 3 or 30 J/cm^2 was applied. PBM 810nm treatment with any of the 3 energy densities reduced dendritic cell activation as evidenced by reducing all measured the cell surface markers (MHC-II, CD86, CD11c), secretion of IL-12 in cells stimulated with LPS or CpG, and reduced the activation of NFkβ in cells activated with CpG. The results suggested PBM treatment at 810nm had an anti-inflammatory effect on dendritic cells by reducing IL-12 and NFkb signal pathway [309].

Studies demonstrated that mitochondrial dysfunction and nitrosative stress play a fundamental role in MS pathogenesis during acute and chronic stages [147, 178-184]. For instance, chronic active plaques obtained from MS subjects present oxidative damage to mitochondrial DNA which correlates with a reduction in the activity of complex I (NADH dehydrogenase) and increased activity of complex IV (cytochrome c

oxidase, CCO) [178]. Microarray analysis showed that postmortem motor cortex samples from MS subjects presented down regulation of mitochondrial genes, as well as the activities of the complexes I and III of the respiratory chain, suggesting that mitochondrial dysfunction in demyelinated axons leads to ATP reduction, which participates in the progression to permanent disability in MS [179]. Cerebrospinal fluid analysis from MS subjects showed increased iNOS activity, nitrite, peroxynitrites, S-nitrosothiols, and reduction in the levels of glutathione [184]. Therefore, the reduction of nitrosative stress and subsequent mitochondrial dysfunction are fundamental to delay the progression of MS.

The results presented here support our previous findings of the potential of PBM treatment in the modulation of cytokines and reduction of nitrosative stress in the EAE model [287, 288]. 830nm ($10J/cm^2$) led to reduced nitrite production by PBMC. In addition, the reduction in nitrite production by PBMC at 830nm at $10J/cm^2$ correlated the increase IL-10 ($p=0.0271$). PBM treatment produced a reduction of nitrite levels regardless of the PDDS score (severity of disease) among MS subjects. These results further support the potential of PBM as an additional therapeutic tool to reduce nitrosative stress in MS to affect disease progression.

CHAPTER 4. CHARACTERIZATION OF THE EFFECTS OF PHOTOBIOMODUATION ON INFLAMMATORY CYTOKINES IN SERUM SAMPLES OBTAINED FROM MS SUBJECTS.

4.1 Abstract

Multiple Sclerosis (MS) is a CD4+ T cell-mediated autoimmune demyelinating disease characterized by the development of plaques (lesions) in the central nervous system (CNS). Some of the symptoms of MS include motor dysfunctions, tremor, pain, numbness, weakness, and muscle fatigue. Currently there is no cure for MS. The drug treatments available focus on the modulation of the immune response during the acute phases of disease but they are not effective during chronic stages. The development of new therapeutic approaches to regulate the immune system and reduce the symptoms of disease at any stage is needed. Photobiomodulation (PBM) is a therapeutic approach showing effective results in the amelioration of neurological disorders as well as reduction of skeletal muscle fatigue, strength loss, and enhanced muscle rehabilitation. It is proposed that the therapeutic effects of PBM are by the improvement of mitochondrial function. Previously our lab studied the effect PBM at 670nm on the Experimental autoimmune encephalopathy (EAE) model, the animal model of MS. 670nm modulated pro-(IFN-ɣ, TNF-α) and anti-(IL-4, IL-10) inflammatory cytokines which correlated with the reduction in severity of EAE.

In this study we evaluated the effects of PBM treatment on muscle fatigue and pro- and anti-inflammatory cytokines in relapsing-remitting MS subjects. The effect of PBM treatment with either an “active device”, emitting simultaneously 640, 875, and

905nm at 40, 80, 120J, or a “placebo device” emitting only 640nm light at 3, 6, and 9 J, on muscle recovery was evaluated in MS subjects over 4 visits. Muscle strength was evaluated pre- and post- PMB treatment by maximal voluntary contractions (MVCs) of the tibialis anterior (TA) muscle. The results showed each patient demonstrated improvement in muscle recovery with the active device at 80J and 120J. An extended PBM treatment protocol showed improvement in muscle recovery in some MS subjects, however statistical significance was not achieved. Most of the levels of IFN-ɣ, IL-6 and IL-10 among MS subjects were below the limit of detection, which correlates with no active disease. TGF-β levels were lower in MS subjects with higher disability status (PDDS≥1) than MS subjects with PDDS=0. The extended PBM treatment with the active device increased TGF-β in MS subjects with PDDS≥1, however, the increase was not significant. The results showed the potential of PBM to improve muscle recovery, reduce muscle fatigue and modulate the immune response in persons with MS.

4.2 Introduction

Multiple sclerosis (MS) is a neurodegenerative CD4+ T mediated autoimmune disease that affects the central nervous system (CNS). MS is characterized by the destruction of the myelin sheath disrupting the nerve impulse transmissions from the CNS to other parts of the body causing the development of symptoms [2]. Some symptoms include motor dysfunctions, walking problems, tremor, pain, numbness, weakness, and fatigue [2]. Approximately 80% of MS subjects present muscle weakness and fatigue due to the combination of compromise function of the central motor drive and intramuscular function [223, 289-294]. Fatigue is additionally related to

alterations in skeletal muscle, such as reduction in the size of muscle fibers and reduction in the activity of mitochondrial enzymes involved in the production of energy [294].

CD4+ T cells play an important role in the pathogenesis of MS. CD4+ T cells can differentiate into pro-inflammatory Th1 and Th17 cell subtypes, which are considered pathogenic in MS. Th1 cells produce TNF-α, IFN-γ and IL-2. Th17 cells produce IL-17, IL-6, IL-21, IL-22, and TNF-α [23, 38]. CD4+ T cells can also differentiate into Th2 and regulatory T cells (Tregs) which are considered protective against the disease due to their production of anti-inflammatory cytokines [23, 38]. Th2 cells produce IL-4, IL-5, IL-6, and IL-10. Treg cells produce TGF-β and IL-10 [23, 38].

PBM is proving to be effective at ameliorating pathology and clinical severity for various neurodegenerative diseases [250, 259-268]. In addition, PBM on healthy subjects showed to reduce skeletal muscle fatigue, strength loss, exercise-induced oxidative stress, and improve muscle rehabilitation after exercise [295-303]. The mechanism of action of PBM is not fully elucidated, however, it is proposed that that during PBM treatment, the light is absorbed by cytochrome c oxidase (CCO) improving mitochondrial function and ATP production[239-242]. Our lab previously focused on the study of PBM for the treatment of MS using the experimental autoimmune encephalomyelitis model (EAE). PBM (670nm, 5J/cm^2) regulated the production of pro- and anti-inflammatory cytokines, reduced nitrosative stress, and ameliorated disease severity in the EAE model [287, 288]. Our next goal was to study the potential effect of PBM on immune regulation and muscle fatigue in MS subjects. We hypothesized that PBM treatment would reduce muscle fatigue and reduce pro-inflammatory cytokines

(IFN-ɣ, IL-6) and increase anti-inflammatory cytokines (IL-10, TGF-β) in serum samples collected from MS subjects after PBM treatment.

4.3 Materials and methods

Subject population. Recruitment of subjects was carried out following the guidelines of the Institutional Review Board of the University of Wisconsin Milwaukee (IRB# 18.020) and Marquette University (IRB# HR-1710020115). Inclusion criteria: RRMS male and female subjects between 20-60 years of age with no history of relapse or immunosuppressive therapy in the previous 6 months. Any current disease-modifying drug treatment was recorded. Exclusion criteria: RRMS subjects with any current infection, any additional neurodegenerative, autoimmune, or mitochondrial disease.

MS patient classification. MS subjects were classified based on the Patient Determined disease steps (PDDS) scale. PDDS scale is a patient reported outcome of disability of multiple sclerosis. PDDS scale is based on motor and ambulatory dysfunction present in MS subjects. PDDS scale has 7 levels ranging from 0= normal to 6= Confined to wheelchair (Table 4) [304, 305].

Photobiomodulation (PBM). PBM treatment was applied using customized "Painaway Post-Op Laser" devices (Multiradiance Medical, Solon, OH). Two different devices were used. The "Placebo" device delivered a single pulsed wavelength at 640nm (VIS, light emitting diode [LED] at 25mW/cm^2). The "Active" device delivered 3 pulsed wavelengths simultaneously, including: 640nm (VIS, light emitting diode [LED]); 875nm (NIR;LED); and 905nm light (NIR; super-pulsed Galium Arsenic laser, at a total power density of 33mW/cm^2). Devices and energies used are summarized in Table 22.

Table 22. Photobiomodulation parameters

Wavelength	Device	Power Density (W/cm^2)	Time (sec)	Energy Density (J/cm^2)	Surface area (4 cm^2)	Total Energy (J)
Type 2A 640 nm	Pulsed LED (MRM)	0.0025 W/cm^2	300 sec	0.75 J/cm^2	4 cm^2	3
			600 sec	1.5 J/cm^2	4 cm^2	6
			900 sec	2.25 J/cm^2	4 cm^2	9
Type 2B 640 nm 875 nm 905 nm	LED LED Superpulsed laser (MRM)	0.033 W/cm^2	300 sec	10 J/cm^2	4 cm^2	40
			600 sec	20 J/cm^2	4 cm^2	80
			900 sec	30 J/cm^2	4 cm^2	120

Study Design. Phase 1: Energy dose optimization. We first sought to determine the best dose of energy able to produce an improvement in muscle function in MS subjects. Using a randomized double blinded repeated measured design, MS subjects were scheduled for 4 appointments. In 3 out of the 4 appointments, each patient received a different dose of energy using the **active device (Type 2B device)** including 40, 80, and 120 J. During the fourth appointment, each patient received a low dose of energy using the **placebo device (Type 2A device)** including 3, 6 and 9 J. PBM treatment was applied in the tibialis anterior of the right leg. Muscle function was measured before and 20 minutes after PBM treatment by Dr. Alexander Ng's lab at Marquette University using techniques standard in his lab. **Phase #2. Extended PBM treatment (crossover**

study). The objective of this phase was to determine the effects of sustained PBM treatment on the reduction of muscle fatigue and immune regulation in MS subjects. For each patient, the best dose of energy that showed an improvement in muscle function during phase 1, it was used in phase 2. Patients were scheduled for 5 appointments. In the first and third appointment, each patient received a PBM device (therapeutic or placebo) to apply the light treatment at home for 2 consecutive weeks. Patients were instructed to apply PBM treatment to the gastrocnemius of both legs every morning, and the tibialis anterior of both legs every night. Patients came back to evaluate the effects of PBM treatment on muscle fatigue (appointments 2 and 4). Then the patients went sent home for a period of two weeks without PBM treatment and then they came back to evaluate the lasting effect of PBM treatment (appointments 3 and 5). In each appointment subjects were evaluated for the effect of PBM treatment on muscle fatigue Figure 14.

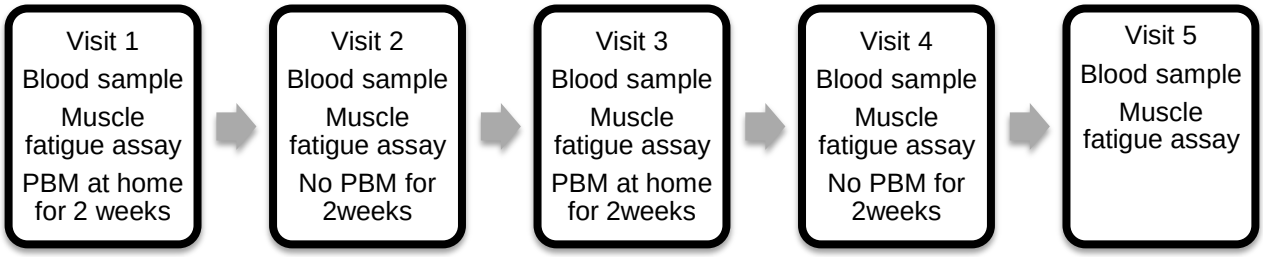

Figure 14. Phase 2 study design.

Blood sample collection. Blood (10ml) was collected at each of the 5 appointments. Blood collected in the absence of anticoagulant and were allowed to clot. Samples were centrifuged (1500g, 10min) and serums were aliquoted and stored at -80C until ELISA quantification.

Cytokine quantification by ELISA. Serum collected from MS subjects were used for quantification of IFN-ɣ (<15.6pg/mL detection limit, Duoset ELISA R&D systems, MN), IL-6 (<9.3pg/mL detection limit, Duoset ELISA R&D systems, MN), IL-10 (<7.8pg/mL detection limit, Quantikine ELISA R&D systems, MN), TGF-β (<31.3pg/mL detection limit, Quantikine ELISA R&D systems, MN) by ELISA following manufacturer instructions. Absorbance was measured using a plate reader (Bio-Tek, model KC4, Winooski, VT) at 450nm. Levels of cytokines were calculated according to a standard curve.

Data analysis. Statistical analysis was performed with SAS 9.4 (Cary, NC). For muscle recovery, McNemar's test was used to test for each light dose compared to placebo and Spearman's correlations were compared with Fisher's r to z transformation. For serum cytokine data, multiple comparisons performed by Wilcoxon Two-Sample Test were performed as appropriate. P<0.05 was considered significant. Statistical analysis was carried out by Chi Cho, MS, in the college of Health Sciences, University of Wisconsin Milwaukee.

4.4 Results

Phase 1. Energy dose optimization. Acute PBM treatment improves muscle strength recovery in MS subjects

To determine an optimal dose for subsequent study, we evaluated the acute effect of PBM treatment on muscle recovery following a fatiguing task on persons with RRMS ("Phase 1"). Using a randomized double blinded repeated measured design, pre-

and post- PBM treatment effect on muscle recovery was evaluated in MS subjects (n=17, males=3, females=14) over the course of 4 visits over a 4-week period. Evaluation of muscle strength consisted in 3 maximal voluntary contractions (MVCs) of tibialis anterior muscle followed by 2min of intermittent isometric contraction at 45% of MVC. Then, PBM treatment was applied to the tibialis anterior muscle using 1 of 3 energy doses with the “active device”: 40, 80, 120J or 1 dose with the “placebo device”: 3, 6, 9 J. Once PBM treatment was applied, a recovery period of 20min was allowed, after which recovery MVCs were evaluated. Muscle fatigue was evaluated by the degree of recovery in the MVC before PBM treatment. Twelve out of 17 subjects recruited finished the 4 visits.

All subjects who completed 4 visits were able to recover strength within 12% of their initial strength after PBM treatment with the active device using a total energy dose of 120J. This difference in force recovery between 120J energy dose and placebo was significant (p=0.03). In addition, the results showed that there was not an optimal dose of energy to improve muscle recovery rather each patient showed improvement in muscle recovery at a specific dose (Table 23). Doses of energy at 80J (5 patients) and 120J (6 patients) showed the best results to improve muscle recovery.

Table 23. Optimal Energy Dose for Subjects.				
Patient #	Gender	Age	PDDS score	Dose of energy
1	Male	59	0	High, 120J, 15min
2	Female	53	0	High, 120J, 15min
3	Female	59	0	High, 120J, 15min
4	Female	56	0	High, 120J, 15min
5	Female	46	4	High, 120J, 15min
6	Female	54	1	Medium, 80J, 10min
7	Female	46	3	Medium, 80J, 10min
8	Female	41	0	Medium, 80J, 10min
9	Female	23	1	Medium, 80J, 10min
10	Female	47	No info	Low, 40J, 5 min
11	Female	55	1	Low, 40J, 5 min
12	Female	47	2	Low, 40J, 5 min

The effect of Extended PBM treatment on muscle fatigue in persons with MS. Following dose optimization, we investigated the effects of an extended PBM treatment on the reduction of muscle fatigue and immune regulation in MS subjects using an extended, 2-week treatment protocol (“Phase 2”). PBM doses used in Phase 2 were individually assigned based on the optimal dose determined in Phase 1(Table 23). MS subjects (n=12; male=1, females=11) were scheduled for 5 appointments. In the first and third appointment, each patient received a PBM device (therapeutic or placebo) to apply the light treatment at home for 2 consecutive weeks. Patients were instructed to apply PBM treatment every morning to the gastrocnemius of both legs. At night, treatment was applied to the tibialis anterior of both legs. Patients came back to evaluate the effects of PBM treatment on muscle fatigue (appointments 2 and 4). Following a 2-week washout period without PBM treatment, subjects returned to the lab to evaluate the lasting effect of PBM treatment (appointments 3 and 5). In each appointment subjects were evaluated for the effect of PBM treatment on muscle fatigue

and a blood sample was collected. The collection of data is completed. However, the analysis of data for the muscle fatigue studies is ongoing.

Effect of extended PBM treatment on serum cytokines

Serum cytokine analysis was performed using blood samples collected during Phase 2. Pro-(IFN-ɣ, IL-6) and anti- (IL-10, TGF-β) inflammatory cytokines were measured by ELISA to investigate the systemic effect of PBM treatment on the immune response. For IFN-ɣ, IL-6, and IL-10 most of the patients showed results below the limits of detection during the 5 appointments. A summary of the results is shown in Appendix Table 24. For IFN-ɣ, 2 out of 12 patients presented detectable values between 10-20 pg/mL. For IL-6, 4 out of 12 patients presented detectable values between 20-80pg/mL. For IL-10, 1 out of 12 patients reported detectable values between 10-15 pg/mL. Analysis of data showed that PBM treatment did not produce a significant change on the production IFN-ɣ, IL-6 and IL-10 among MS subjects.

Contrary to other cytokines measured, all MS subjects presented with measurable TGF-β values between 10,000 and 25,000pg/mL. TGF-β results were plotted against the PDDS scores. Subjects were divided into two groups based on their PDDS score: Group 1 included subjects with PDDS=0 (n=6); Group 2 included subjects with PPDS ≥1 (n=6). The results showed that in MS subjects with PDDS≥1, the mean values of TGF-β were lower compared to MS subjects with PDDS=0. Furthermore, PBM treatment with the active device was associated with an increase in TGF-β with in subjects with PDDS≥1 compared to subjects with PDDS=0. However, the increase was not statistically significant (p=0.2403, Wilcoxon Two-Sample Test) (Figure 15).

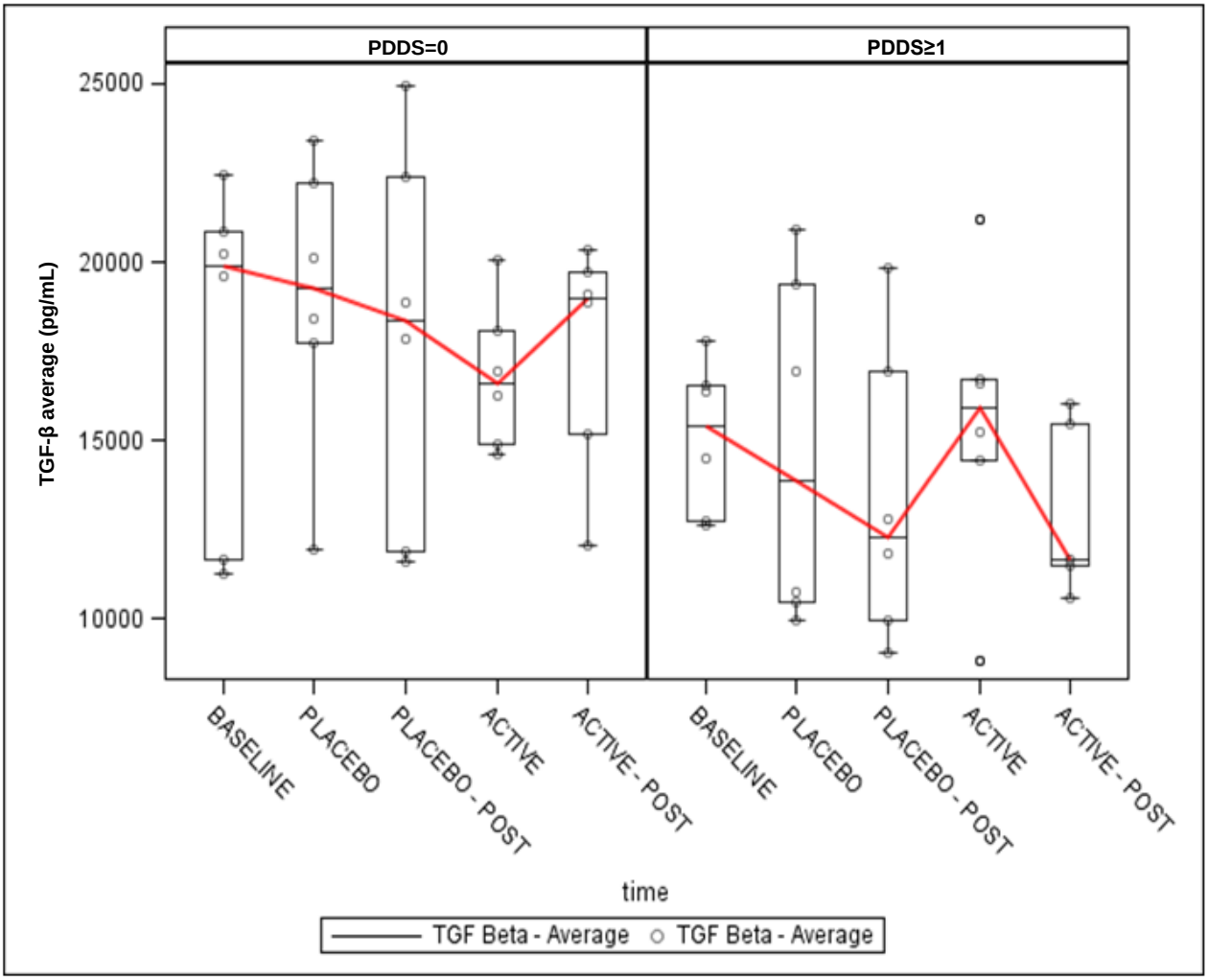

Figure 15. TGF-β values in serum collected from MS subjects during phase 2. MS subjects with PDD≥1 presented lower values of TGF-β in comparison with MS subjects with PDDS=0. During PBM with the active devise, MS subjects with PDDS≥1 showed an increase in TGF-β, however the increase was not statistically significant (p=0.2403, Wilcoxon Two-Sample Test) Box represents interquartile range (75%-25%). The bar within the box is the median. The whiskers are 1.5x the interquartile range. Anything outside these bars is an outlier. The red lines connect the median score at each time point. The circles represent subjects at each visit

4.5 Discussion

The destruction of the myelin sheath in MS interrupts the transmission of nerve impulses from the brain to other parts of the body causing the symptoms of MS [2]. Muscle weakness and fatigue are commonly present in MS subjects due to alterations in both the central motor drive and intramuscular function [223, 289-294]. Fatigue is additionally related to alterations in skeletal muscle, reduction in the size of muscle fibers, and reduction in energy by mitochondria [294]. Currently, there is no cure for MS. Current treatments focus on the suppression of the immune system to slow down disease progression but they are not effective in chronic stages of disease. Photobiomodulation (PBM) is proving to be effective to ameliorate different neurological disorders [250, 259-268]. In addition, in healthy subjects, PBM is effective to reduce muscle fatigue, improve exercise performance, reduce strength loss, and improve muscle rehabilitation after injury or exercise [295-303]. Previously, our laboratory studied the effects of PBM in the experimental autoimmune encephalomyelitis (EAE) [287, 288]. PBM at 670nm on mice with EAE reduced pro-inflammatory cytokines (IFN-ɣ, TNF-α), increased anti-inflammatory cytokines (IL-4, IL-10), and reduced nitrosative stress, which correlated with the reduction in disease severity [287, 288]. Here, we investigated the effect of PBM on immune regulation and muscle fatigue in MS subjects.

The first step in the study (Phase 1) was to evaluate the acute effect of PBM on muscle fatigue in RRMS. RRMS subjects (n=17) where scheduled for 4 visits to the laboratory in a period of 4 weeks. Muscle fatigue pre- and post- PBM treatment was evaluated maximal voluntary contractions (MVCs) of tibialis anterior (TA) muscle in the right leg or dominant leg. Muscle fatigue was evaluated by the degree of recovery in the

MVC before PBM treatment. The results showed that all patients were able to recover strength within 12% of their initial strength after PBM treatment with the active device using a total energy dose of 120J. In addition, the results showed that there was not an optimal energy dose to improve muscle fatigue rather each patient showed improvement in muscle recovery at a unique dose. This differences in energy requirement can be explained due to the fact that MS is a very variable disease, each MS subject is in a different stage of disease and each of them develop different motor problems at a different levels. Therefore the energy requirements to improve muscle function could be different. Energy doses of 80 and 120J showed to best results in muscle recovery. Analysis of data is ongoing. Preliminary analysis suggests that MS subjects with motor dysfunction problems (i.e. walking problems), higher depression, and lower quality of life showed a better response to PBM treatment (data not shown).

Phase 2 employed a cross-over study design to investigate the effect of an extended PBM treatment protocol on muscle fatigue in MS subjects. MS subjects were scheduled for 5 appointments. Patients received a PBM device (therapeutic or placebo) and were instructed to apply the PBM treatment at home using the energy dose from Phase 1 that improved muscle recovery. The PBM treatment was applied for 2 consecutive weeks every morning in the gastrocnemius of both legs and every night in the tibialis anterior of both legs with washout periods (2 weeks) between the extended PBM treatments.

At each appointment, muscle fatigue was evaluated using the maximal voluntary contractions (MVCs) of tibialis anterior (TA), as performed in Phase 1, and a blood sample was collected for serum cytokines quantification. Collection of data is complete

but the analysis of data is still pending. Preliminary analysis of data showed that patients with motor problems (walking problems) or higher disability showed a more noticeable muscle fatigue improvement. The low improvement in muscle fatigue among patients after PBM treatment can be explained due to the low sensitivity of the muscle fatigue task and the short period of time of PBM treatment. In future studies a more sensitive assay and longer PBM treatment will be necessary to evaluate muscle recovery.

Published studies analyzed the cytokine profile of MS subjects with the main goal of identify biomarkers for the diagnosis, identification of disease stages, identification of the correct MS subtype, and monitoring of the drug treatment [314-317]. Our serum cytokine data presented here correlate with these published results. Martins et al. quantified pro-inflammatory Th1 (IFN-ɣ, IL-2, IL-12) and anti-inflammatory Th2 (IL-4, IL-5, IL-10, IL-13) cytokines in serum samples from 833 MS subjects and 117 healthy controls in order to investigate cytokine differences among disease stages [314]. MS subjects included primary progressive (n=27), relapsing remitting (n=656), and secondary progressive (n=150), receiving IFN-β, Glatiramer acetate, other disease-modifying therapy (not specified), or no drug treatment, with no active disease present. When the results of the 3 MS groups were compared individually (pairwise) with each other, no significant differences were found comparing cytokine expression, indicating that the results obtained were not directly related to the subtype of the disease. Significant increases in MS samples in comparison with healthy controls were found for IFN-ɣ (mean 7.5 vs 0.4pg/mL, p=0.0002), IL-2 (mean 5.7 vs 1.0pg/mL, p=0.0002), TNF-α (mean 4.1 vs 1.2pg/mL, p=0.01) IL-4 (mean1.4 vs 0.1pg/ml, p≤0.0001), IL-10 (mean

16.8 vs 7.5pg/mL, p=0.03). The increase in both pro- and anti- inflammatory cytokines correlates with the progression of the disease due to the increase in pro-inflammatory cytokines, and the simultaneous restorative process by anti-inflammatory cytokines [314].

Kallaur et al. also evaluated the serum cytokine profile from RRMS patient with the progression and activity of the disease [315]. Serum cytokines levels in RRMS (n=169) and healthy donors (n=132) were measured by ELISA. All RRMS subjects were in remission period and were prescribed IFN-β1a, IFN-β1b, Glatiramer acetate, Natalizumab, or corticosteroid treatment with no presence of relapse for at least 3 months before the study. Serum cytokine results were analyzed based on the disability and activity of the disease using the expanded disability status scale (EDSS) and Magnetic resonance imaging lesions. IFN-ɣ, IL-6, IL-12, IL-4, and IL-10 were higher in RRMS patient compared to healthy donors. Interestingly, IL-4 levels were higher in RRMS subjects with mild disability compared with those with moderate and severe disability. TNF-α and IL-10 levels were higher in RRMS subjects with inactive disease in comparison with active disease. The results suggested that the production of anti-inflammatory cytokines is to counteract the presence of pro-inflammatory cytokines present during the progression of MS [315].

Nicoletti et al. used ELISA to measure serum levels of TGF-β in RRMS subjects, and SPMS subjects with no MS drug treatment [316]. The control group consisted of age matched healthy subjects (n=29). RRMS subjects (n=65) were divided in 2 groups depending on if they were on remission (n=41), or relapse (n=24). RRMS subjects in remission presented TGF-β values of approximately 70ng/mL. Relapsing patients

showed values of approximately 90pg/mL. The control group presented values of approximately 20ng/ml. In addition, 10 RRMS subjects were monitored for 4-6 months before and during a relapse period. The longitudinal analysis showed that the mean value for TGF-β before the attack was 50ng/mL, and the mean value during the attack was 82ng/mL. The data indicated that the increase in TGF-β during the attack period was due to the activation of immunomodulatory mechanisms in a feedback fashion by the pro-inflammatory events present during the relapse period [316].

In our study, the low levels of pro-(IFN-ɣ, IL-6) or anti-(IL-10, TGF-β) inflammatory cytokines obtained from RRMS subjects through the 5 visits in phase 2 correlate with the lack active disease (i.e., all subjects were in a remission period). In addition, the low serum cytokine levels obtained indicate that the drug treatment used by patients is efficiently modulating the immune response. Our results showed that PBM treatment did not produce significant change on low serum levels of IFN-ɣ, IL6, and IL-10 detected in our study population. On the other hand, PBM treatment resulted in an increase in TGF-β levels in MS subjects with PDDS≥1 during the extended PBM treatment with the active device, however, this increase was not significant. The observation that PBM treatment produced an effect on patients with higher disability (PDDS≥1) but not in patients with normal motor functions or no limitations on activity (PDDS=0) suggests that PBM treatment might be more effective in chronic stages of disease or with higher disability (i.e. motor dysfunctions). Therefore, the lack of significant in the increment of TGF-β after PBM treatment could be explained due to the low number of subjects in our study, the low number of patients with higher disability status, as well the fact that none of our subjects presented with active disease, which

suggest that anti-inflammatory cytokines (IL-10, TGF-β) would not be elevated. The presence of TGF-β and the lack of IL-6 are particularly important because these conditions induce CD4+ T cells to differentiate into Tregs, which are protective in MS. On the other hand, TGF-β and the presence of IL-6 induce CD4+ T cells to differentiate to Th17, which are pathogenic in MS [23, 38].

In conclusion, the results presented here suggest that PBM treatment has the potential to be used as an additional therapeutic tool to modulate immune response and reduce muscle fatigue in MS subjects. Our data suggest that PBM therapy might be effective in MS subjects in chronic stages or with higher disability status. In addition, the serum cytokine data indicate that biomarkers such as IL-10 and TGF-β in combination with PDDS scale can be used to monitor the efficacy of PBM treatment on MS subjects. Future studies are needed to investigate the effect of PBM treatment for extended periods of time on serum cytokines (pro- and anti-inflammatory cytokines), evaluate motor function with more sensitive assays and possibly different muscles in the body (i.e. legs, biceps, triceps, back, muscle fatigue in general) as well as recruit MS subjects in more advanced stages of disease or with higher disability status.

CHAPTER 5.

GENERAL DISCUSSION

In MS, the destruction of myelin blocks the transmission of nerve impulses or messages from the CNS to other parts of the body causing the symptoms of MS such as anxiety, depression, motor dysfunctions, walking problems, pain, muscle fatigue, fatigue in general, etcetera [2]. There is no cure for MS. Currently therapeutic agents impact disease through modulation of the immune response in order to slow down the progression of disease. Importantly, these agents are only approved relapsing-remitting disease and are not effective against progressive stages where nitrosative stress is largely responsible for disease pathogenesis. However, studies demonstrated that nitrosative stress events are in fact present during the acute stages of disease, even before the cellular infiltration in the central nervous system, and play role in pathogenesis [147, 178-184]. Thus, the development of therapeutic approaches that target the generation of nitrosative stress are needed.

Photobiomodulation (PBM) is a therapeutic approach demonstrating potential toward ameliorating pathology and clinical severity for various neurodegenerative conditions, including traumatic brain injury (TBI), acute ischemic stroke (AIS), familial amyotrophic lateral sclerosis (FALS), spinal cord injury (SCI), Alzheimer disease (AD) and Parkinson disease (PD) [250, 259-268]. It is proposed that the biological effects of PBM are elicited through improvement of mitochondrial function. Previous studies demonstrated that during PBM treatment, VIS/NIR light (600-1100nm wavelength range) is absorbed by cytochrome c oxidase (CCO, complex IV), the mitochondrial

enzyme responsible for catalyzing the transfer of electrons from cytochrome c to molecular oxygen in the generation of ATP [239-242].

Our lab previously studied the effect PBM at 670nm on the EAE model of MS. 670nm light reduced pro-inflammatory cytokines (IFN-ɣ, TNF-α), increase anti-inflammatory cytokines (IL-4, IL-10) and reduce nitrosative stress, correlating with a reduction in disease severity [287, 288]. The main goal of the current study was to investigate the effect of PBM in the modulation of pro- and anti-inflammatory cytokines and nitrosative stress in peripheral blood mononuclear cells (PBMC) and CD4+ T cells obtained from MS subjects. Based on our previous work, we evaluated the effect of PBM with 670nm light [287, 288]. In addition, we investigated the effects of different wavelengths with proven effectiveness in other different systems [239, 240, 243, 245, 246, 248].

First, we compared the effect of PBM treatment on the modulation of cytokines between MS subjects and healthy subjects (control group). The threshold for significance was set at ±20% based on changes expected in MS subjects over the course of disease and compared to healthy donors. MS subjects did not present active disease or other inflammatory condition, each of them is on a different stage of disease, and most of them are receiving drug treatment to modulate disease. Our data revealed unique PBM wavelengths and doses effective at modulating cytokine secretion in MS subjects and healthy donors (Chapter 2, Table 6). Importantly, the results showed both MS subjects and healthy donors responded to PBM treatment with the modulation of cytokine production by PBMC and CD4+ T cells under unique conditions. This was unexpected, as the current paradigm in the PBM community supports the notion that

healthy individuals should not respond to PBM treatment. Our results demonstrate that at least some individuals considered “healthy” do in fact respond to PBM therapy. One explanation for this is that many healthy patient present some degree of inflammation that allows to PBM affects the production of cytokines.

Next we analyzed the effect of PBM treatment on cytokine production in MS subjects based on disease severity (Table 13). MS subjects were divided in 2 groups based on the Patient Determined Disease Steps (PDDS) scale, a self-reported measure of disease severity. MS subjects with PDDS=0 showed no change in the production of IFN-ɣ by PBMC. Meanwhile, most MS subjects with PDDS≥1 responded with changes in IFN-ɣ production with these parameters, albeit with mixed results, with equal percentages of subjects responding with increased versus decreased cytokine production. In response to the Type 2b device (640/875/905nm, 1J/cm^2 at 48h), CD4+ T cells from the majority (75%) of subjects with PDDS=0 did not change IFN-ɣ production, while 25% of subjects reduced cytokine secretion under the conditions. On the other hand, 100% of MS subjects with PDDS≥1 showed an increase in IFN-ɣ in response to this same device. Unexpectedly, 735nm light (10J/cm^2) affected cytokine production in MS subjects with PDDS=0, with 66.67% of CD4+ T cell cultures showing increased IFN-ɣ production in response to these conditions. Cells from MS subjects with PDDS≥1 also responded to these conditions, with 25% of cultures presented an increase and 62.5% a reduction in IFN-ɣ.

The results showed that disease severity played a role in the modulatory effect of PBM on cytokines. Then, we evaluated if the magnitude in cytokine production in each patient was different between MS subjects with PDDS=0 compared to MS subjects with

PDDS≥1 after PBM treatment (Table 17). The results showed that MS subjects with PDDS=0, in comparison with MS subjects with PDDS≥1, presented higher levels of IFN-ɣ produced by CD4+ T cells after PBM treatment with 735nm (3J/cm^2 at 120h and 10J/cm^2 at 72h) and higher levels of IFN-ɣ produced by PBMC after treatment with type 2b device (640/875/905nm, with 1 and 3J/cm^2 at 120h). The fact that PBM treatment with 735nm and type 2b device (640/87/905nm) increased the production of IFN-ɣ by CD4+ T cells and PBMC from patients with PDDS=0 will require further investigation in its potential effect on MS subjects. For some time IFN-ɣ has been considered detrimental in MS due to its participation in the development and progression of MS and EAE [46-52]. However, several studies indicate that IFN-ɣ can play a beneficial role in MS and EAE [53-65]. Thus, the increase of IFN-ɣ due to PBM treatment in MS subjects with PDDS=0 might be beneficial to ameliorate disease. Conversely, our results showed that 670nm (3J/cm^2 at 72h) produced a reduction or no change in IFN-ɣ production by PBMC and CD4+ T cells but increased IL-10 by CD4+ T cells from MS subjects with PDDS≥1 compared to MS subjects with PDDS=0, which showed increase in IFN-ɣ and no change in IL-10. These results are very important because they show that the production of cytokine and its regulation among MS subjects with PPDS=0 and PDDS≥1 is different after PBM treatment. In addition, MS subjects with higher severity in disease (PDDS≥1) presented an anti-inflammatory effect after PBM with 670nm (3J/cm^2 at 72h), and patients with normal functions (PDDS=0) presented no effect or a low pro-inflammatory response. Thus, optimization of PBM treatment parameters to support efficacy and prevent unwanted responses will be necessary if PBM therapy is to used successfully in the clinical setting.

Initially, we considered 735nm as a negative control in our experimental design, due to our previous studies that showed that wavelengths around 700nm did not provide significant effect during PBM, correlating with the absorption spectrum of CCO [243]. On the contrary, our results showed that $CD4^+$ T cells from MS subjects with PDDS=0, but not MS subjects with PDDS≥1, expressed higher levels of IFN-ɣ produced by CD4 T cells after PBM treatment with 735nm ($3J/cm^2$ at 120h and $10J/cm^2$ at 72h). This result is important because it indicates that wavelengths in the 700nm range are able to produce a significant effect in at least some circumstances. Therefore, in addition to wavelength, energy densities (J/cm^2), cell type, severity of disease are some of the factors that also need to be considered when optimizing PBM treatment.

Our results correlate with previous observations from other authors that indicate that the effect of PBM treatment is affected by the redox status of the system [248, 249, 307-309]. Karu et al. evaluated the changes in the absorption spectra of HeLa cells before and after PBM [307]. 632.8nm ($103J/m^2$) on HeLa cells with oxidized cytochrome c oxidase resulted in the reduction of the cytochrome C oxidase, followed by its subsequent oxidation, producing a bell-shaped dose-response curve. Conversely, the application of PBM treatment to HeLa cells with reduced cytochrome c oxidase first led to the oxidation, followed by the reduction, of the cytochrome c oxidase, resulting in an inverted bell-shaped curve dose-response curve. These results indicated that PBM can produce reduction or oxidation of CCO depending on the redox status of the enzyme, and the maximum in the bell-shape dose-dependent curve or minimum in the inverted bell-shape dose-dependent curve is the dose threshold or inflection point between the changes in redox state [307]. These results correlate with the observations by others

characterizing the effect of PBM on healthy cells in comparison with cells under oxidative stress. For instance, Chen et al. reported that 830nm ($3J/cm^2$) on healthy embryonic fibroblasts increased CCO activity, mitochondrial membrane potential above normal baseline, and increased ROS production significant enough to activate NFκb [249]. Using primary cultured murine cortical neurons, Huang et al. demonstrated that, under conditions of experimentally-induced oxidative stress, 810nm at $3J/cm^2$ returned mitochondrial membrane potential back to basal levels, increase ATP production, reduced high ROS levels, and reduced cell death [308]. Conversely, cells exposed to the same PBM condition in the absence of oxidative stressors showed a similar increase in mitochondrial membrane potential and ATP production but a modest increase in ROS levels. The results showed that PBM can reduce oxidative stress in compromised systems (oxidative stress conditions) but in healthy cells can increase ROS levels [308].

The reduction of IFN-ɣ after PBM treatment in MS subjects with PDDS≥1 correlates with the observations by Karu and others that indicate that PBM effect will depend of the redox state of the system [248, 249, 307-309]. Our results showed that that PBM treatment on PBMC and CD4+ T cells reduced IFN-ɣ secretion by cells isolated from MS subjects with PDDS≥1 (presence of disability) and increased IFN-ɣ secretion by cells from MS subjects with PDDS=0 (normal patients, no disability present). High levels of IFN-ɣ were previously correlated with the progression of MS and EAE [46-52]. For instance, in a clinical study, RRMS (n=18) patients received recombinant IFN-ɣ over a range of doses [low (1mcg); intermediate (30mcg); and high (1000mcg)]. In a dose-dependent manner, disease was exacerbated in 39% of subjects

receiving exogenous IFN-ɣ, suggesting that IFN-ɣ administration activated the immune response, leading to disease activity clinical relapse. [51]. Conversely, studies demonstrated a protective role of IFN-ɣ in EAE and MS [53-65]. The Billiau group showed that the intraperitoneal administration of anti-IFN-ɣ antibodies into EAE-induced C57BL/6J mice on days -6, 0, 7, and 14 relative to EAE induction increased the incidence, disease severity and mortality [56]. Conversely, the intraperitoneal injections of recombinant-DNA-derived IFN-ɣ into EAE-induced SJL/J mice on days -1, 0, 1, 3, 5, 7, and 9 relative to EAE induction reduced disease severity and mortality [56]. The authors proposed that it is important to differentiate between the local and systemic effects of IFN-ɣ. Local IFN-ɣ promotes inflammation whereas the systemic IFN-ɣ produced an anti-inflammatory effect. Anti-IFN-ɣ antibodies neutralized the IFN-ɣ present in the circulation and peripheral body compartments but not that produced locally in the CNS, which is difficult to reach due to the presence of the blood brain barrier. The blocking of the systemic IFN-ɣ suppresses the anti-inflammatory properties of IFN-ɣ, leading to increase of EAE severity. The endogenous IFN-ɣ formed during the induction or development of EAE, as well as the administration of IFN-ɣ before EAE induction, can play a disease-limiting role therefore it should not be blocked during the inflammation of CNS. [56]. Similarly, the Furlan group showed that the localized over expression of IFN-ɣ in the CNS reduced the severity of disease in EAE-induced mice [65]. Overexpression of IFN-ɣ was carried out by using an IFN-ɣ gene-containing vector inserted in Herpes simplex virus type 1 (HSV-1) which was injected intracisternally in C57BL/6 mice. These mice developed EAE with earlier disease onset, milder disease course, reduction in apoptotic T cells, inflammatory infiltrates, demyelination, axonal

loss, and 83% of mice recovered from disease compared to mice with no IFN-ɣ gene-containing vector (control group) [65]. The results challenge the general idea that the presence of IFN-ɣ in EAE and MS leads to the worsening of disease. Depending on disease stage and site of production (systemic or local), IFN-ɣ can play a dual role in EAE and MS: 1) a protective role to reduce disease severity or 2) a pathogenic role which participates in the progression and development of disease [65]. Thus, the modulation of IFN-ɣ at any stage of MS or EAE (before, during or after relapse) could be potentially useful to reduce the clinical symptoms during the progression of the disease.

Our results showed that PBM at 670nm ($3J/cm^2$) on cells isolated from MS subjects with PDDS≥1 lead to increased IL-10 production by CD4+ T cells in comparison with MS subjects with PDDS=0. These results are very important because they show that MS subjects with higher severity in disease present an anti-inflammatory effect after PBM treatment. Studies demonstrated the protective role of IL-10 in the amelioration of MS and EAE [86, 87]. For instance IL-10 deficient mice, but not IL-4 deficient mice, developed accelerated EAE onset in comparison with WT mice [86]. Spontaneous recovery was present in WT and IL-4 deficient mice but recovery was not present in IL-10 deficient mice suggesting that IL-10 is fundamental in the amelioration or recovery process [86]. In one study, quantification of IFN-ɣ, TNF-α, IL-4, and IL-10 in serum isolated from MS subjects during relapse (n=42) showed higher levels of these cytokines in comparison with healthy controls (n=12). In addition, the quantification of TNF-α, IL-10, and nitric oxide (NO) in 17 MS subjects during active relapse showed higher levels in comparison with healthy subjects [90]. Together, these studies suggested that the simultaneous activation of Th1 and Th2 cells is present during the

acute stages of the disease [89, 90]. Thus, the increased IL-10 production, especially in patients with higher disability can participate in the amelioration of disease.

Nitrosative stress is linked to disease progression in EAE and MS. NO also plays an important role in the modulation of cellular respiration and mitochondrial function. Under either hypoxic conditions or high concentration of NO, NO competes with oxygen and binds reversibly to Cytochrome c oxidase (CCO or complex IV). This leads to inhibition of CCO and subsequent reduction of ATP production [160-162]. In addition, ROS and RNS inhibit the activity of complexes I, II, IV and V of the respiratory chain leading to mitochondria dysfunction and reduction in ATP production [167-169]. MS and EAE studies showed that nitrosative stress and mitochondrial dysfunction are events present in early and chronic stages of disease [147, 178-184]. For instance, Lu et al., showed that chronic active plaques from MS subjects presented high oxidative damage of mitochondrial DNA (mtDNA) which correlated with a reduction in the activity of complex I of the respiratory chain and a possible compensatory increase in the activity of complex IV (CCO) [178]. Qi et al. reported that mitochondrial dysfunction due to oxidative stress was present in the CNS of immunized mice before the infiltration of immune cells the CNS [180]. Mice immunized for the induction of EAE were euthanized 3 days after EAE induction, prior to the appearance of clinical signs, and the optic nerves, retinas, brains, and spinal cords were analyzed for signs of disease pathology [180]. None of the mice showed clinical signs of EAE or cellular infiltration in the CNS, but nitrated proteins, apoptosis of oligondendrocytes, and reduced ATP levels were present in all of the samples [180]. Histological analysis of spinal cords showed positive iNOS immunofluorescence, mitochondrial vacuolization and dissolution of cristae which

correlate with the presence of nitrosative stress and the degeneration of axons at an early stage of EAE [180]. Quantification of nitrosative stress parameters in cerebrospinal fluid and plasma samples collected from MS subjects revealed increased iNOS activity, nitrotyrosine, nitrite, peroxynitrites, and S-nitrosothiols in comparison with controls [184].

Previous work from our lab showed that treatment of MOG_{35-55}-induced EAE in mice with 670nm light reduced nitrosative stress which correlated with the reduction in the severity of disease [288]. In cell culture experiments using lymphocytes isolated from peripheral lymph nodes from mice with EAE incubated with MOG_{35-55}, PBM treatment with 670nm light resulted in a reduction in nitrite (NO_2^-) levels in comparison with control (no light treatment). Similarly, in vivo experiments showed that mice with EAE receiving double light treatment protocol (light treatment for 7 days starting with the day of onset of clinical signs, followed by a period of 7 days without light treatment, with light treatment resuming on days 8 through 14) presented with a reduction the clinical severity of disease [288]. Spinal cords collected during the course of the experiment were used to quantify iNOS expression. INOS expression was not reduced during the acute phase of the disease. However, there was a significant down-regulation iNOS expression in the chronic phase of the disease. In addition, the double treatment protocol was applied on iNOS knockout ($iNOS^{-/-}$) mice and WT C57BL/6 mice immunized with MOG_{35-55}. The double light treatment protocol resulted in amelioration of clinical severity in WT mice but did not produce amelioration in $iNOS^{-/-}$ mice, suggesting that NO produced by iNOS is necessary in the beneficial effects of PBM [288].

Peripheral blood mononuclear cells are a heterogeneous population of cells representing the circulating immune response. In addition to $CD4^+$ T cells, the population contains other lymphocytes and monocytes/macrophages. Important to these studies, monocytes and differentiated macrophages are the principal source of NO produced by iNOS. To investigate the effect of PBM on the generation of NO/nitrosative stress, PBMC were isolated from MS subjects, activated with Phytohemagglutinin (PHA) and received PBM treatment as indicated in materials and methods (Table 5). Supernatants collected at 72h were used to measure nitrite (NO_2^-) levels by fluorescence. PBM treatment at 830nm (10J/cm^2, 72h, p=0.0153) produced a statistically significant reduction in the levels of nitrite in comparison with controls (no light treatment). Some of the other PBM treatments produced mixed results that were not statistically significant.

Further analysis of data showed that 830nm (10J/cm^2) was also capable of cytokine modulation. Analysis demonstrated that 830nm (10J/cm^2, at 72h) produced both a reduction in nitrite and increase in IL-10 produced by PBMC (p=0.0271). These results are important because they show that PBM can participate in the reduction of nitrosative stress and also provide an anti-inflammatory effect due to the increase in IL-10. In addition, 830nm (10J/cm^2, at 72h) produced a reduction in both nitrite levels and IFN-ɣ produced from PBMC in the majority of our subjects. However, this reduction did not reach statistical not significance (p=0.1940) in this study. The lack of significance in the reduction of IFN-ɣ can be explained based by: 1) the small size of our sample; 2) all MS subjects included in the study are not on relapse and therefore the levels of IFN-ɣ were to be low; 3) most of the patients were prescribed MS disease-modifying therapy

to control their disease. One mechanism by which these therapies control MS is through the shift from Th1 to Th2 responses which leads to low levels of pro-inflammatory cytokines such as IFN-ɣ, as was observed in our subject population. Interestingly, unlike what was noted above with respect to immune modulation by PBM, we did not observe significant difference with respect to nitrite, IL-10 and IFN-ɣ correlation and disease severity (PDDS=0 vs PDDS≥1). This is particularly important because it suggests that PBM can be useful to reduce nitrosative stress in MS subjects in early stages of disease with no motor dysfunctions as well as patients in a more advanced stage with motor dysfunction present.

Together with the pro-inflammatory immune response, nitrosative stress plays a central role in MS pathogenesis. Therefore, the reduction of nitrosative stress is fundamental to the development of effective therapies for MS. Furthermore, the expression of pro-inflammatory cytokines such as IFN-ɣ and NO are coordinately regulated. The IFN-ɣ produced by Th1 cells activates macrophages leading to the expression of iNOS and production of high amounts of NO. Similarly, high amounts of NO produced by iNOS inhibit the expansion of Th1 cells and IFN-ɣ by a negative feedback mechanism whereby activated macrophages inhibit IL-12 production which is necessary for Th1 differentiation [121]. Fenyk-Melody, J.E., et al. showed that EAE induction in iNOS-deficient mice result in more severe clinical disease in comparison with disease induced in WT mice, suggesting that the NO produced by iNOS in WT mice-EAE immunized prevents CD4+ T cells differentiation to Th1 cells [122, 123]. Thus, therapeutic targeting on NO will directly target pathogenic mechanisms responsible for disease progression and immune modulation leading to a decrease in

the pro-inflammatory immune response. Together, these actions would be predicted to ameliorate MS disease severity and perhaps prevent disease progression.

In our project we also carried out a pilot clinical study to investigate the effect of PBM treatment on muscle fatigue as well cytokine modulation in serum in MS subjects. PBM studies showed a positive effect on the reduction of skeletal muscle fatigue, exercise performance, reduction of strength loss, reduction in exercise-induced oxidative stress, and enhancement of muscle rehabilitation [295-303]. Phase 1 of the study evaluated the acute effect of PBM in muscle recovery to determine an optimal dose for follow-up studies. The effect of pre and post PBM treatment on muscle recovery in MS subjects was evaluated in 4 different visits by maximal voluntary contractions (MVCs) of tibialis anterior muscle. The results showed that there was not an optimal energy dose for muscle recovery, rather each patient showed improvement in muscle recovery at a specific dose: 5 patients with 120J, 4 patients with 80J and 3 patients with 40J.

In phase 2, we evaluated the effect of an extended (2-week) PBM treatment on the reduction of muscle fatigue and immune regulation in MS subjects. Each MS subject applied their optimal dose of energy determined in Phase 1. Phase 2 consisted in 5 appointments. In the first and third appointment, each subject received a PBM device (therapeutic or placebo) to apply the light treatment at home for 2 weeks every morning in the gastrocnemius of both legs, and every night in the tibialis anterior of both legs. Muscle strength was evaluated by MVCs of tibialis anterior muscle and a blood sample was collected at follow-up appointments (visits 2 and 4). Analysis Visits 3 and 5 assess for a continued effect of PBM treatment after 2 weeks of discontinued treatment.

Analysis of muscle recovery data has not been completed. However, preliminary analysis showed that there was not significant improvement in muscle strength after the extended PBM treatment. The lack of significance in the results can be explained based to the short period of time (2 weeks) of PBM treatment, the small sample size of our patient population, and the low sensitivity of the muscle fatigue task. Therefore, in future studies it will be necessary to increase our sample size, and include more sensitive assays to evaluate muscle recovery, as well as include other muscles to evaluate muscle recovery (i.e. biceps, triceps).

The analysis of blood samples collected during phase 2 showed that the values of IFN-ɣ, IL-6, and IL-10 in most of the MS subjects were below the limits of detection during the 5 appointments. The low values of these cytokines can be explained because the all subjects that were included in the study presented no active disease and most of them were under drug treatment. The main goal of the MS drug is to modulate he immune response MS drug shift Th1 to Th2 responses, thus low values of IFN-ɣ and IL-6 correlate with the use of the drug treatment. These results correlate with the results presented by others where MS subjects in a remission period presented low values of cytokines, and increased values during active periods [314-317]. Those studies showed that the increase in both pro- and anti- inflammatory cytokines correlates with the progression of the disease due to the increase in pro-inflammatory cytokines, and the simultaneous restorative process by anti-inflammatory cytokines [314-317].

Unlike other cytokines measured, TGF-β expression was measurable in all subjects prior to light treatment and showed changes during the PBM treatment in a disease severity dependent manner in phase 2. MS subjects with PDDS=0 presented

higher levels of TGF-β compared to PDDS≥1, however this difference was not significant. Interestingly, MS subjects with PDDS≥1 responded to PBM treatment with the active device with increased levels of TGF-β compared to the placebo treatment, however, this increase was not significant ($p=0.2403$). This increase was not observed in MS subjects with PDDS=0 (Figure 15). The fact that the levels of IL-6 were below of limit of detection while amounts of TGF-β present were significant is particularly important in MS. The presence of TGF-β and the lack of IL-6 induce CD4+ T cells to differentiate in Tregs which are considered protective in MS due to the production of production of anti-inflammatory cytokines (TGF-β, IL-10). Conversely, conditions were TGF-β and IL-6 are present lead to CD4+ T cells to differentiate into Th17, which are pathogenic in MS due to their production of pro inflammatory cytokines (IL-17, IL-6, IL-21, IL-22,TNF-α) [23, 38]. In addition, even though the increase in TGF-β was not significant, it is important in future studies to evaluate the effect of PBM on TGF-β in cell culture and in vivo experiments due to its role in MS and EAE. TGF-β is an anti-inflammatory cytokine that plays an important role in cell development differentiation and immune regulation [91]. TGF-β inhibits Th1 cell activation by the inhibition of both Jak-2 and Tyk-2 kinases and subsequently the phosphorylation of STAT 3 and STAT4. This inhibition leads to reduced T cell proliferation and IFN-ɣ production and increased apoptosis [93]. Several studies evaluated the role of TGFβ1 in the EAE mice [95-99]. Kuruvilla group reported that a daily intraperitoneal injection of TGF-β on SJL/J mice for 2 weeks starting the day of EAE induction delayed the onset of symptoms, reduced the severity of the second episode, and reduced the development of spontaneous relapses [95]. The Racke group showed that the addition of TGF-β to cell cultures inhibited the

activation and proliferation of myelin basic protein-specific lymph nodes cells. When these cells were transferred to naive mice, the EAE induction was reduced [96]. In in vivo experiments, the administration of TGF-β to mice with EAE reduced the severity of the disease, cellular infiltration in CNS, the expression of cell adhesion surface molecule lymphocyte function-associated Ag-1 (LFA-1), and the expression of MHC-II on antigen presenting cells in comparison with EAE mice without TGF-β1 treatment [96].

In conclusion, the results presented here show the potential effect of PBM to modulate immune response and nitrosative stress in MS subjects. The results showed that there was not a specific wavelength and dose of energy (J/cm^2) to modulate the immune response and reduce oxidative stress. The clinical severity of the disease seems to be an important factor during PBM treatment. We observed that MS subjects with higher severity of disease (PDDS≥1) responded better to PBM than those with low disease severity (PDDS=0). One of the most significant results obtained was with 830nm light treatment of PBMC. PBM with 830nm light ($10J/cm^2$, at 72h) produced both a reduction in nitrite and increase in IL-10 produced by PBMC ($p=0.0271$) as well as reduced IFN-ɣ produced by PBMC. The direct application of PBM treatment on MS subjects seems to be safe. The results suggest that it is necessary to recruit MS subjects with higher disability status (PDDS≥1) in order to observe more dramatic effect of PBM. However, the direct application of PBM on MS patient with higher disability must be monitored with extreme caution in order to avoid any imbalance in the immune response that could affect the health of MS subjects.

MODEL OF THE EFFECT OF PBM ON MS

Our results show that PBM has the potential to modulate cytokine production and nitrosative stress in MS subjects which correlate with our previous data collected using the EAE model. Data presented by others showed that PBM is absorbed by CCO in order to improve mitochondrial function and increase ATP production [239-242]. The improvement of mitochondrial function leads to a reduction of nitrosative stress which is a fundamental player in MS and EAE. Our data from the EAE model [287, 288] in combination with the data collected from MS subjects here show that PBM leads to a reduction of iNOS which induces the reduction of nitric oxide, which was indirectly measured by the quantification of nitrite. In the EAE model, the reduction of nitrite correlated with the reduction in the severity of disease, reduction in apoptosis, and reduction in cellular infiltration in the CNS [288]. Future studies are needed to evaluate the effect of PBM treatment in mitochondrial function (i.e. seahorse assay) in mice with EAE as well as in MS subjects.

Our data suggest that the reduction in nitric oxide as well as PBM treatment are involved in the shifting of Th1 responses to Th2 responses leading to an reduction of pro-inflammatory cytokines (IFN-g, IL-6) and an increase in anti-inflammatory cytokines (IL-10, TGF-β). Our data showed that PBM treatment is affected by the severity of disease presented by MS subjects. Therefore, patients with higher severity of disease showed more dramatic results. Future studies need to evaluate the role of MS disease-modifying drugs during PBM treatment. Most of our patients were receiving MS disease-modifying drugs, which mainly function to produce a shift of Th1 to Th2 responses in

order to prevent relapses. PBM in combination with the MS disease-modifying drugs could participate in improving the shift from Th1to Th2 responses.

FUTURE DIRECTIONS

The data collected here suggest that PBM has the potential to regulate immune response, nitrosative stress, and muscle fatigue in MS subjects. Previous work from our lab showed that 670nm (5J/cm^2) on C57BL/6 mice with EAE reduced IFN-ɣ and TNF-α, increased IL-10, and IL-4, and reduced nitrosative stress (NO_2 and iNOS) which correlated with a reduction in disease severity [287, 288]. C57BL/6 mice with EAE are characterized by the development of a chronic disease and only 20-30% of mice present relapses. Here we showed that 830nm was one of the best wavelengths to modulate cytokines and reduce nitrosative stress in MS subjects. Administration of 830nm light (10J/cm^2, at 72h) on PBMC resulted in reduced nitrite and IFN-ɣ ($p=0.1940$) and increased IL-10 ($p=0.0271$). Our results showed that the clinical severity of the disease plays a role during PBM treatment. MS subjects with higher severity of disease (PDDS≥1) showed better results to PBM than patients with low disease severity (PDDS=0). This, to some extent, correlates with the results observed in mice with EAE. Mice with chronic disease showed an improvement after PBM treatment [287, 288]. The fact that 670nm and 830nm regulated cytokines and nitrosative stress in EAE and MS respectively correlate with the observations made by Wong-Riley group where 670nm and 830nm increased CCO activity and ATP production [243]. In addition, they showed

that there was a positive correlation between the action spectra of CCO activity and the ATP content (at 670nm and 830nm) with the absorption spectrum of CCO [243].

MS is an autoimmune disease, however mitochondrial dysfunction and nitrosative stress are also present during acute and chronic stages of disease [147, 178-184]. Our experiments from mice with EAE and MS subjects showed that PBM can regulate the immune response and reduce nitrosative stress. However, the effect of PBM on mitochondrial function MS subjects has not been studied. Future experiments are needed in order to produce a sustained effect by PBM on the regulation of cytokines, reduction of nitrosative stress, and investigate the effect on mitochondrial function. Being able to determine the correct wavelengths and energy doses to improve mitochondrial function and understand how mitochondrial function evolves during PBM treatment can provide pivotal information to improve PBM treatments on MS subjects. Seahorse assay allows the use cells to evaluate mitochondrial function and production of ATP. Therefore, seahorse assay can be used to monitor how mitochondrial function behaves under specific wavelengths and doses of energies in order to find the best conditions to improve mitochondrial function. Furthermore, the seahorse assay can determine the initial state of mitochondria and then monitor their progression throughout PBM treatment. It could be possible that the energy doses needed to improve mitochondrial function would be different depending of disease severity. Therefore, the use of different doses of energy (energy dose curve assays) and the use of the seashore assay to monitor mitochondrial function will help to determine the optimal doses of energy during PBM for MS subjects with specific disease severity. We

hypothesized that the improvement of mitochondrial function will correlate with a reduction in nitrosative stress and regulation of cytokines.

The study of PBM on muscle fatigue in MS subjects needs also to be expanded. Our data showed that PBM reduced muscle fatigue in MS subjects with higher disease severity. However, data did not achieved statistical significance due to the small size of population, low number of patients with higher disease severity, and short period of PBM treatment (2 weeks). Therefore, to address these drawbacks in future experiments it will be necessary to increase our population size, increase the number of MS subjects with higher disease severity (PPDS≥1), apply PBM for longer period of time (i.e. 1 month), include more sensitive assays to evaluate muscle performance (i.e. walking tests, number of repetitions), evaluate serum enzymes related to muscle performance (CK, CKMB, LDH, PCR), evaluate serum cytokines during the course of the study. At different stages of disease, MS subjects develop motor problems, muscle fatigue in different parts of the body (i.e. arms, legs, back) or chronic fatigue en general Therefore, evaluating different muscle groups (i.e. biceps, triceps) could show the potential of PBM to treat different parts of the body to improve muscle activity in MS subjects.

APPENDIX A

Table 24. Phase 2. Serum cytokines				
PBMS #1 No on drug	**IFN-ɣ**	**IL-6**	**TGF-β**	**IL-10**
Visit		mean	mean	mean
1	0	0	12718.7263	0
2	0	0	10477.8341	0
3	0	0	9974.07215	1.74552055
4	0	0	8812.58763	1.83589912
5	0	0	11628.64	2.41773911
PBMC #6, COPAXONE				
Visit	**IFN-ɣ**	**IL-6**	**TGF-β**	**IL-10**
1	0	0	22459.3002	5.97012211
2	0	0	23433.9321	0
3	0	0	22400.5556	2.46357524
4	0	0	16932.3233	1.1266452
5	0	0	19745.4444	1.39736355
PBMS#14 OCREVUS				
Visit	**IFN-ɣ**	**IL-6**	**TGF-β**	**IL-10**
1	0	0	12592.4592	4.76855078
2	0	0	16600.5296	4.95307585
3	0	0	10566.3162	4.76831511
4	0	0	9921.95786	4.30605042
5	0	0	9063.48748	3.61280463
PBMS #10 REBIF				
Visit	**IFN-ɣ**	**IL-6**	**TGF-β**	**IL-10**
1	2.94898637	51.5240978	11674.5572	12.7005531
2	1.29298628	41.775989	14890.0912	10.0080058
3	1.39546597	48.3109143	12049.5792	8.66000166
4	0	41.6851965	11949.0826	9.5165494
5	0	48.4530275	11590.4679	8.70220676
PBMS #17 GILENYA				
Visit	**IFN-ɣ**	**IL-6**	**TGF-β**	**IL-10**
1	6.87711101	61.71561	17773.48	0
2	7.32600608	74.7527985	16709.0213	1.44014512
3	7.26926837	73.2116544	15441.0018	1.70154463
4	10.0519821	73.2728667	19349.032	2.05789447
5	8.44337528	71.831385	19812.133	0
	0	0	0	0
PBMS #18, betaseron				
Visit	**IFN-ɣ**	**IL-6**	**TGF-β**	**IL-10**
1	0	0	19591.9203	12.7449621
2	0	0	18429.1715	10.3602818

3	0	0	17862.7382	3.98179006
4	0	0	18092.6441	5.41620128
5	0	0	19085.225	4.25935237
PBMS #7 GILENYA				
Visit	**IFN-ɣ**	**IL-6**	**TGF-β**	**IL-10**
1	0	0	11238.6134	3.15010852
2	0	0	16267.1026	0
3	0	0	20355.9881	4.53726978
4	0	0	22211.4102	2.31312066
5	1.9693794	0	11875.9331	1.74646812
PBMS #13 GILENYA				
Visit	**IFN-ɣ**	**IL-6**	**TGF-β**	**IL-10**
1	0	2.68914523	20832.5446	0
2	0	5.82705739	20040.0433	0
3	0	3.56073298	18876.5231	1.3266452
4	0	2.88724344	20103.6391	1.70912442
5	0	3.75471019	24918.0458	1.72013461
PBMS #4 No on Drug				
Visit	**IFN-ɣ**	**IL-6**	**TGF-β**	**IL-10**
1	0	0	20200.9095	0
2	0	0	17722.9096	0
3	0	0	18837.1404	0
4	0	0	14624.451	1.77013461
5	0	0	15173.4319	0
PBMS #3 COPAXONE				
Visit	**IFN-ɣ**	**IL-6**	**TGF-β**	**IL-10**
1	19.5442543	82.606487	16528.7463	1.61385166
2	17.1022064	77.3337887	14460.5177	5.41633814
3	16.0330914	80.2054393	11505.2837	3.65913273
4	15.4429519	71.948152	16927.6269	1.75756871
5	12.793903	70.8422623	11816.7011	2.39160364
PBMS #11 Tecfidera				
Visit	**IFN-ɣ**	**IL-6**	**TGF-β**	**IL-10**
1	9.88521891	31.1689317	14483.1586	2.12770151
2	12.9502414	31.5987165	10762.9151	1.18464977
3	12.901799	31.7221459	12770.5176	2.19402789
4	11.6999615	31.762209	15257.403	3.30141138
5	10.9333311	27.2321192	16042.0072	1.72280162
PBMS #21 No on Drug				
Visit	**IFN-ɣ**	**IL-6**	**TGF-β**	**IL-10**
1	0	0	16355.8775	2.51488913
2	0	0	20887.8034	1.1266452
3	0	0	16957.2835	3.7054598

4	0	0	21169.8565	3.42687064
5	No sample	No sample	No sample	No sample

References.

1. Dutta, R. and B.D. Trapp, *Mechanisms of neuronal dysfunction and degeneration in multiple sclerosis.* Prog Neurobiol, 2011. **93**(1): p. 1-12.
2. *MS Overview.* Multiple Sclerosis Association of America, Update June 15, 2015. (http://www.mymsaa.org/about-ms/overview/#TypesofMS).
3. Scalfari, A., et al., *Mortality in patients with multiple sclerosis.* Neurology, 2013. **81**(2): p. 184-92.
4. *Who gets MS? (Epidemiology).* National Multiple Sclerosis Society, 2015(http://www.nationalmssociety.org/What-is-MS/Who-Gets-MS).
5. Koch-Henriksen, N. and P.S. Sorensen, *The changing demographic pattern of multiple sclerosis epidemiology.* Lancet Neurol, 2010. **9**(5): p. 520-32.
6. Sadovnick, A.D., P.A. Baird, and R.H. Ward, *Multiple sclerosis: updated risks for relatives.* Am J Med Genet, 1988. **29**(3): p. 533-41.
7. *HLA-DRB1.* Genetics Home Reference, 2014(http://ghr.nlm.nih.gov/gene=HLA-DRB1).
8. Ebers, G.C., *Environmental factors and multiple sclerosis.* Lancet Neurol, 2008. **7**(3): p. 268-77.
9. Files, D.K., et al., *Multiple sclerosis.* Prim Care, 2015. **42**(2): p. 159-75.
10. Compston, A. and A. Coles, *Multiple sclerosis.* Lancet, 2008. **372**(9648): p. 1502-17.
11. Bashinskaya, V.V., et al., *A review of genome-wide association studies for multiple sclerosis: classical and hypothesis-driven approaches.* Hum Genet, 2015. **134**(11-12): p. 1143-62.
12. Hindorff, L.A., et al., *Potential etiologic and functional implications of genome-wide association loci for human diseases and traits.* Proc Natl Acad Sci U S A, 2009. **106**(23): p. 9362-7.
13. De Jager, P.L., et al., *Meta-analysis of genome scans and replication identify CD6, IRF8 and TNFRSF1A as new multiple sclerosis susceptibility loci.* Nat Genet, 2009. **41**(7): p. 776-82.
14. Sawcer, S., et al., *Genetic risk and a primary role for cell-mediated immune mechanisms in multiple sclerosis.* Nature, 2011. **476**(7359): p. 214-9.
15. Madsen, L.S., et al., *A humanized model for multiple sclerosis using HLA-DR2 and a human T-cell receptor.* Nat Genet, 1999. **23**(3): p. 343-7.
16. Burton, P.R., et al., *Association scan of 14,500 nonsynonymous SNPs in four diseases identifies autoimmunity variants.* Nat Genet, 2007. **39**(11): p. 1329-37.
17. Beecham, A.H., et al., *Analysis of immune-related loci identifies 48 new susceptibility variants for multiple sclerosis.* Nat Genet, 2013. **45**(11): p. 1353-60.
18. Wingerchuk, D.M., C.F. Lucchinetti, and J.H. Noseworthy, *Multiple sclerosis: current pathophysiological concepts.* Lab Invest, 2001. **81**(3): p. 263-81.
19. Comabella, M. and S.J. Khoury, *Immunopathogenesis of multiple sclerosis.* Clin Immunol, 2012. **142**(1): p. 2-8.
20. Ben-Nun, A., H. Wekerle, and I.R. Cohen, *The rapid isolation of clonable antigen-specific T lymphocyte lines capable of mediating autoimmune encephalomyelitis.* Eur J Immunol, 1981. **11**(3): p. 195-9.
21. Miljkovic, D. and I. Spasojevic, *Multiple sclerosis: molecular mechanisms and therapeutic opportunities.* Antioxid Redox Signal, 2013. **19**(18): p. 2286-334.
22. Corthay, A., *A three-cell model for activation of naive T helper cells.* Scand J Immunol, 2006. **64**(2): p. 93-6.

23. Riedhammer, C. and R. Weissert, *Antigen Presentation, Autoantigens, and Immune Regulation in Multiple Sclerosis and Other Autoimmune Diseases.* Front Immunol, 2015. **6**: p. 322.
24. Goverman, J., *Autoimmune T cell responses in the central nervous system.* Nat Rev Immunol, 2009. **9**(6): p. 393-407.
25. Gutcher, I. and B. Becher, *APC-derived cytokines and T cell polarization in autoimmune inflammation.* J Clin Invest, 2007. **117**(5): p. 1119-27.
26. Kamradt, T. and N.A. Mitchison, *Tolerance and autoimmunity.* N Engl J Med, 2001. **344**(9): p. 655-64.
27. Xing, Y. and K.A. Hogquist, *T-cell tolerance: central and peripheral.* Cold Spring Harb Perspect Biol, 2012. **4**(6).
28. Harrington, C.J., et al., *Differential tolerance is induced in T cells recognizing distinct epitopes of myelin basic protein.* Immunity, 1998. **8**(5): p. 571-80.
29. Seamons, A., A. Perchellet, and J. Goverman, *Immune tolerance to myelin proteins.* Immunol Res, 2003. **28**(3): p. 201-21.
30. Macchi, B., et al., *Impaired apoptosis in mitogen-stimulated lymphocytes of patients with multiple sclerosis.* Neuroreport, 1999. **10**(2): p. 399-402.
31. Moreno, M., et al., *Activation-induced cell death in T lymphocytes from multiple sclerosis patients.* J Neuroimmunol, 2014. **272**(1-2): p. 51-5.
32. Lovett-Racke, A.E., et al., *Decreased dependence of myelin basic protein-reactive T cells on CD28-mediated costimulation in multiple sclerosis patients. A marker of activated/memory T cells.* J Clin Invest, 1998. **101**(4): p. 725-30.
33. Scholz, C., et al., *Expansion of autoreactive T cells in multiple sclerosis is independent of exogenous B7 costimulation.* J Immunol, 1998. **160**(3): p. 1532-8.
34. Oliveira, E.M., et al., *CTLA-4 dysregulation in the activation of myelin basic protein reactive T cells may distinguish patients with multiple sclerosis from healthy controls.* J Autoimmun, 2003. **20**(1): p. 71-81.
35. Markovic-Plese, S., et al., *CD4+CD28- costimulation-independent T cells in multiple sclerosis.* J Clin Invest, 2001. **108**(8): p. 1185-94.
36. Ortiz, G.G., et al., *Role of the blood-brain barrier in multiple sclerosis.* Arch Med Res, 2014. **45**(8): p. 687-97.
37. Sospedra, M. and R. Martin, *Immunology of multiple sclerosis.* Annu Rev Immunol, 2005. **23**: p. 683-747.
38. Duffy, S.S., J.G. Lees, and G. Moalem-Taylor, *The contribution of immune and glial cell types in experimental autoimmune encephalomyelitis and multiple sclerosis.* Mult Scler Int, 2014. **2014**: p. 285245.
39. Korner, H., et al., *Unimpaired autoreactive T-cell traffic within the central nervous system during tumor necrosis factor receptor-mediated inhibition of experimental autoimmune encephalomyelitis.* Proc Natl Acad Sci U S A, 1995. **92**(24): p. 11066-70.
40. Korner, H., et al., *Tumor necrosis factor blockade in actively induced experimental autoimmune encephalomyelitis prevents clinical disease despite activated T cell infiltration to the central nervous system.* Eur J Immunol, 1997. **27**(8): p. 1973-81.
41. Sean Riminton, D., et al., *Challenging cytokine redundancy: inflammatory cell movement and clinical course of experimental autoimmune encephalomyelitis are normal in lymphotoxin-deficient, but not tumor necrosis factor-deficient, mice.* J Exp Med, 1998. **187**(9): p. 1517-28.
42. Eugster, H.P., et al., *Severity of symptoms and demyelination in MOG-induced EAE depends on TNFR1.* Eur J Immunol, 1999. **29**(2): p. 626-32.
43. Selmaj, K., et al., *Prevention of chronic relapsing experimental autoimmune encephalomyelitis by soluble tumor necrosis factor receptor I.* J Neuroimmunol, 1995. **56**(2): p. 135-41.

44. Hovelmeyer, N., et al., *Apoptosis of oligodendrocytes via Fas and TNF-R1 is a key event in the induction of experimental autoimmune encephalomyelitis.* J Immunol, 2005. **175**(9): p. 5875-84.
45. Liu, J., et al., *TNF is a potent anti-inflammatory cytokine in autoimmune-mediated demyelination.* Nat Med, 1998. **4**(1): p. 78-83.
46. Brosnan, C.F., et al., *Cytokine localization in multiple sclerosis lesions: correlation with adhesion molecule expression and reactive nitrogen species.* Neurology, 1995. **45**(6 Suppl 6): p. S16-21.
47. Olsson, T., *Cytokines in neuroinflammatory disease: role of myelin autoreactive T cell production of interferon-gamma.* J Neuroimmunol, 1992. **40**(2-3): p. 211-8.
48. Renno, T., et al., *Cytokine production by cells in cerebrospinal fluid during experimental allergic encephalomyelitis in SJL/J mice.* J Neuroimmunol, 1994. **49**(1-2): p. 1-7.
49. Renno, T., et al., *Interferon-gamma in progression to chronic demyelination and neurological deficit following acute EAE.* Mol Cell Neurosci, 1998. **12**(6): p. 376-89.
50. Renno, T., et al., *TNF-alpha expression by resident microglia and infiltrating leukocytes in the central nervous system of mice with experimental allergic encephalomyelitis. Regulation by Th1 cytokines.* J Immunol, 1995. **154**(2): p. 944-53.
51. Panitch, H.S., et al., *Treatment of multiple sclerosis with gamma interferon: exacerbations associated with activation of the immune system.* Neurology, 1987. **37**(7): p. 1097-102.
52. Skurkovich, S., et al., *Randomized study of antibodies to IFN-gamma and TNF-alpha in secondary progressive multiple sclerosis.* Mult Scler, 2001. **7**(5): p. 277-84.
53. Ferber, I.A., et al., *Mice with a disrupted IFN-gamma gene are susceptible to the induction of experimental autoimmune encephalomyelitis (EAE).* J Immunol, 1996. **156**(1): p. 5-7.
54. Krakowski, M. and T. Owens, *Interferon-gamma confers resistance to experimental allergic encephalomyelitis.* Eur J Immunol, 1996. **26**(7): p. 1641-6.
55. Willenborg, D.O., et al., *IFN-gamma plays a critical down-regulatory role in the induction and effector phase of myelin oligodendrocyte glycoprotein-induced autoimmune encephalomyelitis.* J Immunol, 1996. **157**(8): p. 3223-7.
56. Billiau, A., et al., *Enhancement of experimental allergic encephalomyelitis in mice by antibodies against IFN-gamma.* J Immunol, 1988. **140**(5): p. 1506-10.
57. Duong, T.T., et al., *Effect of anti-interferon-gamma and anti-interleukin-2 monoclonal antibody treatment on the development of actively and passively induced experimental allergic encephalomyelitis in the SJL/J mouse.* J Neuroimmunol, 1992. **36**(2-3): p. 105-15.
58. Lublin, F.D., et al., *Monoclonal anti-gamma interferon antibodies enhance experimental allergic encephalomyelitis.* Autoimmunity, 1993. **16**(4): p. 267-74.
59. Chu, C.Q., S. Wittmer, and D.K. Dalton, *Failure to suppress the expansion of the activated CD4 T cell population in interferon gamma-deficient mice leads to exacerbation of experimental autoimmune encephalomyelitis.* J Exp Med, 2000. **192**(1): p. 123-8.
60. Voorthuis, J.A., et al., *Suppression of experimental allergic encephalomyelitis by intraventricular administration of interferon-gamma in Lewis rats.* Clin Exp Immunol, 1990. **81**(2): p. 183-8.
61. Heremans, H., et al., *Chronic relapsing experimental autoimmune encephalomyelitis (CREAE) in mice: enhancement by monoclonal antibodies against interferon-gamma.* Eur J Immunol, 1996. **26**(10): p. 2393-8.
62. Duong, T.T., et al., *Effect of anti-interferon-gamma monoclonal antibody treatment on the development of experimental allergic encephalomyelitis in resistant mouse strains.* J Neuroimmunol, 1994. **53**(1): p. 101-7.
63. Sabatino, J.J., Jr., et al., *Loss of IFN-gamma enables the expansion of autoreactive CD4+ T cells to induce experimental autoimmune encephalomyelitis by a nonencephalitogenic myelin variant antigen.* J Immunol, 2008. **180**(7): p. 4451-7.

64. Xiao, B.G., et al., *IL-12/IFN-gamma/NO axis plays critical role in development of Th1-mediated experimental autoimmune encephalomyelitis.* Mol Immunol, 2008. **45**(4): p. 1191-6.
65. Furlan, R., et al., *Intrathecal delivery of IFN-gamma protects C57BL/6 mice from chronic-progressive experimental autoimmune encephalomyelitis by increasing apoptosis of central nervous system-infiltrating lymphocytes.* J Immunol, 2001. **167**(3): p. 1821-9.
66. Rothaug, M., C. Becker-Pauly, and S. Rose-John, *The role of interleukin-6 signaling in nervous tissue.* Biochim Biophys Acta, 2016. **1863**(6 Pt A): p. 1218-27.
67. Kaur, S., et al., *A panoramic review of IL-6: Structure, pathophysiological roles and inhibitors.* Bioorg Med Chem, 2020. **28**(5): p. 115327.
68. Chalaris, A., et al., *The soluble Interleukin 6 receptor: generation and role in inflammation and cancer.* Eur J Cell Biol, 2011. **90**(6-7): p. 484-94.
69. Taga, T., et al., *Interleukin-6 triggers the association of its receptor with a possible signal transducer, gp130.* Cell, 1989. **58**(3): p. 573-81.
70. Hibi, M., et al., *Molecular cloning and expression of an IL-6 signal transducer, gp130.* Cell, 1990. **63**(6): p. 1149-57.
71. Samoilova, E.B., et al., *IL-6-deficient mice are resistant to experimental autoimmune encephalomyelitis: roles of IL-6 in the activation and differentiation of autoreactive T cells.* J Immunol, 1998. **161**(12): p. 6480-6.
72. Okuda, Y., et al., *IL-6-deficient mice are resistant to the induction of experimental autoimmune encephalomyelitis provoked by myelin oligodendrocyte glycoprotein.* Int Immunol, 1998. **10**(5): p. 703-8.
73. Eugster, H.P., et al., *IL-6-deficient mice resist myelin oligodendrocyte glycoprotein-induced autoimmune encephalomyelitis.* Eur J Immunol, 1998. **28**(7): p. 2178-87.
74. Serada, S., et al., *IL-6 blockade inhibits the induction of myelin antigen-specific Th17 cells and Th1 cells in experimental autoimmune encephalomyelitis.* Proc Natl Acad Sci U S A, 2008. **105**(26): p. 9041-6.
75. Wullschleger, A., et al., *Cerebrospinal fluid interleukin-6 in central nervous system inflammatory diseases.* PLoS One, 2013. **8**(8): p. e72399.
76. Frei, K., et al., *Interleukin-6 is elevated in plasma in multiple sclerosis.* J Neuroimmunol, 1991. **31**(2): p. 147-53.
77. Lanzillo, R., et al., *Immunometabolic profiling of patients with multiple sclerosis identifies new biomarkers to predict disease activity during treatment with interferon beta-1a.* Clin Immunol, 2017. **183**: p. 249-253.
78. Maimone, D., G.C. Guazzi, and P. Annunziata, *IL-6 detection in multiple sclerosis brain.* J Neurol Sci, 1997. **146**(1): p. 59-65.
79. Lubina-Dabrowska, N., et al., *Effects of IFN-beta1a and IFN-beta1b treatment on the expression of cytokines, inducible NOS (NOS type II), and myelin proteins in animal model of multiple sclerosis.* Arch Immunol Ther Exp (Warsz), 2017. **65**(4): p. 325-338.
80. Bitan, M., et al., *Heparanase upregulates Th2 cytokines, ameliorating experimental autoimmune encephalitis.* Mol Immunol, 2010. **47**(10): p. 1890-8.
81. Zhang, G.X., et al., *Glucosamine abrogates the acute phase of experimental autoimmune encephalomyelitis by induction of Th2 response.* J Immunol, 2005. **175**(11): p. 7202-8.
82. Falcone, M., et al., *A critical role for IL-4 in regulating disease severity in experimental allergic encephalomyelitis as demonstrated in IL-4-deficient C57BL/6 mice and BALB/c mice.* J Immunol, 1998. **160**(10): p. 4822-30.
83. Furlan, R., et al., *Central nervous system delivery of interleukin 4 by a nonreplicative herpes simplex type 1 viral vector ameliorates autoimmune demyelination.* Hum Gene Ther, 1998. **9**(17): p. 2605-17.

84. Furlan, R., et al., *Central nervous system gene therapy with interleukin-4 inhibits progression of ongoing relapsing-remitting autoimmune encephalomyelitis in Biozzi AB/H mice.* Gene Ther, 2001. **8**(1): p. 13-9.
85. Lu, C.Z., M.A. Jensen, and B.G. Arnason, *Interferon gamma- and interleukin-4-secreting cells in multiple sclerosis.* J Neuroimmunol, 1993. **46**(1-2): p. 123-8.
86. Samoilova, E.B., J.L. Horton, and Y. Chen, *Acceleration of experimental autoimmune encephalomyelitis in interleukin-10-deficient mice: roles of interleukin-10 in disease progression and recovery.* Cell Immunol, 1998. **188**(2): p. 118-24.
87. Bettelli, E., et al., *IL-10 is critical in the regulation of autoimmune encephalomyelitis as demonstrated by studies of IL-10- and IL-4-deficient and transgenic mice.* J Immunol, 1998. **161**(7): p. 3299-306.
88. Brod, S.A., et al., *Increased in vitro induced CD4+ and CD8+ T cell IFN-gamma and CD4+ T cell IL-10 production in stable relapsing multiple sclerosis.* Int J Neurosci, 1997. **90**(3-4): p. 187-202.
89. Hohnoki, K., A. Inoue, and C.S. Koh, *Elevated serum levels of IFN-gamma, IL-4 and TNF-alpha/unelevated serum levels of IL-10 in patients with demyelinating diseases during the acute stage.* J Neuroimmunol, 1998. **87**(1-2): p. 27-32.
90. Rodriguez-Sainz Mdel, C., et al., *Th1/Th2 cytokine balance and nitric oxide in cerebrospinal fluid and serum from patients with multiple sclerosis.* Eur Cytokine Netw, 2002. **13**(1): p. 110-4.
91. Lee, P.W., M.E. Severin, and A.E. Lovett-Racke, *TGF-beta regulation of encephalitogenic and regulatory T cells in multiple sclerosis.* Eur J Immunol, 2017. **47**(3): p. 446-453.
92. Kehrl, J.H., et al., *Production of transforming growth factor beta by human T lymphocytes and its potential role in the regulation of T cell growth.* J Exp Med, 1986. **163**(5): p. 1037-50.
93. Bright, J.J. and S. Sriram, *TGF-beta inhibits IL-12-induced activation of Jak-STAT pathway in T lymphocytes.* J Immunol, 1998. **161**(4): p. 1772-7.
94. Gorelik, L. and R.A. Flavell, *Abrogation of TGFbeta signaling in T cells leads to spontaneous T cell differentiation and autoimmune disease.* Immunity, 2000. **12**(2): p. 171-81.
95. Kuruvilla, A.P., et al., *Protective effect of transforming growth factor beta 1 on experimental autoimmune diseases in mice.* Proc Natl Acad Sci U S A, 1991. **88**(7): p. 2918-21.
96. Racke, M.K., et al., *Prevention and treatment of chronic relapsing experimental allergic encephalomyelitis by transforming growth factor-beta 1.* J Immunol, 1991. **146**(9): p. 3012-7.
97. Johns, L.D., et al., *Successful treatment of experimental allergic encephalomyelitis with transforming growth factor-beta 1.* J Immunol, 1991. **147**(6): p. 1792-6.
98. Racke, M.K., et al., *Long-term treatment of chronic relapsing experimental allergic encephalomyelitis by transforming growth factor-beta 2.* J Neuroimmunol, 1993. **46**(1-2): p. 175-83.
99. Huss, D.J., et al., *TGF-beta enhances effector Th1 cell activation but promotes self-regulation via IL-10.* J Immunol, 2010. **184**(10): p. 5628-36.
100. Nelson, E.J., J. Connolly, and P. McArthur, *Nitric oxide and S-nitrosylation: excitotoxic and cell signaling mechanism.* Biol Cell, 2003. **95**(1): p. 3-8.
101. Pannu, R. and I. Singh, *Pharmacological strategies for the regulation of inducible nitric oxide synthase: neurodegenerative versus neuroprotective mechanisms.* Neurochem Int, 2006. **49**(2): p. 170-82.
102. Hall, C.N. and J. Garthwaite, *What is the real physiological NO concentration in vivo?* Nitric Oxide, 2009. **21**(2): p. 92-103.
103. Herulf, M., et al., *Increased nitric oxide in infective gastroenteritis.* J Infect Dis, 1999. **180**(2): p. 542-5.
104. Aktan, F., *iNOS-mediated nitric oxide production and its regulation.* Life Sci, 2004. **75**(6): p. 639-53.

105. Xue, Q., et al., *Regulation of iNOS on Immune Cells and Its Role in Diseases.* Int J Mol Sci, 2018. **19**(12).
106. Mao, K., et al., *Nitric oxide suppresses NLRP3 inflammasome activation and protects against LPS-induced septic shock.* Cell Res, 2013. **23**(2): p. 201-12.
107. Mishra, B.B., et al., *Nitric oxide controls the immunopathology of tuberculosis by inhibiting NLRP3 inflammasome-dependent processing of IL-1beta.* Nat Immunol, 2013. **14**(1): p. 52-60.
108. Hernandez-Cuellar, E., et al., *Cutting edge: nitric oxide inhibits the NLRP3 inflammasome.* J Immunol, 2012. **189**(11): p. 5113-7.
109. Bogdan, C., *Nitric oxide synthase in innate and adaptive immunity: an update.* Trends Immunol, 2015. **36**(3): p. 161-78.
110. Bauer, H., et al., *Nitric oxide inhibits the secretion of T-helper 1- and T-helper 2-associated cytokines in activated human T cells.* Immunology, 1997. **90**(2): p. 205-11.
111. Kahn, D.A., et al., *Adjuvant immunotherapy is dependent on inducible nitric oxide synthase.* J Exp Med, 2001. **193**(11): p. 1261-8.
112. Niedbala, W., et al., *Effects of nitric oxide on the induction and differentiation of Th1 cells.* Eur J Immunol, 1999. **29**(8): p. 2498-505.
113. Wei, X.Q., et al., *Altered immune responses in mice lacking inducible nitric oxide synthase.* Nature, 1995. **375**(6530): p. 408-11.
114. McInnes, I.B., et al., *Septic arthritis following Staphylococcus aureus infection in mice lacking inducible nitric oxide synthase.* J Immunol, 1998. **160**(1): p. 308-15.
115. MacLean, A., et al., *Mice lacking inducible nitric-oxide synthase are more susceptible to herpes simplex virus infection despite enhanced Th1 cell responses.* J Gen Virol, 1998. **79 (Pt 4)**: p. 825-30.
116. Kies, M.W. and E.C. Alvord, Jr., *[Prevention of allergic encephalomyelitis by prior injection of adjuvants].* Nature, 1958. **182**(4642): p. 1106.
117. Hempel, K., et al., *Unresponsiveness to experimental allergic encephalomyelitis in Lewis rats pretreated with complete Freund's adjuvant.* Int Arch Allergy Appl Immunol, 1985. **76**(3): p. 193-9.
118. Stevens, D.B., et al., *Studies of V beta 8 T cell receptor peptide treatment in experimental autoimmune encephalomyelitis.* J Neuroimmunol, 1992. **37**(1-2): p. 123-9.
119. Lisak, R.P. and B. Zweiman, *Immune responses to myelin basic protein in mycobacterial-induced suppression of experimental allergic encephalomyelitis.* Cell Immunol, 1974. **14**(2): p. 242-54.
120. Falk, G.A., M.W. Kies, and E.C. Alvord, Jr., *Passive transfer of experimental allergic encephalomyelitis: mechanisms of suppression.* J Immunol, 1969. **103**(6): p. 1248-53.
121. Huang, F.P., et al., *Nitric oxide regulates Th1 cell development through the inhibition of IL-12 synthesis by macrophages.* Eur J Immunol, 1998. **28**(12): p. 4062-70.
122. S. Ibiza, J.M.S., *The role of nitric oxide in the regulation of adaptive immune responses.* Inmunologia, 2008. **27**(3): p. 103-117.
123. Fenyk-Melody, J.E., et al., *Experimental autoimmune encephalomyelitis is exacerbated in mice lacking the NOS2 gene.* J Immunol, 1998. **160**(6): p. 2940-6.
124. Niedbala, W., et al., *Nitric oxide preferentially induces type 1 T cell differentiation by selectively up-regulating IL-12 receptor beta 2 expression via cGMP.* Proc Natl Acad Sci U S A, 2002. **99**(25): p. 16186-91.
125. Bingisser, R.M., et al., *Macrophage-derived nitric oxide regulates T cell activation via reversible disruption of the Jak3/STAT5 signaling pathway.* J Immunol, 1998. **160**(12): p. 5729-34.
126. Mazzoni, A., et al., *Myeloid suppressor lines inhibit T cell responses by an NO-dependent mechanism.* J Immunol, 2002. **168**(2): p. 689-95.

127. Sato, K., et al., *Nitric oxide plays a critical role in suppression of T-cell proliferation by mesenchymal stem cells.* Blood, 2007. **109**(1): p. 228-34.
128. Ferguson, B., et al., *Axonal damage in acute multiple sclerosis lesions.* Brain, 1997. **120 (Pt 3)**: p. 393-9.
129. Kornek, B., et al., *Distribution of a calcium channel subunit in dystrophic axons in multiple sclerosis and experimental autoimmune encephalomyelitis.* Brain, 2001. **124**(Pt 6): p. 1114-24.
130. Bjartmar, C., J.R. Wujek, and B.D. Trapp, *Axonal loss in the pathology of MS: consequences for understanding the progressive phase of the disease.* J Neurol Sci, 2003. **206**(2): p. 165-71.
131. Trapp, B.D., et al., *Axonal transection in the lesions of multiple sclerosis.* N Engl J Med, 1998. **338**(5): p. 278-85.
132. Arancibia-Carcamo, I.L. and D. Attwell, *The node of Ranvier in CNS pathology.* Acta Neuropathol, 2014. **128**(2): p. 161-75.
133. Craner, M.J., et al., *Molecular changes in neurons in multiple sclerosis: altered axonal expression of Nav1.2 and Nav1.6 sodium channels and Na+/Ca2+ exchanger.* Proc Natl Acad Sci U S A, 2004. **101**(21): p. 8168-73.
134. Stys, P.K., S.G. Waxman, and B.R. Ransom, *Ionic mechanisms of anoxic injury in mammalian CNS white matter: role of Na+ channels and Na(+)-Ca2+ exchanger.* J Neurosci, 1992. **12**(2): p. 430-9.
135. Stys, P.K., *White matter injury mechanisms.* Curr Mol Med, 2004. **4**(2): p. 113-30.
136. Gunter, T.E. and S.S. Sheu, *Characteristics and possible functions of mitochondrial Ca(2+) transport mechanisms.* Biochim Biophys Acta, 2009. **1787**(11): p. 1291-308.
137. Trapp, B.D., R. Ransohoff, and R. Rudick, *Axonal pathology in multiple sclerosis: relationship to neurologic disability.* Curr Opin Neurol, 1999. **12**(3): p. 295-302.
138. Ganter, P., C. Prince, and M.M. Esiri, *Spinal cord axonal loss in multiple sclerosis: a post-mortem study.* Neuropathol Appl Neurobiol, 1999. **25**(6): p. 459-67.
139. Lovas, G., et al., *Axonal changes in chronic demyelinated cervical spinal cord plaques.* Brain, 2000. **123 (Pt 2)**: p. 308-17.
140. Bjartmar, C., et al., *Neurological disability correlates with spinal cord axonal loss and reduced N-acetyl aspartate in chronic multiple sclerosis patients.* Ann Neurol, 2000. **48**(6): p. 893-901.
141. Trapp, B.D. and K.A. Nave, *Multiple sclerosis: an immune or neurodegenerative disorder?* Annu Rev Neurosci, 2008. **31**: p. 247-69.
142. Baines, C.P., et al., *Loss of cyclophilin D reveals a critical role for mitochondrial permeability transition in cell death.* Nature, 2005. **434**(7033): p. 658-62.
143. Forte, M., et al., *Cyclophilin D inactivation protects axons in experimental autoimmune encephalomyelitis, an animal model of multiple sclerosis.* Proc Natl Acad Sci U S A, 2007. **104**(18): p. 7558-63.
144. Yin, X., et al., *Myelin-associated glycoprotein is a myelin signal that modulates the caliber of myelinated axons.* J Neurosci, 1998. **18**(6): p. 1953-62.
145. Lappe-Siefke, C., et al., *Disruption of Cnp1 uncouples oligodendroglial functions in axonal support and myelination.* Nat Genet, 2003. **33**(3): p. 366-74.
146. Klugmann, M., et al., *Assembly of CNS myelin in the absence of proteolipid protein.* Neuron, 1997. **18**(1): p. 59-70.
147. Dutta, R. and B.D. Trapp, *Pathogenesis of axonal and neuronal damage in multiple sclerosis.* Neurology, 2007. **68**(22 Suppl 3): p. S22-31; discussion S43-54.
148. Wujek, J.R., et al., *Axon loss in the spinal cord determines permanent neurological disability in an animal model of multiple sclerosis.* J Neuropathol Exp Neurol, 2002. **61**(1): p. 23-32.
149. De Stefano, N., et al., *Axonal damage correlates with disability in patients with relapsing-remitting multiple sclerosis. Results of a longitudinal magnetic resonance spectroscopy study.* Brain, 1998. **121 (Pt 8)**: p. 1469-77.

150. Gonen, O., et al., *Total brain N-acetylaspartate: a new measure of disease load in MS.* Neurology, 2000. **54**(1): p. 15-9.
151. Fu, L., et al., *Imaging axonal damage of normal-appearing white matter in multiple sclerosis.* Brain, 1998. **121 (Pt 1)**: p. 103-13.
152. Khan, O., et al., *Axonal metabolic recovery and potential neuroprotective effect of glatiramer acetate in relapsing-remitting multiple sclerosis.* Mult Scler, 2005. **11**(6): p. 646-51.
153. Foster, R.E., C.C. Whalen, and S.G. Waxman, *Reorganization of the axon membrane in demyelinated peripheral nerve fibers: morphological evidence.* Science, 1980. **210**(4470): p. 661-3.
154. Felts, P.A., T.A. Baker, and K.J. Smith, *Conduction in segmentally demyelinated mammalian central axons.* J Neurosci, 1997. **17**(19): p. 7267-77.
155. Reddy, H., et al., *Evidence for adaptive functional changes in the cerebral cortex with axonal injury from multiple sclerosis.* Brain, 2000. **123 (Pt 11)**: p. 2314-20.
156. Koopman, W.J., P.H. Willems, and J.A. Smeitink, *Monogenic mitochondrial disorders.* N Engl J Med, 2012. **366**(12): p. 1132-41.
157. Poyton, R.O., K.A. Ball, and P.R. Castello, *Mitochondrial generation of free radicals and hypoxic signaling.* Trends Endocrinol Metab, 2009. **20**(7): p. 332-40.
158. Castello, P.R., et al., *Mitochondrial cytochrome oxidase produces nitric oxide under hypoxic conditions: implications for oxygen sensing and hypoxic signaling in eukaryotes.* Cell Metab, 2006. **3**(4): p. 277-87.
159. Basu, S., et al., *Nitrite reductase activity of cytochrome c.* J Biol Chem, 2008. **283**(47): p. 32590-7.
160. Cleeter, M.W., et al., *Reversible inhibition of cytochrome c oxidase, the terminal enzyme of the mitochondrial respiratory chain, by nitric oxide. Implications for neurodegenerative diseases.* FEBS Lett, 1994. **345**(1): p. 50-4.
161. Sarti, P., et al., *Nitric oxide and cytochrome c oxidase: mechanisms of inhibition and NO degradation.* Biochem Biophys Res Commun, 2000. **274**(1): p. 183-7.
162. Mason, M.G., et al., *Nitric oxide inhibition of respiration involves both competitive (heme) and noncompetitive (copper) binding to cytochrome c oxidase.* Proc Natl Acad Sci U S A, 2006. **103**(3): p. 708-13.
163. Hamblin, M.R., *MECHANISMS OF LOW LEVEL LIGHT THERAPY.* 2008.
164. Poderoso, J.J., et al., *Nitric oxide regulates oxygen uptake and hydrogen peroxide release by the isolated beating rat heart.* Am J Physiol, 1998. **274**(1 Pt 1): p. C112-9.
165. Poderoso, J.J., et al., *Nitric oxide inhibits electron transfer and increases superoxide radical production in rat heart mitochondria and submitochondrial particles.* Arch Biochem Biophys, 1996. **328**(1): p. 85-92.
166. Borutaite, V. and G.C. Brown, *Nitric oxide induces apoptosis via hydrogen peroxide, but necrosis via energy and thiol depletion.* Free Radic Biol Med, 2003. **35**(11): p. 1457-68.
167. Borutaite, V., A. Budriunaite, and G.C. Brown, *Reversal of nitric oxide-, peroxynitrite- and S-nitrosothiol-induced inhibition of mitochondrial respiration or complex I activity by light and thiols.* Biochim Biophys Acta, 2000. **1459**(2-3): p. 405-12.
168. Riobo, N.A., et al., *Nitric oxide inhibits mitochondrial NADH:ubiquinone reductase activity through peroxynitrite formation.* Biochem J, 2001. **359**(Pt 1): p. 139-45.
169. Brown, G.C., *Regulation of mitochondrial respiration by nitric oxide inhibition of cytochrome c oxidase.* Biochim Biophys Acta, 2001. **1504**(1): p. 46-57.
170. Bal-Price, A. and G.C. Brown, *Inflammatory neurodegeneration mediated by nitric oxide from activated glia-inhibiting neuronal respiration, causing glutamate release and excitotoxicity.* J Neurosci, 2001. **21**(17): p. 6480-91.

171. Trabace, L. and K.M. Kendrick, *Nitric oxide can differentially modulate striatal neurotransmitter concentrations via soluble guanylate cyclase and peroxynitrite formation.* J Neurochem, 2000. **75**(4): p. 1664-74.
172. McNaught, K.S. and G.C. Brown, *Nitric oxide causes glutamate release from brain synaptosomes.* J Neurochem, 1998. **70**(4): p. 1541-6.
173. Brown, G.C., *Nitric oxide and neuronal death.* Nitric Oxide, 2010. **23**(3): p. 153-65.
174. Groom, A.J., T. Smith, and L. Turski, *Multiple sclerosis and glutamate.* Ann N Y Acad Sci, 2003. **993**: p. 229-75; discussion 287-8.
175. Nicholls, D.G. and S.L. Budd, *Neuronal excitotoxicity: the role of mitochondria.* Biofactors, 1998. **8**(3-4): p. 287-99.
176. Polster, B.M., et al., *Calpain I induces cleavage and release of apoptosis-inducing factor from isolated mitochondria.* J Biol Chem, 2005. **280**(8): p. 6447-54.
177. Landshamer, S., et al., *Bid-induced release of AIF from mitochondria causes immediate neuronal cell death.* Cell Death Differ, 2008. **15**(10): p. 1553-63.
178. Lu, F., et al., *Oxidative damage to mitochondrial DNA and activity of mitochondrial enzymes in chronic active lesions of multiple sclerosis.* J Neurol Sci, 2000. **177**(2): p. 95-103.
179. Dutta, R., et al., *Mitochondrial dysfunction as a cause of axonal degeneration in multiple sclerosis patients.* Ann Neurol, 2006. **59**(3): p. 478-89.
180. Qi, X., et al., *Mitochondrial protein nitration primes neurodegeneration in experimental autoimmune encephalomyelitis.* J Biol Chem, 2006. **281**(42): p. 31950-62.
181. Qi, X., et al., *Suppression of mitochondrial oxidative stress provides long-term neuroprotection in experimental optic neuritis.* Invest Ophthalmol Vis Sci, 2007. **48**(2): p. 681-91.
182. O'Brien, N.C., et al., *Nitric oxide plays a critical role in the recovery of Lewis rats from experimental autoimmune encephalomyelitis and the maintenance of resistance to reinduction.* J Immunol, 1999. **163**(12): p. 6841-7.
183. Jolivalt, C.G., et al., *A novel nitric oxide scavenger in combination with cyclosporine A ameliorates experimental autoimmune encephalomyelitis progression in mice.* J Neuroimmunol, 2003. **138**(1-2): p. 56-64.
184. Calabrese, V., et al., *Nitric oxide synthase is present in the cerebrospinal fluid of patients with active multiple sclerosis and is associated with increases in cerebrospinal fluid protein nitrotyrosine and S-nitrosothiols and with changes in glutathione levels.* J Neurosci Res, 2002. **70**(4): p. 580-7.
185. Damal, K., E. Stoker, and J.F. Foley, *Optimizing therapeutics in the management of patients with multiple sclerosis: a review of drug efficacy, dosing, and mechanisms of action.* Biologics, 2013. **7**: p. 247-58.
186. Rommer, P.S., et al., *Immunological Aspects of Approved MS Therapeutics.* Front Immunol, 2019. **10**: p. 1564.
187. Neuhaus, O., B.C. Kieseier, and H.P. Hartung, *Pharmacokinetics and pharmacodynamics of the interferon-betas, glatiramer acetate, and mitoxantrone in multiple sclerosis.* J Neurol Sci, 2007. **259**(1-2): p. 27-37.
188. White, J.T., et al., *Incidence, characterization, and clinical impact analysis of peginterferon beta1a immunogenicity in patients with multiple sclerosis in the ADVANCE trial.* Ther Adv Neurol Disord, 2016. **9**(4): p. 239-49.
189. Markowitz, C.E., *Interferon-beta: mechanism of action and dosing issues.* Neurology, 2007. **68**(24 Suppl 4): p. S8-11.
190. Zhang, J., G. Hutton, and Y. Zang, *A comparison of the mechanisms of action of interferon beta and glatiramer acetate in the treatment of multiple sclerosis.* Clin Ther, 2002. **24**(12): p. 1998-2021.

191. Kay, M., Z. Hojati, and F. Dehghanian, *The molecular study of IFNbeta pleiotropic roles in MS treatment.* Iran J Neurol, 2013. **12**(4): p. 149-56.
192. Wandinger, K.P., et al., *Complex immunomodulatory effects of interferon-beta in multiple sclerosis include the upregulation of T helper 1-associated marker genes.* Ann Neurol, 2001. **50**(3): p. 349-57.
193. *Interferon beta-1b in the treatment of multiple sclerosis: final outcome of the randomized controlled trial. The IFNB Multiple Sclerosis Study Group and The University of British Columbia MS/MRI Analysis Group.* Neurology, 1995. **45**(7): p. 1277-85.
194. *Interferon beta-1b is effective in relapsing-remitting multiple sclerosis. I. Clinical results of a multicenter, randomized, double-blind, placebo-controlled trial. The IFNB Multiple Sclerosis Study Group.* Neurology, 1993. **43**(4): p. 655-61.
195. Vermersch, P., et al., *Interferon beta1a (Avonex) treatment in multiple sclerosis: similarity of effect on progression of disability in patients with mild and moderate disability.* J Neurol, 2002. **249**(2): p. 184-7.
196. Ben-Nun, A., et al., *The autoimmune reactivity to myelin oligodendrocyte glycoprotein (MOG) in multiple sclerosis is potentially pathogenic: effect of copolymer 1 on MOG-induced disease.* J Neurol, 1996. **243**(4 Suppl 1): p. S14-22.
197. Teitelbaum, D., et al., *Synthetic copolymer 1 inhibits human T-cell lines specific for myelin basic protein.* Proc Natl Acad Sci U S A, 1992. **89**(1): p. 137-41.
198. Teitelbaum, D., et al., *Copolymer 1 inhibits chronic relapsing experimental allergic encephalomyelitis induced by proteolipid protein (PLP) peptides in mice and interferes with PLP-specific T cell responses.* J Neuroimmunol, 1996. **64**(2): p. 209-17.
199. Neuhaus, O., et al., *Multiple sclerosis: comparison of copolymer-1- reactive T cell lines from treated and untreated subjects reveals cytokine shift from T helper 1 to T helper 2 cells.* Proc Natl Acad Sci U S A, 2000. **97**(13): p. 7452-7.
200. Chen, M., et al., *Glatiramer acetate induces a Th2-biased response and crossreactivity with myelin basic protein in patients with MS.* Mult Scler, 2001. **7**(4): p. 209-19.
201. Vieira, P.L., et al., *Glatiramer acetate (copolymer-1, copaxone) promotes Th2 cell development and increased IL-10 production through modulation of dendritic cells.* J Immunol, 2003. **170**(9): p. 4483-8.
202. Ziemssen, T., et al., *Glatiramer acetate-specific T-helper 1- and 2-type cell lines produce BDNF: implications for multiple sclerosis therapy. Brain-derived neurotrophic factor.* Brain, 2002. **125**(Pt 11): p. 2381-91.
203. Aharoni, R., R. Arnon, and R. Eilam, *Neurogenesis and neuroprotection induced by peripheral immunomodulatory treatment of experimental autoimmune encephalomyelitis.* J Neurosci, 2005. **25**(36): p. 8217-28.
204. Johnson, K.P., et al., *Copolymer 1 reduces relapse rate and improves disability in relapsing-remitting multiple sclerosis: results of a phase III multicenter, double-blind placebo-controlled trial. The Copolymer 1 Multiple Sclerosis Study Group.* Neurology, 1995. **45**(7): p. 1268-76.
205. Comi, G., M. Filippi, and J.S. Wolinsky, *European/Canadian multicenter, double-blind, randomized, placebo-controlled study of the effects of glatiramer acetate on magnetic resonance imaging--measured disease activity and burden in patients with relapsing multiple sclerosis. European/Canadian Glatiramer Acetate Study Group.* Ann Neurol, 2001. **49**(3): p. 290-7.
206. Ford, C., et al., *Continuous long-term immunomodulatory therapy in relapsing multiple sclerosis: results from the 15-year analysis of the US prospective open-label study of glatiramer acetate.* Mult Scler, 2010. **16**(3): p. 342-50.

207. Xie, J.H., et al., *Sphingosine-1-phosphate receptor agonism impairs the efficiency of the local immune response by altering trafficking of naive and antigen-activated CD4+ T cells.* J Immunol, 2003. **170**(7): p. 3662-70.
208. Chiba, K., et al., *FTY720, a novel immunosuppressant, induces sequestration of circulating mature lymphocytes by acceleration of lymphocyte homing in rats. I. FTY720 selectively decreases the number of circulating mature lymphocytes by acceleration of lymphocyte homing.* J Immunol, 1998. **160**(10): p. 5037-44.
209. Yanagawa, Y., Y. Masubuchi, and K. Chiba, *FTY720, a novel immunosuppressant, induces sequestration of circulating mature lymphocytes by acceleration of lymphocyte homing in rats, III. Increase in frequency of CD62L-positive T cells in Peyer's patches by FTY720-induced lymphocyte homing.* Immunology, 1998. **95**(4): p. 591-4.
210. Fujino, M., et al., *Amelioration of experimental autoimmune encephalomyelitis in Lewis rats by FTY720 treatment.* J Pharmacol Exp Ther, 2003. **305**(1): p. 70-7.
211. Miron, V.E., et al., *Fingolimod (FTY720) enhances remyelination following demyelination of organotypic cerebellar slices.* Am J Pathol, 2010. **176**(6): p. 2682-94.
212. Cohen, J.A., et al., *Oral fingolimod or intramuscular interferon for relapsing multiple sclerosis.* N Engl J Med, 2010. **362**(5): p. 402-15.
213. Kappos, L., et al., *Long-term effects of fingolimod in multiple sclerosis: the randomized FREEDOMS extension trial.* Neurology, 2015. **84**(15): p. 1582-91.
214. Wierinckx, A., et al., *Detoxication enzyme inducers modify cytokine production in rat mixed glial cells.* J Neuroimmunol, 2005. **166**(1-2): p. 132-43.
215. Albrecht, P., et al., *Effects of dimethyl fumarate on neuroprotection and immunomodulation.* J Neuroinflammation, 2012. **9**: p. 163.
216. Linker, R.A., et al., *Fumaric acid esters exert neuroprotective effects in neuroinflammation via activation of the Nrf2 antioxidant pathway.* Brain, 2011. **134**(Pt 3): p. 678-92.
217. Dubey, D., et al., *Dimethyl fumarate in relapsing-remitting multiple sclerosis: rationale, mechanisms of action, pharmacokinetics, efficacy and safety.* Expert Rev Neurother, 2015. **15**(4): p. 339-46.
218. Peng, H., et al., *Dimethyl fumarate inhibits dendritic cell maturation via nuclear factor kappaB (NF-kappaB) and extracellular signal-regulated kinase 1 and 2 (ERK1/2) and mitogen stress-activated kinase 1 (MSK1) signaling.* J Biol Chem, 2012. **287**(33): p. 28017-26.
219. Schilling, S., et al., *Fumaric acid esters are effective in chronic experimental autoimmune encephalomyelitis and suppress macrophage infiltration.* Clin Exp Immunol, 2006. **145**(1): p. 101-7.
220. de Jong, R., et al., *Selective stimulation of T helper 2 cytokine responses by the anti-psoriasis agent monomethylfumarate.* Eur J Immunol, 1996. **26**(9): p. 2067-74.
221. Kappos, L., et al., *Efficacy and safety of oral fumarate in patients with relapsing-remitting multiple sclerosis: a multicentre, randomised, double-blind, placebo-controlled phase IIb study.* Lancet, 2008. **372**(9648): p. 1463-72.
222. Gold, R., et al., *Placebo-controlled phase 3 study of oral BG-12 for relapsing multiple sclerosis.* N Engl J Med, 2012. **367**(12): p. 1098-107.
223. Kurtzke, J.F., *Rating neurologic impairment in multiple sclerosis: an expanded disability status scale (EDSS).* Neurology, 1983. **33**(11): p. 1444-52.
224. Fox, R.J., et al., *Placebo-controlled phase 3 study of oral BG-12 or glatiramer in multiple sclerosis.* N Engl J Med, 2012. **367**(12): p. 1087-97.
225. Havrdova, E., et al., *Oral BG-12 (dimethyl fumarate) for relapsing-remitting multiple sclerosis: a review of DEFINE and CONFIRM. Evaluation of: Gold R, Kappos L, Arnold D, et al. Placebo-controlled phase 3 study of oral BG-12 for relapsing multiple sclerosis. N Engl J Med*

2012;367:1098-107; and Fox RJ, Miller DH, Phillips JT, et al. Placebo-controlled phase 3 study of oral BG-12 or glatiramer in multiple sclerosis. N Engl J Med 2012;367:1087-97. Expert Opin Pharmacother, 2013. **14**(15): p. 2145-56.
226. Bar-Or, A., et al., *Teriflunomide and its mechanism of action in multiple sclerosis.* Drugs, 2014. **74**(6): p. 659-74.
227. Ruckemann, K., et al., *Leflunomide inhibits pyrimidine de novo synthesis in mitogen-stimulated T-lymphocytes from healthy humans.* J Biol Chem, 1998. **273**(34): p. 21682-91.
228. Loffler, M., et al., *Dihydroorotate dehydrogenase mRNA and protein expression analysis in normal and drug-resistant cells.* Nucleosides Nucleotides Nucleic Acids, 2004. **23**(8-9): p. 1281-5.
229. Gold, R. and J.S. Wolinsky, *Pathophysiology of multiple sclerosis and the place of teriflunomide.* Acta Neurol Scand, 2011. **124**(2): p. 75-84.
230. Wostradowski, T., et al., *In vitro evaluation of physiologically relevant concentrations of teriflunomide on activation and proliferation of primary rodent microglia.* J Neuroinflammation, 2016. **13**(1): p. 250.
231. Iglesias-Bregna, D., et al., *Effects of prophylactic and therapeutic teriflunomide in transcranial magnetic stimulation-induced motor-evoked potentials in the dark agouti rat model of experimental autoimmune encephalomyelitis.* J Pharmacol Exp Ther, 2013. **347**(1): p. 203-11.
232. Merrill, J.E., et al., *Teriflunomide reduces behavioral, electrophysiological, and histopathological deficits in the Dark Agouti rat model of experimental autoimmune encephalomyelitis.* J Neurol, 2009. **256**(1): p. 89-103.
233. O'Connor, P., et al., *Randomized trial of oral teriflunomide for relapsing multiple sclerosis.* N Engl J Med, 2011. **365**(14): p. 1293-303.
234. Confavreux, C., et al., *Oral teriflunomide for patients with relapsing multiple sclerosis (TOWER): a randomised, double-blind, placebo-controlled, phase 3 trial.* Lancet Neurol, 2014. **13**(3): p. 247-56.
235. Mulero, P., L. Midaglia, and X. Montalban, *Ocrelizumab: a new milestone in multiple sclerosis therapy.* Ther Adv Neurol Disord, 2018. **11**: p. 1756286418773025.
236. Hauser, S.L., et al., *Ocrelizumab versus Interferon Beta-1a in Relapsing Multiple Sclerosis.* N Engl J Med, 2017. **376**(3): p. 221-234.
237. Montalban, X., et al., *Ocrelizumab versus Placebo in Primary Progressive Multiple Sclerosis.* N Engl J Med, 2017. **376**(3): p. 209-220.
238. Chung, H., et al., *The nuts and bolts of low-level laser (light) therapy.* Ann Biomed Eng, 2012. **40**(2): p. 516-33.
239. Pastore, D., M. Greco, and S. Passarella, *Specific helium-neon laser sensitivity of the purified cytochrome c oxidase.* Int J Radiat Biol, 2000. **76**(6): p. 863-70.
240. Greco, M., et al., *Increase in RNA and protein synthesis by mitochondria irradiated with helium-neon laser.* Biochem Biophys Res Commun, 1989. **163**(3): p. 1428-34.
241. Karu, T., *Primary and secondary mechanisms of action of visible to near-IR radiation on cells.* J Photochem Photobiol B, 1999. **49**(1): p. 1-17.
242. Pastore, D., et al., *Increase in <--H+/e- ratio of the cytochrome c oxidase reaction in mitochondria irradiated with helium-neon laser.* Biochem Mol Biol Int, 1994. **34**(4): p. 817-26.
243. Wong-Riley, M.T., et al., *Photobiomodulation directly benefits primary neurons functionally inactivated by toxins: role of cytochrome c oxidase.* J Biol Chem, 2005. **280**(6): p. 4761-71.
244. Huang, Y.Y., et al., *Biphasic dose response in low level light therapy.* Dose Response, 2009. **7**(4): p. 358-83.
245. Hu, W.P., et al., *Helium-neon laser irradiation stimulates cell proliferation through photostimulatory effects in mitochondria.* J Invest Dermatol, 2007. **127**(8): p. 2048-57.

246. Karu, T., L. Pyatibrat, and G. Kalendo, *Irradiation with He-Ne laser increases ATP level in cells cultivated in vitro.* J Photochem Photobiol B, 1995. **27**(3): p. 219-23.
247. de Freitas, L.F. and M.R. Hamblin, *Proposed Mechanisms of Photobiomodulation or Low-Level Light Therapy.* IEEE J Sel Top Quantum Electron, 2016. **22**(3).
248. Sharma, S.K., et al., *Dose response effects of 810 nm laser light on mouse primary cortical neurons.* Lasers Surg Med, 2011. **43**(8): p. 851-9.
249. Chen, A.C., et al., *Low-level laser therapy activates NF-kB via generation of reactive oxygen species in mouse embryonic fibroblasts.* PLoS One, 2011. **6**(7): p. e22453.
250. Xuan, W., et al., *Transcranial low-level laser therapy improves neurological performance in traumatic brain injury in mice: effect of treatment repetition regimen.* PLoS One, 2013. **8**(1): p. e53454.
251. Xuan, W., L. Huang, and M.R. Hamblin, *Repeated transcranial low-level laser therapy for traumatic brain injury in mice: biphasic dose response and long-term treatment outcome.* J Biophotonics, 2016. **9**(11-12): p. 1263-1272.
252. Salehpour, F., et al., *Brain Photobiomodulation Therapy: a Narrative Review.* Mol Neurobiol, 2018. **55**(8): p. 6601-6636.
253. Huang, Y.Y., et al., *Biphasic dose response in low level light therapy - an update.* Dose Response, 2011. **9**(4): p. 602-18.
254. Li, N. and M. Karin, *Is NF-kappaB the sensor of oxidative stress?* FASEB J, 1999. **13**(10): p. 1137-43.
255. Tergaonkar, V., *NFkappaB pathway: a good signaling paradigm and therapeutic target.* Int J Biochem Cell Biol, 2006. **38**(10): p. 1647-53.
256. Ball, K.A., P.R. Castello, and R.O. Poyton, *Low intensity light stimulates nitrite-dependent nitric oxide synthesis but not oxygen consumption by cytochrome c oxidase: Implications for phototherapy.* J Photochem Photobiol B, 2011. **102**(3): p. 182-91.
257. Hayashi, T., et al., *Fourier transform infrared characterization of a CuB-nitrosyl complex in cytochrome ba3 from Thermus thermophilus: relevance to NO reductase activity in heme-copper terminal oxidases.* J Am Chem Soc, 2007. **129**(48): p. 14952-8.
258. Zhang, R., et al., *Near infrared light protects cardiomyocytes from hypoxia and reoxygenation injury by a nitric oxide dependent mechanism.* J Mol Cell Cardiol, 2009. **46**(1): p. 4-14.
259. Yu, Z., et al., *Near infrared radiation rescues mitochondrial dysfunction in cortical neurons after oxygen-glucose deprivation.* Metab Brain Dis, 2015. **30**(2): p. 491-6.
260. Oron, A., et al., *Low-level laser therapy applied transcranially to rats after induction of stroke significantly reduces long-term neurological deficits.* Stroke, 2006. **37**(10): p. 2620-4.
261. Moges, H., et al., *Light therapy and supplementary Riboflavin in the SOD1 transgenic mouse model of familial amyotrophic lateral sclerosis (FALS).* Lasers Surg Med, 2009. **41**(1): p. 52-9.
262. Byrnes, K.R., et al., *Light promotes regeneration and functional recovery and alters the immune response after spinal cord injury.* Lasers Surg Med, 2005. **36**(3): p. 171-85.
263. Naeser, M.A., et al., *Improved cognitive function after transcranial, light-emitting diode treatments in chronic, traumatic brain injury: two case reports.* Photomed Laser Surg, 2011. **29**(5): p. 351-8.
264. Lampl, Y., et al., *Infrared laser therapy for ischemic stroke: a new treatment strategy: results of the NeuroThera Effectiveness and Safety Trial-1 (NEST-1).* Stroke, 2007. **38**(6): p. 1843-9.
265. Detaboada, L., et al., *Transcranial application of low-energy laser irradiation improves neurological deficits in rats following acute stroke.* Lasers Surg Med, 2006. **38**(1): p. 70-3.
266. Purushothuman, S., et al., *Photobiomodulation with near infrared light mitigates Alzheimer's disease-related pathology in cerebral cortex - evidence from two transgenic mouse models.* Alzheimers Res Ther, 2014. **6**(1): p. 2.

267. Grillo, S.L., et al., *Non-invasive infra-red therapy (1072 nm) reduces beta-amyloid protein levels in the brain of an Alzheimer's disease mouse model, TASTPM.* J Photochem Photobiol B, 2013. **123**: p. 13-22.
268. Trimmer, P.A., et al., *Reduced axonal transport in Parkinson's disease cybrid neurites is restored by light therapy.* Mol Neurodegener, 2009. **4**: p. 26.
269. Aloisi, F., et al., *Relative efficiency of microglia, astrocytes, dendritic cells and B cells in naive CD4+ T cell priming and Th1/Th2 cell restimulation.* Eur J Immunol, 1999. **29**(9): p. 2705-14.
270. Akama, K.T., et al., *Amyloid beta-peptide stimulates nitric oxide production in astrocytes through an NFkappaB-dependent mechanism.* Proc Natl Acad Sci U S A, 1998. **95**(10): p. 5795-800.
271. Goodwin, J.L., M.E. Kehrli, Jr., and E. Uemura, *Integrin Mac-1 and beta-amyloid in microglial release of nitric oxide.* Brain Res, 1997. **768**(1-2): p. 279-86.
272. Wallace, M.N., et al., *Nitric oxide synthase in reactive astrocytes adjacent to beta-amyloid plaques.* Exp Neurol, 1997. **144**(2): p. 266-72.
273. Combs, C.K., et al., *beta-Amyloid stimulation of microglia and monocytes results in TNFalpha-dependent expression of inducible nitric oxide synthase and neuronal apoptosis.* J Neurosci, 2001. **21**(4): p. 1179-88.
274. Lee, S.C., et al., *Inducible nitric oxide synthase immunoreactivity in the Alzheimer disease hippocampus: association with Hirano bodies, neurofibrillary tangles, and senile plaques.* J Neuropathol Exp Neurol, 1999. **58**(11): p. 1163-9.
275. Vodovotz, Y., et al., *Inducible nitric oxide synthase in tangle-bearing neurons of patients with Alzheimer's disease.* J Exp Med, 1996. **184**(4): p. 1425-33.
276. Brown, G.C. and J.J. Neher, *Inflammatory neurodegeneration and mechanisms of microglial killing of neurons.* Mol Neurobiol, 2010. **41**(2-3): p. 242-7.
277. Knott, A.B. and E. Bossy-Wetzel, *Nitric oxide in health and disease of the nervous system.* Antioxid Redox Signal, 2009. **11**(3): p. 541-54.
278. De Taboada, L., et al., *Transcranial laser therapy attenuates amyloid-beta peptide neuropathology in amyloid-beta protein precursor transgenic mice.* J Alzheimers Dis, 2011. **23**(3): p. 521-35.
279. Darlot, F., et al., *Near-infrared light is neuroprotective in a monkey model of Parkinson disease.* Ann Neurol, 2016. **79**(1): p. 59-75.
280. Shaw, V.E., et al., *Neuroprotection of midbrain dopaminergic cells in MPTP-treated mice after near-infrared light treatment.* J Comp Neurol, 2010. **518**(1): p. 25-40.
281. El Massri, N., et al., *Near-infrared light treatment reduces astrogliosis in MPTP-treated monkeys.* Exp Brain Res, 2016. **234**(11): p. 3225-3232.
282. El Massri, N., et al., *The effect of different doses of near infrared light on dopaminergic cell survival and gliosis in MPTP-treated mice.* Int J Neurosci, 2016. **126**(1): p. 76-87.
283. El Massri, N., et al., *Photobiomodulation-induced changes in a monkey model of Parkinson's disease: changes in tyrosine hydroxylase cells and GDNF expression in the striatum.* Exp Brain Res, 2017. **235**(6): p. 1861-1874.
284. O'Brien, J.A. and P.J. Austin, *Effect of Photobiomodulation in Rescuing Lipopolysaccharide-Induced Dopaminergic Cell Loss in the Male Sprague-Dawley Rat.* Biomolecules, 2019. **9**(8).
285. San Miguel, M., et al., *Photobiomodulation Mitigates Cerebrovascular Leakage Induced by the Parkinsonian Neurotoxin MPTP.* Biomolecules, 2019. **9**(10).
286. Jackson, R.F., et al., *Application of low-level laser therapy for noninvasive body contouring.* Lasers Surg Med, 2012. **44**(3): p. 211-7.
287. Muili, K.A., et al., *Amelioration of experimental autoimmune encephalomyelitis in C57BL/6 mice by photobiomodulation induced by 670 nm light.* PLoS One, 2012. **7**(1): p. e30655.

288. Muili, K.A., et al., *Photobiomodulation induced by 670 nm light ameliorates MOG35-55 induced EAE in female C57BL/6 mice: a role for remediation of nitrosative stress.* PLoS One, 2013. **8**(6): p. e67358.
289. Krupp, L.B., et al., *The fatigue severity scale. Application to patients with multiple sclerosis and systemic lupus erythematosus.* Arch Neurol, 1989. **46**(10): p. 1121-3.
290. Sharma, K.R., et al., *Evidence of an abnormal intramuscular component of fatigue in multiple sclerosis.* Muscle Nerve, 1995. **18**(12): p. 1403-11.
291. Kent-Braun, J.A., et al., *Postexercise phosphocreatine resynthesis is slowed in multiple sclerosis.* Muscle Nerve, 1994. **17**(8): p. 835-41.
292. Kent-Braun, J.A., et al., *Effects of exercise on muscle activation and metabolism in multiple sclerosis.* Muscle Nerve, 1994. **17**(10): p. 1162-9.
293. Rice, C.L., T.L. Vollmer, and B. Bigland-Ritchie, *Neuromuscular responses of patients with multiple sclerosis.* Muscle Nerve, 1992. **15**(10): p. 1123-32.
294. Kent-Braun, J.A., et al., *Strength, skeletal muscle composition, and enzyme activity in multiple sclerosis.* J Appl Physiol (1985), 1997. **83**(6): p. 1998-2004.
295. Leal Junior, E.C., et al., *Effect of 655-nm low-level laser therapy on exercise-induced skeletal muscle fatigue in humans.* Photomed Laser Surg, 2008. **26**(5): p. 419-24.
296. Leal Junior, E.C., et al., *Effect of 830 nm low-level laser therapy in exercise-induced skeletal muscle fatigue in humans.* Lasers Med Sci, 2009. **24**(3): p. 425-31.
297. Leal Junior, E.C., et al., *Effects of low-level laser therapy (LLLT) in the development of exercise-induced skeletal muscle fatigue and changes in biochemical markers related to postexercise recovery.* J Orthop Sports Phys Ther, 2010. **40**(8): p. 524-32.
298. Baroni, B.M., et al., *Low level laser therapy before eccentric exercise reduces muscle damage markers in humans.* Eur J Appl Physiol, 2010. **110**(4): p. 789-96.
299. Toma, R.L., et al., *Effect of 808 nm low-level laser therapy in exercise-induced skeletal muscle fatigue in elderly women.* Lasers Med Sci, 2013. **28**(5): p. 1375-82.
300. De Marchi, T., et al., *Low-level laser therapy (LLLT) in human progressive-intensity running: effects on exercise performance, skeletal muscle status, and oxidative stress.* Lasers Med Sci, 2012. **27**(1): p. 231-6.
301. Larkin-Kaiser, K.A., et al., *Near-infrared light therapy to attenuate strength loss after strenuous resistance exercise.* J Athl Train, 2015. **50**(1): p. 45-50.
302. Larkin-Kaiser, K.A., et al., *Photobiomodulation delays the onset of skeletal muscle fatigue in a dose-dependent manner.* Lasers Med Sci, 2016. **31**(7): p. 1325-32.
303. de Oliveira, A.R., et al., *Pre-Exercise Infrared Photobiomodulation Therapy (810 nm) in Skeletal Muscle Performance and Postexercise Recovery in Humans: What Is the Optimal Power Output?* Photomed Laser Surg, 2017. **35**(11): p. 595-603.
304. Hohol, M.J., E.J. Orav, and H.L. Weiner, *Disease steps in multiple sclerosis: a simple approach to evaluate disease progression.* Neurology, 1995. **45**(2): p. 251-5.
305. Hohol, M.J., E.J. Orav, and H.L. Weiner, *Disease steps in multiple sclerosis: a longitudinal study comparing disease steps and EDSS to evaluate disease progression.* Mult Scler, 1999. **5**(5): p. 349-54.
306. Quah, B.J., H.S. Warren, and C.R. Parish, *Monitoring lymphocyte proliferation in vitro and in vivo with the intracellular fluorescent dye carboxyfluorescein diacetate succinimidyl ester.* Nat Protoc, 2007. **2**(9): p. 2049-56.
307. Karu, T.I., et al., *Absorption measurements of cell monolayers relevant to mechanisms of laser phototherapy: reduction or oxidation of cytochrome c oxidase under laser radiation at 632.8 nm.* Photomed Laser Surg, 2008. **26**(6): p. 593-9.

308. Huang, Y.Y., et al., *Low-level laser therapy (LLLT) reduces oxidative stress in primary cortical neurons in vitro.* J Biophotonics, 2013. **6**(10): p. 829-38.
309. Chen, A.C., et al., *Effects of 810-nm laser on murine bone-marrow-derived dendritic cells.* Photomed Laser Surg, 2011. **29**(6): p. 383-9.
310. Heo, J.C., et al., *Photobiomodulation (660 nm) therapy reduces oxidative stress and induces BDNF expression in the hippocampus.* Sci Rep, 2019. **9**(1): p. 10114.
311. Zhang, J., et al., *Illumination with 630 nm Red Light Reduces Oxidative Stress and Restores Memory by Photo-Activating Catalase and Formaldehyde Dehydrogenase in SAMP8 Mice.* Antioxid Redox Signal, 2019. **30**(11): p. 1432-1449.
312. Rupel, K., et al., *Photobiomodulation at Multiple Wavelengths Differentially Modulates Oxidative Stress In Vitro and In Vivo.* Oxid Med Cell Longev, 2018. **2018**: p. 6510159.
313. Sun, Q., et al., *Red light-emitting diode irradiation regulates oxidative stress and inflammation through SPHK1/NF-kappaB activation in human keratinocytes.* J Photochem Photobiol B, 2018. **186**: p. 31-40.
314. Martins, T.B., et al., *Analysis of proinflammatory and anti-inflammatory cytokine serum concentrations in patients with multiple sclerosis by using a multiplexed immunoassay.* Am J Clin Pathol, 2011. **136**(5): p. 696-704.
315. Kallaur, A.P., et al., *Cytokine profile in relapsingremitting multiple sclerosis patients and the association between progression and activity of the disease.* Mol Med Rep, 2013. **7**(3): p. 1010-20.
316. Nicoletti, F., et al., *Blood levels of transforming growth factor-beta 1 (TGF-beta1) are elevated in both relapsing remitting and chronic progressive multiple sclerosis (MS) patients and are further augmented by treatment with interferon-beta 1b (IFN-beta1b).* Clin Exp Immunol, 1998. **113**(1): p. 96-9.
317. Carrieri, P.B., et al., *Profile of cerebrospinal fluid and serum cytokines in patients with relapsing-remitting multiple sclerosis: a correlation with clinical activity.* Immunopharmacol Immunotoxicol, 1998. **20**(3): p. 373-82.

Curriculum Vitae

Miguel Tolentino tolenti4@uwm.edu

Education

2013-2019 PhD Student in Health Sciences (Immunology). Fall-2013-present. Biomedical Sciences Department, University of Wisconsin Milwaukee.
Dissertation project: Characterization of the Effect of Photobiomodulation at 670nm, 830nm, and 735 nm on Human Lymphoid Cells.

2013 Master in Biomedical Sciences. Biomedical Sciences Department, University of Wisconsin Milwaukee.
Thesis title: Metformin-induced PEDF expression regulates cell proliferation and lipid metabolism in prostate cancer cells.

2006 B. S. Biomedical Sciences (Pharmaceutical-Biologist Chemist). University of Guanajuato, Mexico.

Honors

2018 National Multiple Sclerosis Society (NMSS) Travel Award. November 16-19, 2018. Autumn Immunology Conference, Chicago Illinois. Abstract selected among the top five abstracts related to Multiple Sclerosis or general autoimmunity.

2014-2017 CONACYT grantee from Government of Mexico. Fall 2014-Spring 2017. PhD in Health Sciences. College of Health Sciences. University of Wisconsin Milwaukee.

2015-2016 Chancellor's Graduate Student Award. Fall 2015-Spring 2016. College of Health Sciences PhD program. University of Wisconsin Milwaukee.

2016 Randall S. Lambrecht Honor Code Scholarship. College of Health Sciences. University of Wisconsin Milwaukee.

2015 Molly Yeffet Krain Iirwin Amira Scholarship. College of Health Sciences. University of
2015 Wisconsin Milwaukee.
Clinical Laboratory Scholarship. Biomedical Sciences Department. College of Health
2014-2015 Sciences. University of Wisconsin Milwaukee.
Chancellor's Graduate Student Award. Fall 2014-Spring 2015. College of Health Sciences.
2011-2013 University of Wisconsin Milwaukee.
Fulbright-Garcia Robles grantee. Fall 2011-Spring 2013. Master In Biomedical Sciences. University of Wisconsin Milwaukee.

Professional Experience

2015-2019 Teaching assistant. Fall 2015-present. Current position held. Biomedical Sciences Department. College of Health Sciences. University of Wisconsin Milwaukee. Subjects assigned include Nutrition, Medical Diagnosis, Human Pathophysiology, Public Health Microbiology laboratory, Hematology laboratory, Microbiology laboratory, and Immunology laboratory.
Assignments:
-Assist professors, undergrad and graduate students during classes and laboratory sessions.
-Assist students by answering questions, providing examples, emotional support, friendly attitude and general guidance.
-Assure student understanding of classroom rules and procedures.
-Assist with the grading of homework, exams, written assignments, and laboratory

reports.

2009-2011 -Assist and set up exams.
-Prepare reagents and materials for laboratory practices.

Laboratory Chief and Medical Technologist. April 2009-July 2011. Clinical laboratory area, Juventino Rosas General Hospital, Mexico.
Assignments:
-Perform chemical analysis on blood samples in different clinical areas including hematology, clinical chemistry, immunology, microbiology, blood bank.
-Analysis of laboratory results.
-Operation of laboratory equipment.
-Participate in public health programs including tuberculosis screening, and control/monitoring of gestational diabetes.
-Management of laboratory in general: acquisition of reagents, supplies, purchases, laboratory maintenance, staff training.

2007-2009 Medical Technologist. May 2007-March 2009. Clinical Laboratory area. Dolores Hidalgo General Hospital, Mexico.
Assignments:
-Perform chemical analysis on blood samples in different clinical areas including hematology, clinical chemistry, immunology, microbiology, blood bank.
-Analysis of laboratory results.
-Operation of laboratory equipment.

2005 Internship. January 4-28. Clinical Laboratory, PEMEX Hospital, Salamanca, Mexico.
Assignments:
-Perform chemical analysis on blood samples in different clinical areas including hematology, clinical chemistry, immunology, microbiology, blood bank.
-Analysis of laboratory results.
-Operation of laboratory equipment.

Research Experience

2011-2013 Lab Assistant. Fall 2011-Spring 2013. Health Sciences Department, University of Wisconsin Milwaukee, USA. Thesis title: Metformin-induced PEDF expression regulates cell proliferation and lipid metabolism in prostate cancer cells.

2005-2006 Full-time Research Assistant. Fall 2005-Fall 2006. Chemistry Department, University of Guanajuato, Mexico.
Assignments:
-Work in the synthesis of organic molecules i.e. bi-ciclobutendiones molecules starting from squaric acid. These molecules can work as intermediates for the synthesis of poly-aryl molecules which are present in compounds with biological activity such as antibiotics.
-Assist with academic research.
-Analyze data.
-Prepare reagents and materials for current research projects in the lab.
-Organize, maintain and update lab books, inventory and data bases.
-Supervise undergraduate students working on assignment research projects.
-Attend to lab discussions, meetings and seminars.

2006 Full-Time Research Assistant. Summer research project. Chemistry Department, West

Virginia University, USA.
Assignments:
-Work in the synthesis of organic molecules i.e. pyrrolopyrimidines using palladium catalysts. Palladium catalysts provide an alternative pathway for cross-coupling reaction of cyclic compounds.
-Assist with academic research.
-Analyze data.
-Prepare reagents and materials for current research projects in the lab.
-Organize, maintain and update lab books, inventory and data bases.
-Supervise undergraduate students working on assignment research projects.
-Attend to lab discussions, meetings and seminars.

2005 Full-Time Research Assistant, Chemistry Department, U. of Guanajuato, Mexico.
Assignments:
-Work in the synthesis of organic molecules i.e. bi-aryl compounds with biological activities using boronic acids. The use of boronic acids allows the production of poly-aryl molecules which are present in different kind of compounds with biological activity such as antibiotics and antivirals.
-Assist with academic research.
-Analyze data.
-Prepare reagents and materials for current research projects in the lab.
-Organize, maintain and update lab books, inventory and data bases.
-Supervise undergraduate students working on assignment research projects.
-Attend to lab discussions, meetings and seminars.

Knowledge/skills in laboratory techniques and equipment

-Knowledge in tissue culture techniques, ELISA, western blot, PCR, Nuclear Magnetic Resonance spectrophotometry (NMRS), High Performance Liquid Chromatography (HPLC), electrophoresis, clinical lab equipment, flow-cytometry, data analysis software.
-Knowledge in methodologies related to neuroscience, neuroimmunology, multiple sclerosis, and prostate cancer.
-Ability to develop and follow research methodology and protocols.
-Ability to design, organize, and coordinate scientific research projects.
-Self-motivated, capable to design and conduct experiments.
-Knowledge of lab bio-hazards, safety practices, as well as care and use of laboratory equipment.

Grants obtained in the College of Health Sciences

2019 Student Research Grant Award (SRGA). Fall 2019-Spring 2020. College of Health Sciences. University of Wisconsin Milwaukee. Project title: Evaluation of the potential effect of Photobiomodulation Therapy (PBMT) on nitrosative stress and mitochondrial function in Multiple Sclerosis (MS) patients. Grant: $2000.00 USD.

2018 Student Research Grant Award (SRGA). Fall 2018-Spring 2019. College of Health Sciences. University of Wisconsin Milwaukee. Project title: Study to evaluate Photobiomodulation at 670, 830, and 735 nm on both immune and mitochondrial functions of human lymphoid cells. Grant: $2000.00 USD.

2015 Student Research Grant Award (SRGA). Fall 2015-Spring 2016. College of Health Sciences. University of Wisconsin Milwaukee. Project title: Characterization of the

Effect of Photobiomodulation at 670, 830, and 735nm on human activated CD4+ T cells. Grant: $2000.00 USD.

2013 Student Research Grant Award (SRGA). Fall2013-Spring 2014. College of Health Sciences. University of Wisconsin. Project title: Investigation of the Effect of 670nm light-mediated Photomodulation on Human Lymphoid Cells. Grant: $2000.00 USD.

Publications

2018-2019 Book chapter. Book title: “Photobiomodulation and the Brain” subtitle "Low-level Laser (Light) Therapy in Neurology and Neuroscience” edited by Michael R Hamblin and Yingying Huang. Published by Elsevier. Chapter 21: PBM for MS in animal models, Photobiomodulation in the Brain. **Miguel A. Tolentino** and Jeri-Anne Lyons

2014 Book chapter. Low-Level Laser Therapy: A Treatment Modality for Multiple Sclerosis Targeting Autoimmunity and Oxidative Stress. Zenas George, **Miguel A. Tolentino**, and Jeri-Anne Lyons. Handbook of Low-Level Laser Therapy. Edited by y Michael Hamblin, Tanupriya Agrawal, Marcelo de Sousa. Pan Stanford Publishing.

Conference Presentations

2019 Poster and podium presentation. Photobiomodulation therapy (PBMT) regulates the production of IL-10 and IFN-ɣ by peripheral blood mononuclear cells (PBMC) and CD4+ T cells isolated from subjects with Multiple Sclerosis (MS). The American Association of Immunologists. May 9-13. Abstract selected accepted for podium

2019 and poster presentation.

Poster presentation. Photobiomodulation therapy (PBMT) regulates the production of IL-10 and IFN-ɣ by peripheral blood mononuclear cells (PBMC) and CD4+ T cells

2018 isolated from subjects with Multiple Sclerosis (MS). May 3. University of Milwaukee Health Research Symposium.

Poster and podium presentation. Poster title: “Photobiomodulation therapy (PBMT) regulates production of inflammatory cytokines IL-10 and IFN-ɣ involved in multiple sclerosis”. Autumn Immunology Conference, Chicago Illinois, November 16-19. Abstract selected among the top five abstracts related to multiple sclerosis or general autoimmunity.

2016 Speaker. The Role of the Clinical Lab in the Control of Diabetes Mellitus. June 26. General Hospital Juventino Rosas. Guanajuato Health Department, Mexico.

2015 Poster title: Potential Antioxidant Function of PEDF in Prostate Tissue and Prostate Cancer. Crump, L, M Tolentino, SM Wcislak, and JA Doll. Medical College of Wisconsin Cancer Center.

2015 Speaker: Updates on Pulmonary Tuberculosis. August 7. General Hospital Juventino Rosas. Guanajuato Health Department, Mexico.

2014 Speaker. Course/training: Medic Microbiology. July 2-4. General Hospital Juventino Rosas. Guanajuato Health Department, Mexico.

2013 Speaker. Blood Transfusion and Blood Bank Updates. July 29-31. General Hospital Juventino Rosas. Guanajuato Health Department, Mexico.

2012 Poster title: “Metformin-induced PEDF expression regulates cell proliferation and lipid metabolism in prostate cancer cells”. Miguel Tolentino, Susan M. Wcislak, Ayesha T. Chawla, Betsy Abroe, Akash Patnaik, Massa Mafi, Lewis C. Cantley and Jennifer A. Doll. *Fall Research Symposium*, U. of Wisconsin Milwaukee.

2012 Poster title: “Metformin’s anti-prostate cancer effect may be via increased PEDF levels and lipolytic activity”. Miguel Tolentino, Massa Mafi, Akash Patnaik, Susan M. Wcislak, Betsy Abroe, Ayesha T. Chawla, Lewis C. Cantley and Jennifer A. Doll. *Spring Research Symposium*. U. of Wisconsin Milwaukee.

2011 Speaker. Training: updates on Tuberculosis. March 24. Guanajuato Health Department. General Hospital Juventino Rosas. Mexico.

2010 Speaker. Training on blood transfusion services. August 31. Guanajuato Health Department. General Hospital Juventino Rosas. Mexico.

Training and Conferences Attended

2018 Training: Biosafety Course on Bloodborne Pathogens. December 29. Occupational Safety and Health Administration (OSHA). University of Wisconsin Milwaukee.

2018 Autumn Immunology Conference. November 16-19. Poster and oral presentation. Chicago IL.

2017 College of Health Sciences Research Symposium. Fall. University of Wisconsin Milwaukee.

2017 Training: Bloodborne Pathogens. October 3. University Safety and Assurances. University of Wisconsin Milwaukee.

2017 Training: Satellite Hazardous Waste Accumulation. September 6. University Safety and Assurances. University of Wisconsin Milwaukee.

2017 Course: Checkpoint, Data Security and Privacy. October 2. EVERFI. University of Wisconsin- Milwaukee.

2017 Training: Biological Safety. September 8. University of Wisconsin Milwaukee.

2017 Course: Intersections preventing Harassment and Sexual Violence. February 19. EVERFI. University of Wisconsin- Milwaukee.

2017 Course/Training: Medical Parasitology. January 6. General Hospital Juventino Rosas. Guanajuato Health Department, Mexico.

2016 College of Health Sciences Research Symposium. Fall. University of Wisconsin Milwaukee.

2016 Autumn Immunology Conference. Chicago IL.

2015 College of Health Sciences Research Symposium. Fall. University of Wisconsin Milwaukee.

2014 Autumn Immunology Conference. Chicago IL.

2014 College of Health Sciences Research Symposium. Fall. University of Wisconsin Milwaukee.

2013 Fulbright seminar: “From Lab to Market”. Boston, MA.

2013 College of Health Sciences Spring Research Symposium. Poster presentation. May 3. University of Wisconsin Milwaukee.

2012 College of Health Sciences Spring Research Symposium. Poster presentation. May 4. University of Wisconsin Milwaukee.

2012 Training: Chemical hygiene plan and laboratory safety. February 2. University Safety and Assurances. University of Wisconsin Milwaukee.

2011 Academic English Program. August 1-26. University of California San Diego.

2009 Seminar: “Reduction of Stigma and Discrimination of Personnel who Live with HIV AIDS”. July 7. Institute of Public Health, Guanajuato, Mexico.

2009 Course-workshop: “Tuberculosis and Bacilloscopy”. April 27-29. State Laboratory Of Public Health, Guanajuato, Mexico.

2008 Congress: “The Process for Standardization of Bacteriological Studies in the Clinical Area”. October 10-12. University of Guanajuato, Mexico.

2008 XIV Congress of Chemists of the State of Guanajuato. July 25-27. University of Guanajuato. Mexico.

2008 Course: “Clinical Mycology”. February 29-March 1. The Mexican Association of Medical Clinical Mycology, Guanajuato, Mexico.

2007 Training on: “Procedures in the Area of Blood Donation and Transfusion Service”. December 3-7. General Hospital of Dolores Hidalgo, Mexico.

2007 Course: “Liquids and electrolytes”. August 7. Medical College of Guanajuato, Mexico.

2007 Congress: “2nd International Cycle of Conferences on Quality”. June 30. International Federation of Clinical Chemistry and Laboratory Medicine (IFCC), Mexico.

2007 Course: “Use and Handling of Blood and its Derivatives”. May 16 and 23. General Hospital Dolores Hidalgo, Mexico.

2007 Course: “Updating in Clinical Analysis”. General Hospital of Dolores Hidalgo. Mexico.

2006 Congress: “16th International Conference on Organic Synthesis”. June 11-15, IUPAC, Mexico.

2006 Course: “Asymmetric Synthesis”. February 20-22. Mexican Academy of Organic Chemistry. University of Guanajuato, Mexico.

2006 Course: “Design of Pharmaceuticals”. February 20-22. Mexican Academy of Organic Chemistry. University of Guanajuato, Mexico.

2004 Workshop: “Formulation of Medicines and Cosmetics”. October 7-8. University of Guanajuato, Mexico.

2004 Biomedical Sciences Conference. October 7-8. University of Guanajuato, Mexico.